AD-782 656

THEORETICAL AND MECHANICAL MODELS OF THE HUMAN NECK

Gaylen A. Thurston, et al

Denver University

Prepared for:

Office of Naval Research

June 1974

THEORETICAL AND MECHANICAL MODELS OF THE HUMAN NECK

-Prepared for-

Office of Naval Research
Contract No. N00014-67-A-0394-0002

-Prepared by-

Gaylen A. Thurston
Richard J. Fay

Mechanical Sciences and
Environmental Engineering Department
Denver Research Institute
University of Denver

June 1974

TABLE OF CONTENTS

LIST OF FIGURES

I. INTRODUCTION

The University of Denver's part in the Office of Naval Research Project on Aircraft Crashworthiness has been directed at head and neck motion during crashes. Specifically, it has been concerned with possible constraint systems to protect the head of an aircraft occupant against violent rotation about the torso and subsequent loss of consciousness during emergency landings and survivable crashes.

The restraint concept that has been tested is an inflatable collar to limit head motion. The collar would fit under the chin and cushion the impact of the chin on the thorax during hyperflexion of the neck. During the first year of the contract, an airbag was tested using a single-degree-of-freedom mechanical system. An anthropometric dummy head was mounted on a rigid bar that simulated the neck. This assembly was mounted on a sled that was accelerated by compressed air.

The results of tests on this mechanical system showed that the airbag is a feasible method of limiting head motion during flexion.

The second part of the contract has been devoted to further exploration of this concept. A mechanical model has been built to better simulate the human neck. This model allows stretching of the neck and relative angular motion between the head and neck similar to head rotation about the occipital condyles. This more realistic model allows more confidence in the experimental results evaluating the effectiveness of the airbag.

In addition to the experimental work, theoretical work has been devoted to modelling the motion of the head and neck during acceleration. The acceleration levels of this motion must be kept at low levels in order to survive a crash without serious injury. Part of the resistance to this motion comes from the muscles of the neck themselves. The muscle tension during the normal range of motion affects the response. After the rotation exceeds the voluntary response limits, additional torque is produced by attempting to further stretch muscles and ligaments.

The main theoretical problem is arriving at a tractable set of constitutive relations to compute neck moments as a function of neck displacements and velocities. Many different representations have been used. The simplest are linear springs and dashpots connected in parallel or in series. More sophisticated models use nonlinear springs, stops, and viscoelastic elements. The number of degrees of freedom varies from one or two, to models allowing three degrees of freedom for each cervical vertebrae.

Muscle contraction is varied by the central nervous system. The total tension in the muscles depends on the number of fibers excited. The force does not depend on the length of the muscle during the normal range of motion. This independence of force on length during initial phases of the motion indicates that linear springs are not satisfactory elements for the mathematical modelling of the effect of muscle tension.

The recent literature has used viscoelastic elements to simulate this type of muscle force. These elements contain viscous damping terms.

A different approach has been used in the present study. The voluntary resistance of the neck muscles to motion is treated as a constant torque during the normal range of rotation. The constant torque resisting the motion is analoguous mathematically to solid friction (or Coulomb damping) rather than viscous damping.

Nonlinear hard springs are used in the mathematical model to simulate the increased torque when the head and neck rotations exceed the voluntary limits.

A second feature of the theoretical part of the study is an attempt to incorporate a systematic approach for estimating the parameters in the new constitutive relations. Given the motion of the head and neck from experimental data, the problem is to deduce the equations of motion. This estimation of parameters is treated by finding the effect of varying each parameter by Newton's method (quasilinearization) and applying a least-squares fit of the experimental data to compute the variation in each parameter. This method of estimation theory has been used for process dynamics in chemical engineering, and for other applications, but we have not seen it used in the field of biomechanics of human motion.

The computer program to predict the response for given initial conditions and given parameters was straight forward to write and soon gave numerical results.

The estimation theory is an iterative procedure because of the nonlinear nature of the differential equations of motion. This part of the numerical computations showed poor convergence. The least-squares subroutine to calculate changes in the assumed parameters in the constitutive equations contains a set of linear algebraic equations that must be solved to find the corrections to the current values of the constants appearing in the constitutive equation. The determinant of this matrix was nearly singular. In addition, several of the submatrices were also nearly singular.

The slow convergence of the iteration due to linear dependence is discussed at length in the body of the report. Numerical solutions were finally achieved by varying one parameter at a time.

The lack of sensitivity to parameter variations is of more than academic interest. There are at least two physical explanations of the linear dependence that are of major significance. First of all, the lack of convergence can merely mean that there is not a unique set of parameters that minimizes the sum of the squares of the differences between theory and experiment. This implies that if there is not a unique set of parameters for a given theory, then more than one theory can be used to explain the same data. This line of reasoning leads back to the principle that one experiment can disprove a theory and any

number of experiments cannot "prove" a theory.

A second explanation of the linear dependence is related to the first. The least-squares analysis was based on computed and measured angular rotations of the head and neck. The rotations are calculated by integrating the equations of motion for the angular acceleration. An integral of a function is not as sensitive to a change in a parameter as a function itself. A change in momentum depends on the impulse and different forces can be integrated with time to give the same impulse.

The logical step would be to base the least-squares analysis on measured angular accelerations. However, practical problems presented themselves in following this approach. A complete set of plotted experimental data for live subjects was available for sled accelerations, angular accelerations of the head and neck, and head accelerations plus the velocities and the displacements associated with these accelerations.

However, the linear acceleration of the base of the neck at vertebrae T-1 was not plotted and this acceleration is required for input data to the theory. This T-1 acceleration appears to differ markedly from the sled acceleration because of slack in the shoulder harness, elasticity of the harness and of the thorax and shoulders of the human subject.

The results in this report are computed using the sled acceleration in lieu of the T-1 acceleration. This was sufficient for computing theoretical angular deflections, but the correct set of acceleration data is necessary before proceeding further with the least-squares analysis of the acceleration.

II. CONCLUSIONS AND RECOMMENDATIONS

Before going into the details of the work on the second phase of the contract, it might be useful to outline the results obtained thus far, how they fit into the current literature on head and neck motion, and the directions that future work should take in this field.

1. The mechanical neck developed under the contract has some novel features that add realism to its function as a means of evaluating proposed head restraint. The use of shock cords to simulate muscle tension allows adjusting this variable without major modification of the model. A catch has been designed to oppose rebound from the fully flexed position. This prevents the oscillation observed in the simple one-degree-of-freedom model used on the previous evaluation of an airbag and is closer to experimental observations on human subjects.

2. The airbag acts to relieve the neck forces due to flexion. This is achieved at the price of inducing forces on the jaw and sternum. Data are scarce for a trade-off study between neck injuries and jaw and chest injuries.

3. The head acceleration curve is smoothed by the airbag without a significant reduction from the peak values. However, by limiting the excursion of the head, the inflatable collar could be effective in reducing head injury due to impact on the instrument panel or other parts of a collapsing cockpit. In other words, the airbag does not significantly reduce peak accelerations in the range up to 10 g in sled acceleration. However, its effectiveness at higher accelerations is still an open question. Cadaver or animal tests would be needed at higher acceleration levels, before risking live subjects with inflatable collars.

4. The "Coulomb damping" model used for the neck moment in the analytical part of the work shows good agreement with experiment for acceleration levels which do not result in neck injury in human subjects. The solid damping in the voluntary range of neck rotation plus nonlinear hard springs to stop the motion is therefore presented in this report as an alternative to viscoelastic models.

5. The check on the theory using the experimental data reported by Ewing, Thomas, et.al., Ref. (1), was hampered by the absence of plots of the acceleration of the base of the neck (T-1 acceleration). The reported sled acceleration was used in checking out the computer program for the current analysis as an approximation for the T-1 acceleration, but this is not satisfactory for establishing realistic values for the parameters involved.

   The difference between the sled acceleration and the neck

acceleration is due to the mechanics of the restraint system of lap belt, shoulder harness, and chest strap. This difference was recognized by Ewing, Thomas, et. al. as they note the following: "The effect of the restraint variable is assumed to be independent of the fundamental relationship between the T_1 acceleration and the head acceleration. However, as a practical matter, each individual restraint system was adjusted as tightly as possible for each run, both as a safety measure and to keep the photographic targets within the field of view of the sled-mounted cameras. Parenthetically, it should be noted that the restraint adjustment procedure was determined experimentally to result in apparent excellent control of the restraint variable, as will be shown later. An analysis of the precise effects of variations in the restraint of an individual subject on the dynamic response of the head and neck must be performed, but has not yet been accomplished."

Therefore, the data necessary to plot the T-1 accelerations were recorded with the intent of analyzing it as required. One of the concluding remarks in Ref. (1) is "However, the variables presented in the report are only a partial sampling of what is presently available. Exhaustive and effective use of the data requires large scale digital computer interaction with the data base on a continuing basis. The specific interaction should be determined by the specific problem posed."

It seems worth proposing that the T-1 acceleration data be plotted and compared with the sled acceleration data and the head acceleration data.

6. The experimental run profile for each subject in Ref. (1) contained runs with sled accelerations from 3G to 10G. The plotted results are for runs at levels greater than 5.5G. Presumably, this is because the head rotation response was not as dramatic at the lower levels. However, this data would be useful in comparing the theory in the present report and the usual viscoelastic models. The solid damping model would predict little response below a threshhold level of acceleration while a viscoelastic model would react to any acceleration.

7. The estimation of parameters in the constitutive relations by using Newton's method provides a rational means of calculation that can be incorporated into digital computer programs along with the solution of the equations of motion. The lack of uniqueness in the normal equations for the least-squares curve fit was a nuisance, but varying one constant at a time gave satisfactory answers. The difficulty in inverting the normal equations for polynomial curve fits is well-known and is one of the reasons for using orthogonal polynomials as coordinate functions.

On the practical side, the lack of uniqueness is an advantage. Different laws can be used to fit the same data with good accuracy. Therefore, different mathematical models can be proposed, e.g., the solid damping plus nonlinear springs compared to viscoelastic models.

8. After the least-squares iteration, the computer program calculates head and neck moments supplied by the muscles. In the normal rotation range, these results are comparable in magnitude to measured static results and dynamic results reported in the literature. This correlation supports the assumptions of the theory derived here.

Further work is desirable in several areas:

1. The upper limits for the present theory should be determined and an injury criterion developed for neck injuries. Moment and/or angular impulse levels that produce ruptured discs, fractured vertebrae, and torn ligaments need to be established. Experimental data in this area cannot be obtained from human volunteers. Therefore, indirect methods using cadavers, animals, and mathematical models are necessary.

2. Aircraft structure accelerations are transmitted to the head through the seat and harness restraint. The optimum design of this system can reduce peak head and neck accelerations. The quasilinearization technique used in the current theory can be extended to the optimization problem of the system as a whole.

3. The trend in the literature is to write occupant simulation programs that predict gross motion of vehicles and passengers using as few degrees-of-freedom as possible. Then, using the gross motion as input data, more detailed programs are written to describe selected parts of the overall system. This results in a great saving in computer cost at no loss in physical understanding of the mechanisms affecting the motion. The computer program described in this report can be extended to give a more detailed simulation of the head and neck and it can also be coupled to a program for simulation of a complete crash situation.

4. The experimental sled should be modified so that the effect of the harness on the T-1 impulse can be included. This will require that the base of the neck be allowed to move longitudinally with respect to the sled against the retarding force of a non-linear spring. Slack in the harness will also be simulated.

5. The modified sled can be used to study the effect of harness parameters on the motion of the head under impulsive loading.

III. EXPERIMENTAL

The objective of the experimental program, as mentioned earlier, was to study the potential of an inflatable collar as a means of reducing head and neck rotations of naval flight personnel in the instance of crash induced frontal accelerations. Our previous program, Ref. (19) involved the development of a small test sled for imposing accelerations on a simulated full size head and neck. This consisted of a 35 lb. sled mounted on cylindrical guides and accelerated by a pneumatic launching system as shown in Figure 1. A pneumatic snubbing system, Figure 2, brings the sled to rest. The launching system provides a square wave pulse up to 50 g's in magnitude over a stroke of 2 ft. The pneumatic snubbing system produces a triangular stopping impulse over a stroke of 2 ft. with adjustable onset rate, peak acceleration and fall-off rate. The head may be oriented so that the test pulse is imposed either in starting or stopping of the sled.

On the previous program, a set of experiments was conducted with an Alderson aluminum and rubber anthropometric dummy head attached to the sled with a simple pinned linkage the same length as the human neck. An inflated section of fire hose was used under the chin to reduce head rotations. The simple hinge was an over simplification of the neck; however, these experiments indicated that significant reductions in head accelerations could be achieved if the chin bag or an inflatable collar could be developed. The test results also provided a valuable object of comparison for the analytical head rotation model developed on the program for use in a parameter study.

The results of the experimentation on the first program indicated that the current program should address itself to the development of a more realistic model of the human neck so that better experimental results could be obtained.

An iterative approach was taken in the design of the neck. After consulting an anatomy book, the critical elements were simulated with mechanical parts, (Figure 3). The seven vertebrae simulated with plastic discs, were separated with discs of foam rubber and the assembly held together with strands of steel cable. The primary muscles were simulated with elastic cord covered with a fabric braid (called shock cord). Four muscles were used; one at each side and two at the back. Sled tests were conducted with the head and neck to evaluate neck performance. Accelerometer and high speed photographic data were compared with data from one of the live subject tests from Ref. 1 (Subject 004, 6.9 g's) for which a high-speed film was available. Adjustments were made in the neck until the motion of the head and neck closely simulated that of the live subject. The final neck design is shown in Figure 4.

To facilitate the comparison of the model test data with live subject data, a small analogue computer was built to provide directly the vector sum of the radial and tangential head accelerometers for display and recording on the oscilloscope. This resulted in a considerable reduction in the effort required to make the desired comparisons. The instrumentation used for the sled tests is shown in Figure 5.

A comparison of the resultant accelerations of the model head with that of two live subjects is given in Figure 6. The neck base impulse for the model test was the same as that measured by an accelerometer at the base of the neck of Subject 003, Ref. (1) (Figure 7); subject LMP of Ref. 16 was subjected to a 9.6 g half sine wave impulse.* These curves have the same characteristic shape which, with the exception of the initial peak, closely resembles the shape of the sled impulse. The time and amplitude of the initial peak were found in the model tests to be a function of the head translation which occurs before head rotation begins. A greater resistance to head translation results in less translation and less jerking just before head rotation begins. It was noticed that the orientation of the neck base plate on the model influenced the size of the initial peak. It is suggested, therefore, that the size of the initial peak and the time required to achieve it can be affected by the posture of the subject in the seat as well as the subject's general ability to resist head translation. Also, it is believed that the harness and seat characteristics have an effect since slack in this system can serve to sharpen the pulse transmitted to the subject.

As previously indicated, the motion of the model was compared to the head motion of subject 004 through the use of high speed film sequences of the tests; such a comparison for the final neck design is presented in Figures 8 and 9. As can be seen here, the motions are very similar.

An important feature of the model neck is the cable restraint which holds the chin down when the head rotates forward. This simulates the live subject's ability to prevent his head from bobbing. The cable feeds freely through a guide as the head rotates forward (Figure 4) but is secured by a knurled eccentric wheel when the direction of the head rotation is reversed.

The effectiveness of the inflatable collar concept was evaluated using an inflated bag under the chin. This bag was made from a section of fire hose as illustrated in Figure 10. A series of tests was made with the head facing the launcher so that a testing impulse approximating a square wave was applied to the base of the neck during the test period. The resultant head acceleration for impulses of 10 g's is plotted in Figure 11 for the head without restraint and with the chin bag inflated to 5, 10, and 25 psi. A similar plot for 5 g's is presented in Figure 12 for the unrestrained head and the head with the 25 psi chin bag. In general, without the chin restraint, the resultant head acceleration curve is similar in shape to the applied impulse except for the initial peak and is greater in magnitude and longer in duration. The curves in Figure 12 indicate that the chin bag reduces the size of

---

* Neck base accelerometer data was not available for subject 004 so the data for subject 003 was used. It is assumed that these were similar.

the resultant head impulse but that increases in bag pressure over 5 psi have little effect.

Static tests were also conducted to measure the effect of the chin restraint. The test set up is illustrated in Figure 13. Weights were used to impose a horizontal force on the top of the head and head rotations were measured. Plots of head rotation as a function of applied force are presented in Figure 14. It is interesting to note here that the greatest single effect at large rotations is achieved with the 5 psi inflation pressure. While pressures up to 25 psi were used in the bag, it is believed that these higher bag pressures might pose a threat to a person's jaw structure.

In summary, the experimental program set out to build an improved model of the human neck in order to obtain data on the potential of a chin bag or inflatable collar as a means of reducing head rotations associated with crash induced frontal accelerations on Navy flight personnel. A neck was developed which closely simulates the behavior of the human neck in the desired mode of operation. This neck was used for experiments with an inflated chin bag. The chin bag test results indicate that some reduction in head accelerations can be achieved. Aside from chin bag tests, the mechanical neck model has also been useful in gaining an understanding of neck and head motions and accelerations under impulsive frontal loading similar to that experienced by flight personnel in crash landings.

IV. THEORY

The analytical work described in this section of the report paralleled the experimental work in the previous section, but the objective was not to write equations of motion for the mechanical neck. The intent was to develop a theory to describe the head and neck motion of humans. Then, the sensitivity of parameters appearing in the theory were evaluated by Newton's method and the parameters evaluated by a least-squares curve fit between the theory and the experiments on volunteers reported by Ewing and Thomas in Ref. 1.

The emphasis was on the estimation theory, so the equations of motions were restricted to a two-degree-of-freedom model containing six free parameters. The two degrees of freedom are head rotation and neck rotation.

The rigid-body equations of motion for the head and neck are (see Figure 15).

$$-\underline{F}_1 = m_h \underline{a}_h \tag{1}$$

$$\underline{F}_2 + \underline{F}_1 = m_n \underline{a}_n \tag{2}$$

$$-M_1\underline{k} + \underline{\rho}_h \times \underline{F}_1 = I_h \ddot{\phi} \underline{k} \tag{3}$$

$$-M_2\underline{k} + M_1\underline{k} + (\underline{\rho}_1-\underline{\rho}_2) \times F_1-\underline{\rho}_2 \times \underline{F}_2 = I_n\ddot{\alpha} \underline{k} \tag{4}$$

The kinematic relations are

$$\underline{r}_n = \underline{R}_n + \underline{\rho}_2 \tag{5}$$

$$\underline{r}_h = \underline{R}_n + \underline{\rho}_1 + \underline{\rho}_h \tag{6}$$

$$\ddot{\underline{r}}_n = \underline{a}_n = \ddot{\underline{R}}_n + \ddot{\alpha} \underline{k} \times \underline{\rho}_2 - \dot{\alpha}^2\underline{\rho}_2 \tag{7}$$

$$\ddot{\underline{r}}_h = \underline{a}_h = \ddot{R}_n + \ddot{\alpha}\underline{k} \times \underline{\rho}_1 -\dot{\alpha}^2\underline{\rho}_1 + \ddot{\phi}\underline{k} \times \underline{\rho}_h -\dot{\phi}^2\underline{\rho}_h \tag{8}$$

The forces $\underline{F}_1$ and $\underline{F}_2$ can be eliminated from Eqs. (3) and (4) by solving in terms of $\underline{a}_h$ and $\underline{a}_n$ from Eqs. (1) and (2). Then replacing $\underline{a}_h$ and $\underline{a}_n$ results in the differential equations

$$(I_h + m_h\rho_h^2) \ddot{\phi} + m_h\rho_h\rho_1\ddot{\alpha} \cos (\phi-\alpha)$$
$$= -M_1 + m_h\rho_h \left[\ddot{x}_n \cos \phi + \ddot{y}_n \sin \phi -\rho_1\dot{\alpha}^2 \sin (\phi-\alpha)\right] \tag{9}$$

$$m_h\rho_h\rho_1\ddot{\phi} \cos (\phi-\alpha) + (I_n + m_n\rho_2^2 + m_h\rho_1^2) \ddot{\alpha}$$
$$= M_1 -M_2 + m_h\rho_h\rho_1 \dot{\phi}^2 \sin (\phi-\alpha) + (m_h\rho_1 + m_n\rho_2)(\ddot{x}_n \cos\alpha + \ddot{y}_n \sin \alpha)$$
$$\tag{10}$$

The acceleration components at the base of the neck, $\ddot{x}_n$ and $\ddot{y}_n$, are given functions of time. The mass properties and length are anthropometric data that can be measured or estimated from volume measurements

NOTATION (see Figure 15)

I_h — Moment of inertia of head about its center of mass, pound-in-seconds^2.

I_n — Moment of inertia of neck about its center of mass, pound-in-seconds^2.

$\underline{F_1} = N_1 \underline{e_t} - Q_1 \underline{e_\alpha}$ — Force between head and neck, pounds.

$\underline{F_2} = N_1 \underline{e_t} + Q_2 \underline{e_\alpha}$ — Force between neck and shoulders, pounds.

M_1, M_2 — Moments at occipital condyles and moment at T_1 vertebrae, respectively inch-pounds.

m_h, m_n — Mass of head and neck respectively, pounds - second^2/inch.

$\underline{i}, \underline{j}, \underline{k}$ — Right-handed set of unit vectors. $\underline{j}$ is vertical and $\underline{k}$ is out-of-plane of paper.

$\underline{e_t} = -\sin\alpha\, \underline{i} + \cos\alpha\, \underline{j}$ — Unit vector fixed to neck.

$\underline{e_\alpha} = -\cos\alpha\, \underline{i} - \sin\alpha\, \underline{j}$ — Unit vector perpendicular to neck.

ϕ — Angle of head rotation from the vertical (measured from $\underline{j}$ direction), radians.

α — Angle of neck rotation.

ρ_h — Distance from occipital condyles to center of mass of the head, inches.

ρ_1 — Length of neck from T_1 vertebrae to occipital condyles, inches.

ρ_2 — Distance from T_1 vertebrae to center of mass of the neck, inches.

$\underline{\ddot{R}_n} = \ddot{x}_n\, \underline{i} + \ddot{y}_n\, \underline{j}$ — Acceleration of the neck at T_1 vertebrae, inches/second^2.

g — Acceleration of gravity, inches/second^2.

and assumptions on mass density.

The key problem is the constitutive relations that determine the head and neck moments M_1 and M_2

$$M_1 = M_1\ (t,\phi,\dot{\phi},\ddot{\phi},\alpha,\dot{\alpha},\ddot{\alpha})$$

$$M_2 = M_2\ (t,\phi,\dot{\phi},\ddot{\phi},\alpha,\dot{\alpha},\ddot{\alpha})$$

Until these relations are defined, the equations of motion cannot be integrated explicitly.

Several different constitutive relations have been proposed for the head and neck.

Bowman and Robbins (2)* adopted the Maxwell element of a linear spring and a linear viscous damper in series. The spring and damper coefficients are assumed to be linear functions of "the voluntary static moment". This latter moment is not clearly defined. The Maxwell element was proposed by Moffat, Harris, and Haslam (3) based on a study of knee moments. They obtained coefficients for the knee by impressing a sinusoidal motion on the leg and measuring directly the total moment necessary to produce the motion. The resultant moment was split into components and the moment due to the muscles was fit to the Maxwell model using least-squares. In the experiment, a voluntary knee moment was measured for the knee reacting against a foot plate before the test apparatus was set in motion.

In the notation of the present report, the constitutive relations would be

$$\dot{M}_1 + \frac{k_1}{c_1} M_1 = + k_1\ (\dot{\phi}-\dot{\alpha}) \qquad (11)$$

$$\dot{M}_2 + \frac{k_2}{c_2} M_2 = + k_2\dot{\alpha} \qquad (12)$$

where the k_i and c_i coefficients are linear functions of initial muscle tension. This proposed relation has the advantage that the angular velocity and acceleration resulting from an applied impulse do not depend on the initial values of the angles. This independence from initial values seems in agreement with experimental data. However, the Maxwell element responds to any applied moment, no matter how small or slowly applied. This feature does not seem in agreement with experimental observations.

A general linear viscoelastic element similar to the Maxwell element was used in the analysis of whiplash reported by McKenzie and Williams (4). The same type of viscoelastic elements are included in the analytical neck simulation of Melvin, McElhaney, and Roberts (5). The linear viscoelastic element was first assumed by Orne and Liu (6) as constitutive relations for intervertebral discs in their mathematical model for spinal response to axial impact simulating the pilot ejection problem.

---

* Number in parentheses refer to list of references.

The linear viscoelastic model would assume the relations

$$M_1 + p_1\dot{M}_1 = q_{o1} \left[\phi-\alpha-\phi(o) + \alpha(o)\right] + q_{11} \left[\dot{\phi}-\dot{\alpha}\right] \tag{13}$$

$$M_2 + p_2\dot{M}_2 = q_{o2} \left[\alpha-\alpha(o)\right] + q_{12}\dot{\alpha} \tag{14}$$

during the normal range of motion. Stops would be included in the mathematical model to limit the angular motion. The linear spring constants q_{oi} multiplying angular displacement is certainly inappropriate for simulating the effect of muscles for quasi-static loadings.

The constitutive relations actually used in the present study were

$$M_1 = \left[C_1 + D_1 \ (\phi-\alpha)^{n_1}\right] m_h g \qquad (\dot{\phi}-\dot{\alpha})>0, \ (\phi-\alpha)>0 \tag{15a}$$

$$M_2 - M_1 = \left[C_2 + D_2\alpha^{n_2}\right] m_h g \qquad \dot{\alpha} > 0 \tag{15b}$$

$$M_1 = -C_1 m_h g \quad (\dot{\phi}-\dot{\alpha})<0 \tag{15c}$$

$$M_2 - M_1 = \left[-C_2 + D_2\alpha^{n_2}\right] m_h g \qquad \dot{\alpha}<0 \tag{15d}$$

The equations are scaled by head weight, $m_h g$. The equations are designed to represent flexion such as produced by the sled accelerations in the experiments described in Ref. (1). The constant terms C_1 and C_2 oppose the angular motion no matter in which direction the head is moving, in the same manner as Coulomb (solid) friction. The nonlinear springs are assumed to have large positive exponents, n_1 and n_2, so that these hard spring terms become significant near the limits of voluntary motion and act effectively as stops. For hyperextension or whiplash problems, Eqs. (15c) and (15d) would need to be modified to include similar stops for negative values of the head and neck rotation. Also, since the neck is not as strong in extension as it is in flexion, the constants C_1 and C_2 should be replaced with different values when the neck is extending. This point is discussed further in the results section of this report.

As pointed out recently by Soechting and Paslay (7), there will be a response time before the muscles can react to resist the motion. The algebraic sign associated with the constant terms C_1 and C_2 should depend on angular velocities at $(t-\tau)$ where τ is a neural delay time rather than at the current value of time to t. This delay time is on the order of .1 second for the stretch reflex of relaxed arm muscles. The reaction time of the neck muscles of human subjects expecting an acceleration pulse is not known, however, if it is on the order of 100 msec, this delay time could be a significant fraction of the total time for the event. One way of measuring this effect on volunteers would be to reproduce constant acceleration levels with different onset rates.

A logical modification of the constitutive relations in Eqs. (15) is to include a delay time. However, the results presented later do not contain this effect.

Aside from differences in the assumed form of the constitutive

relations in biomechanics, there is general agreement that experimental data are lacking to fix the values of the constant parameters that appear in the equations. "Appropriate parameter values for the neck are not available in the literature, but Moffat, Harris and Haslam (9) give experimentally determined values for the knee joint. These values were used following application of appropriate scaling procedures using other available experimental data to obtain rough, order-or-magnitude values for corresponding neck quantities."*

"In particular, it should be noted that the values of the material properties governing the viscoelastic behavior of the intervertebral discs were those used by Orne and Liu (1971). These authors found that a wide range and combination of material parameters had little effect on the magnitude of the peak force response."**

". . . muscle and neural feedback parameters are difficult to obtain. The time constant D appears to be reasonably well established, however, values for the muscle spring constant K and the feedback parameter C have been determined only for isolated sets of muscles."***

In addition to the lack of data, the usefulness of certain basic studies, e.g., Ref. (3) and Ref. (10), has been impaired by the authors fitting the results to a mathematical model rather than presenting the raw data. There is no objection to trying to analyze data, but it should not be at the expense of obscuring the basic measurements.

Since there is a lack of data on proper parameters for constitutive relations for muscles and joints, it seems necessary to adopt an indirect apprcach. This approach consists of formulating the theoretical model and then adjusting the parameters to fit the data of tests such as Ref. (1). If the theory is consistent, the known parameters can be used to predict responses to sets of applied forces different from the test data. This approach is commonly used in mechanics; in a particular example in biomechanics, Melvin, McElhaney, and Roberts, Ref. (5), fit their mathematical model to the tests of Mertz and Patrick (11).

The main aim of the present study has been to develop a systematic method for arriving at the parameters in the constitutive equations so that the theory fits the experimental data of Ref. (1). The result has been a computer program that automates the search for parameters that fit the data. The program is an improvement over varying different parameters in a random fashion and comparing the resulting motion to the experimental results. As will be shown, the current version of the program is probably not an optimum algorithm in terms of computer time, and in some cases, the search procedure does not converge. However, the progress thus far has shed important light on the interpretation of the experimental results of Ref. (1) and could serve as a guide in conducting

---

* Ref. (2) Bowman and Robbins

** Ref. (4) McKenzie and Williams

*** Ref. (7) Soechting and Paslay

future experiments. The theoretical results to date have also suggested improvements in the analytical model.

The estimation of parameters in the constitutive relations is treated by finding the effect of varying each parameter by Newton's method, Ref. (12) and Ref. (13). The variation in each parameter is computed by a least-squares fit of the experimental data. This method of estimation theory has been used for process dynamics in chemical engineering by Lee, Ref. (14), and others. Bellman, Ref. (15), describes other applications, but the method does not seem to be in common use for the biomechanics of human motion.

The procedure is an iterative one. First, a trial set of parameters is assumed along with the initial conditions and the rest of the data to solve the nonlinear equations of motion, Eqs. (9) and (10), for $\phi = \phi_o(t)$ and $\alpha = \alpha_o(t)$. This initial solution is calculated in the computer program by a Runge-Kutta subroutine. The next step is to compute the effect of a change in each parameter by means of a Taylor series expansion about the initial solution, $\phi_o(t)$ and $\alpha_o(t)$.

$$\phi = \phi_o + \delta\phi \tag{16a}$$

$$\alpha = \alpha_o + \delta\alpha \tag{16b}$$

Before the integration of the initial solution was programmed, the equations of motion were normalized by dividing through by the mass of the head, m_h. The constitutive relations are scaled by dividing the moments by the weight of the head, $m_h g$, as indicated in Eqs. (15). The expansion in the parameters is then of the form

$$\frac{M_1}{m_h} = \frac{M_1^{(o)}}{m_h} + \frac{\delta M_1}{m_h} \tag{17}$$

where

$$\frac{M_1^{(o)}}{m_h} = g\left[C_1^{(o)} + D_1^{(o)}(\phi_o - \alpha_o)^{n_1}\right] \qquad (\dot{\phi}_o - \dot{\alpha}_o) > o, \ (\phi - \alpha) > o$$

$$\frac{\delta M_1}{m_h} = g\left\{\delta C_1 + \delta D_1 (\phi_o - \alpha_o)^{n_1} + n_1 D_1 (\phi_o - \alpha_o)^{n_1 - 1} (\delta\phi - \delta\alpha) + \delta n_1 \left[\ln(\phi_o - \alpha_o)\right] (\phi_o - \alpha_o)^{n_1}\right\}$$

etc.

Note that the expansion is truncated at first order terms in the corrections. For example, the term $D_1(\phi - \alpha)^{n_1}$ is expanded $(D_1^{(o)} + \delta D_1)$

$$(\phi_o + \delta\phi - \alpha_o - \delta\alpha)^{n_1 + \delta n_1} = D_1^{(o)}(\phi_o - \alpha_o)^{n_1} + \delta D_1(\phi_o - \alpha_o)^{n_1} + D_1(\phi_o - \alpha_o)^{n_1 - 1}$$

$(\delta\phi - \delta\alpha) + \delta n_1 \ln(\phi_o - \alpha_o)\ (\phi_o - \alpha_o)^{n_1} + \ldots$ and quadratic and higher terms in the corrections and their products are dropped. Similarly, in substituting Eqs. (16) into the equations of motion, only linear terms

are retained, such as

$$\dot{\phi}^2 \sin(\phi-\alpha) = \dot{\phi}_o^2 \sin(\phi_o-\alpha_o) + 2\dot{\phi}_o\delta\dot{\phi} \sin(\phi_o-\alpha_o) + \dot{\phi}_o^2 \cos(\phi_o-\alpha_o)(\delta\phi-\delta\alpha)$$

The resulting "variational" equations of motion can be written as

$$L_{11}(\delta\phi) + L_{12}(\delta\alpha) = \sum_{i=1}^{6} g_{1i}(\phi_o,\alpha_o)\delta C_i \qquad (18a)$$

$$L_{21}(\delta\phi) + L_{22}(\delta\alpha) = \sum_{i=1}^{6} g_{2i}(\phi_o,\alpha_o)\delta C_i \qquad (18b)$$

where the six subscripted variables δC_i are δC_1, δC_2, δD_1, δD_2, δn_1, and δn_2 in that order. The L_{ij} are second order linear differential operators.

Since Eqs. (18) are linear differential equations, a particular solution $(\delta\phi_i, \delta\alpha_i)$ can be obtained for each term in the series on the right and the results superposed to obtain

$$\phi = \phi_o + \delta\phi = \phi_o + \sum_{i=1}^{6} \delta C_i\ \delta\phi_i \qquad (19a)$$

$$\alpha = \alpha + \delta\alpha = \alpha_o + \sum_{i=1}^{6} \delta C_i\ \delta\alpha_i \qquad (19b)$$

The correction terms $\delta\phi$ and $\delta\alpha$, are linear functions of the δC_i so that the original intent was to use Eqs. (19) in a linear regression function and to compute the δC_i by the method of least-squares using the experimental data of Ref. (1).

Angular accelerations would seem intuitively to be the choice for the linear regression function since the moment terms affect the angular accelerations directly. However, there were problems interpreting the acceleration data. These problems will be discussed in more detail later.

The regression function was programmed to fit the measured angular deflections. The idea was to solve the "normal equations" for the six δC_i, solve Eqs. (19) explicitly for ϕ and α, repeat the iteration with ϕ and α replacing ϕ_o and α_o respectively in Eqs. (16). The iteration continues until the corrections δC_i become small. However, this procedure failed to converge because the matrix of the normal equations was nearly singular. This difficulty took considerable time to overcome because it is not clear what caused the trouble. Are the coordinate functions, $\delta\phi_i$ and $\delta\alpha_i$ in Eqs. (19), linearly dependent? Does the numerical analysis contain truncation and round-off errors that affect the inversion of the normal equations? Is the difficulty a combination of using nearly linearly dependent functions and numerical errors?

Hamming, R. and Feigenbaum (17) explain the situation by saying "It frequently happens that the system of equations does not determine the parameters very accurately. This tends to worry the beginner. The reason they are poorly determined is often that the minimum is broad and rather flat. It is true that the optimum values are then poorly known, but it is also true that whichever set you choose (among those that look good) does not very much affect the value of the function you

were minimizing; thus, the uncertainty does you little harm."

As an example, they cite the linear regression problem using powers of x. They are linearly independent functions; but as the degree of the regression polynomial get larger, the accurate inversion of the normal equations becomes more difficult.

It is not difficult to construct counter examples where the normal equations are actually singular. The simple linear oscillator is a familiar case that illustrates this point. The steps in the numerical solution can be shown explicitly so it makes a good illustrative example. The differential equation

$$m\ddot{x} + kx = 0 \tag{20}$$

governs the motion. Assume that the mass m is given and an experimental curve

$$x_e = A \sin \omega t$$

is available. The problem is to find the spring constant k by Newton's method. In general, the linear variational equations have variable coefficients and can't be solved in closed form, but can be solved numerically.

The procedure is to assume an initial value of $k = k_o$ and seek a correction δk so that $k = k_o + \delta k$ gives an improved approximation to the experimental data. The solution of Eq.(20) for $k = k_o$ is denoted by $x = x_o$. When k is varied by δk the variation in x is δx. Substituting in Eq.(20) gives

$$m(\ddot{x}_o + \delta\ddot{x}) + (k_o + \delta k)(x_o + \delta x) = 0 \tag{21}$$

Dropping the nonlinear term in the variations and using the fact that by definition

$$m\ddot{x}_o + k_o x_o = 0 \tag{22a}$$

$$x_o = A_o \sin \omega_o t \qquad \omega_o^2 = k_o/m \tag{22b}$$

leads to the variational equation

$$m\delta\ddot{x} + k_o\delta x = -\delta k \, A_o \sin \omega_o t \tag{23}$$

The solution of Eq. (23) is

$$\delta x = \frac{A_o}{2\omega_o m} \delta k \; t \cos \omega_o t \tag{24}$$

The current approximation for x is

$$x = x_o + \delta x = A_o \sin \omega_o t + \frac{A_o}{2\omega_o m} \delta k \; t \cos \omega_o t$$

This approximation is compared to the experimental curve x_e by a linear

regression analysis to determine the correction δk

$$\frac{A_o}{2\omega_o m} \delta k \int_o^T t^2 \cos \omega_o t \; dt = \int_o^T (A \sin \omega t - A_o \sin \omega_o t)$$

$$t \cos \omega_o t \; dt \qquad (25)$$

The integrals in Eq. (25) depend on the upper limit T, but the leading term for δk does not.

$$\delta k = 2\omega_o m(\omega-\omega_o) + \ldots \qquad (26)$$

Setting

$$k_1 = k_o + \delta k$$

the iteration can be repeated. In general, equations such as Eqs. (22a), Eq. (23) and Eq. (25) must be integrated numerically. In this simple example, Eq. (26) for the correction on k_o can be checked directly since the solution of the original problem can be written in closed form.

$$\omega^2 = \frac{k}{m} = \frac{k_o + \delta k}{m} = \omega_o^2 + \frac{\delta k}{m}$$

$$\delta k = m(\omega+\omega_o)(\omega-\omega_o) = 2m\omega_o(\omega-\omega_o) + m(\omega-\omega_o)^2 \qquad (27)$$

Comparing Eqs. (26) and Eqs. (27) shows that the approximate expression differs from the exact expression by a quadratic term in the error in the current approximation to the angular frequency so that convergence is rapid and the correct value of k is determined easily. However, if the mass m is unknown as well as the spring constant k, the procedure breaks down. Varying both m and k results in an expression for the variation in x as

$$\delta x = \frac{A_o}{2\omega_o m_o} \delta k \, t \cos \omega t - \frac{A_o \omega_o}{2m_o} \delta m \, t \cos \omega t$$

The pair of linear normal equations equivalent to Eq. (25) are obviously singular. In the closed form solution, it can be seen that the ratio k/m is a single independent parameter and the singular normal equations reflect this.

The mass of the head m_h is used to normalize Eqs. (9), (10), and (15) so that this particular variable is not redundant in the analysis of head and neck motion. In the example of the linear oscillator, the rank of the matrix of the normal equations is one or one less than the number of variables when the mass and spring constant are both varied. During the checkout of the computer program for head and neck motion, different sub-matrices of the normal equations were inverted to see if sub-sets of the six parameters could be varied independently. In some cases, they could and in others, the sub-matrices were also nearly singular. The final version of the computer program varies only one parameter at a time, however, the possibility of varying more than one

but less than six in a systematic fashion is a possible variation of the program.

Before leaving the example of the linear oscillator, another feature of that solution should be mentioned. The particular solution, Eq. (24), of the variational equation grows linearly with time. This linear growth affects the convergence of the normal equations, Eq. (25), if the interval of integration T is larger than several cycles. This nonuniform convergence can be avoided if a weighting factor t^{-2} is introduced in the error analysis. A weighting factor of t^{-1} was introduced arbitrarily in the regression analysis for the head and neck but it did not improve the convergence and was subsequently removed. All variational equations do not have particular solutions with amplitudes that grow linearly with time so that this feature of autonomous systems with periodic solutions is not always present, Ref. (18).

Another possible source of error was checked. The six solutions of Eqs. (18) are assumed to be particular solutions. However, since the differential equations are solved numerically, it is possible to pick up an unstable homogeneous solution as part of the numerical solution. If the homogeneous solution is dominant, this will affect the linear independence of the six solutions used in the regression analysis. A seventh homogeneous solution of Eqs. (18) was computed numerically for nonzero initial conditions. The six particular solutions were made orthogonal to the homogeneous solution. The resulting six solutions were essentially unchanged so that this check was also removed from the program.

The conclusion from the checks run on the program is that the results are insensitive to the six parameters in the sense that more than one combination of parameters will give virtually the same response curve. This conclusion was also reached by Orne and Liu, Ref. (6), for their viscoelastic model of the spine. The current version of the computer program varies one parameter at a time. The parameter that is varied is computed in the analysis. A regression analysis is run for the effect of the variation of each parameter while the others are held constant and the fractional change of each parameter computed. The parameter with the smallest change based on the linear analysis is selected to be changed. If the fractional change is less than a small input number, the parameter with the next smallest fractional change is varied. The iteration is continued until all the changes are less than the tolerance number or until an iteration counter is exceeded. The results are then printed and plotted.

V. RESULTS

Typical results are plotted in Figures 16-45. Each computer run generates five graphs. The runs are identified by the subject number and peak acceleration from Ref. (1) and by the six parameters, C_1, D_1, n_1, C_2, D_2 and n_2, that appear in the constitutive relations, Eqs. (15). The first two plots show the head rotation and neck rotation as a function of time. These are the two variables in the regression analysis that are fitted to the experimental data of Ref. (1). The experimental points used as input to the program are also plotted. The experimental data in Ref. (1) extends over a longer time period than the points shown on the plots. It was found that the head rotation reaches a maximum and then rebounds to a more or less constant value. The numerical analysis consistently arrives at the equilibrium condition at a higher angle than experiment. There are at least two possible explanations for this. First, it is known that the neck is stronger in flexion than in extension, Ref. (11). Therefore, the constants in Eqs. (15c) and Eqs. (15d) should be modified for flexion. This would essentially introduce additional parameters which could be used to fit the data on the rebound part of the curve. A more direct way of arriving at these constants would be with hyperextension tests.

The second explanation of the apparent higher strength of the model in extension is that a delay time should be introduced in the constitutive relations, Eqs. (15). The subject must sense the rebound and tense opposing muscles to resist it. Meanwhile, the head continues to rebound until the subject can bring it to rest.

Whichever explanation is valid, the present theory is restricted to flexion in one direction and the curve fitting was done on this part of the curve where the maximum velocities and accelerations occur.

The head moment about the occipital condyles and the neck moment about T_1 are the third and fourth plots. These are normalized by division by the head weight so that the units on the plots are inch-pounds per pound. An average head weight is about 10 pounds; to convert the plotted values for this weight to foot-pounds, multiply by 10/12. These computed values of the moments shown in the plots are in good agreement with measured dynamic and static moments reported in the literature.

The last graph is the computed resultant acceleration of the center of gravity of the head. This plot shows a peak acceleration on the order of twice the peak sled acceleration.

It was intended to do the regression analysis on the measured head accelerations, but the experimental data from Ref. (1) show two peaks in the acceleration curve. The two relative maxima are approximately the same magnitude. A typical experimental plot is shown in Fig. 6 of this report.

The first acceleration peak is not as pronounced in the analytical

results and is of much lower magnitude than the experimental result. The agreement between the theory and experiment is better for the second peak. The computed amplitude is consistently lower, but the discrepancy between theory and experiment is less than for the first peak.

As mentioned earlier, the analysis uses the sled acceleration as input for the neck acceleration since the neck acceleration data were not readily available. It seems likely that the peak acceleration at the neck of the experimental subjects was considerably higher than the peak sled acceleration and occurs later in time. The elasticity and slack in the shoulder harness and torso which transmit the acceleration from the sled to the upper torso act to prevent the neck from having an identical acceleration with the sled.

The one figure of raw data in Ref. (1), Figure DP-4,, tends to support this assumption. Shulman, et.al., Ref. (20), measured a time lag between the beginning sled and subject accelerations for negative vertical acceleration of a seated pilot.

The analytical model does not have an axial degree-of-freedom. The slow motion film of one of the tests reported in Ref. (1) shows an apparent stretching of the neck. An acceleration in this mode could be an alternate explanation of the first acceleration peak exhibited by the experimental data. However, the computed stretching of the neck plotted in Ref. (1) does not indicate that this is a significant variable.

Whatever the explanation for the first acceleration peak in the experimental data, it would be desirable to have the neck acceleration data to use as input data for the computer program rather than the sled accelration.

The plots in this report are based on data for subjects 3 and 10 from Ref. (1). For subject 3, the constants in the constitutive relation were computed by the computer program for each sled acceleration level. For subject 10, the constants were computed by the regression analysis for the 7.1g sled acceleration. As a check on the theory, the other runs on subject 10 were made with the same constants.

The poorest agreement between theory and experiment is for subject 3 at 9.5 g acceleration. It is not apparent whether different initial choices of the six constants in the constitutive relations would improve the regression analysis or whether the limitations in the input data and the theory that have been discussed earlier are more pronounced at higher acceleration levels.

In summary, the results thus far are encouraging. They support the assumption of this report and of other investigations that the neck muscles affect the head motion at survivable acceleration levels. A "solid friction" type of constitutive relation for the moments fits the experimental data as well as the viscoelastic models found in the

literature, although a delay time should be added to the theory to allow for the reaction time of the subject.

VI. LIST OF REFERENCES

1. Ewing, C. L. and Thomas, D. J., "Human Head and Neck Response to Impact Acceleration," NAMRL Monograph 21, Naval Aerospace Medical Research Laboratory, August, 1972.

2. Bowman, B. M. and Robbins, D. H., "Parameter Study of Biomechanical Quantities in Analytical Neck Models", Proceedings of 16th. Stapp Car Crash Conference, SAE, New York, N.Y. pp. 14-44.

3. Moffatt, C. A., Harris, E. H., and Haslam, E. T., "An Experimental and Analytic Study of the Dynamic Properties of the Human Leg", Journal of Biomechanics, Vol. 2, 1969, pp. 373-387.

4. McKenzie, J. A. and Williams, J. F., "The Dynamic Behavior of the Head and Cervical Spine During 'Whiplash', "Journal of Biomechanics, Vol. 4., 1971, pp. 477-490.

5. Melvin, J. W., McElhaney, J. H. and Roberts, V. L., "Improved Neck Simulation for Antropometric Dummies", Proceedings of 16th. Stapp Car Crash Conference, SAE, New York, N.Y. pp. 45-60.

6. Orne, D. and Liu, Y. K., "A Mathematical Model of Spinal Response to Impact," Journal of Biomechanics, Vol. 4, 1971, pp. 49-71.

7. Soechting, J. F. and Paslay, P. R., "A Model for the Human Spine During Impact Including Muscalature Influence," Journal of Biomechanics, Vol. 6, 1973, pp. 195-203.

8. Mains, R. E. and Soechting, J. F., "A Model for the Neuro-Muscular Response to Sudden Disturbances," Journal of Dynamic Systems, Measurement and Control, Vol. 93, 1971, p. 247.

9. Soechting, J. F., Stewart, P. A., Hawley, R. H., Paslay, P. R., and Duffy, J., "Evaluation of Neuro-Muscular Parameters Describing Reflex Motion", Journal of Dynamic Systems, Measurement and Control, Vol. 92, 1971, p. 221.

10. Kazarian, L., "Dynamic Response Characteristics of the Human Vertebral Column," Acta Orthopaedica Scandinavica, Supplementum No. 146, Munksgaard, Copenhagen, 1972.

11. Mertz, H. J. and Patrick, L. M., "Strength and Response of the Human Neck", Proceeding of 15th. Stapp Conference, SAE, New York, N.Y. pp. 207-268.

12. Thurston, G. A., "Newton's Method Applied to Problems in Nonlinear Mechanics," Journal of Applied Mechanics, Vol. 32, Series E, No. 2, 1965, pp. 383-388.

13. Perrone, N. and Kao, R., "A General Nonlinear Relaxation Iteration Technique for Solving Nonlinear Problems in Mechanics," ASME

Paper No. 70-WA/APM-43.

14. Lee, E. S., "Quasilinearization and the Estimation of Parameters in Differential Equations," I and EC Fundamentals, Vol. 7, No. 1, February, 1968, pp. 153-158.

15. Bellman, R., Kagiwada, H., Kalaba, R., "Quasilinearization, System Identification, and Prediction," RAND Corp. RM-3812-PR, August, 1963.

16. Mertz, H. J. and Patrick, L. M., "Investigation of the Kinematics and Kinetics of Whiplash," SAE Transactions, Vol. 76, 1967, paper #670919.

17. Hamming, R. and Feigenbaum, E., "Introduction to Applied Numerical Analysis," McGraw-Hill, 1971.

18. Thurston, G. A., "Floquet Theory and Newton's Method", Journal of Applied Mechanics, Vol. 95, Series E, December, 1973, pp. 1091-1096.

19. Thurston, G. A., Fay, R., and Rowell, G., "Analytical and Experimental Evaluation of a Pilot Chin-Airbag System" Report of Office of Naval Research Contract No. N00014-67-A-0394-003, University of Denver, April, 1972.

20. Schulman, M., Critz, G., Highly, F., and Hendler, E., "Determination of Human Tolerance to Negative Impact Acceleration," U.S. Naval Air Engineering Center, Aerospace Crew Equipment Laboratory, Report NAEC-ACEL-510, 1963.

VII. APPENDIX

Certain anthropometric data is necessary as input data for the computer program. These numbers were not readily available for the subjects of Ref. (1). One set of assumed data was used for all the calculations. The numerical values are the following:

$(I_h/m_h) + \rho_h^2 = 16.18\ m^2$, $(I_n+m_n\rho_2^2)\ /\ m_h = 2.66\ in^2$

$\rho_h = 3.0$ in., $\rho_1 = 4.5$ in., $\rho_2 = 2.25$ in.,

$m_n/m_h = .318$

VIII. ACKNOWLEDGEMENT

The authors wish to acknowledge the helpful discussions with Drs. N. Perrone and K. Saczalski of the Office of Naval Research during the course of the contract. Mr. M. Chaszeyka of the ONR Branch Office in Chicago also reviewed the work in progress.

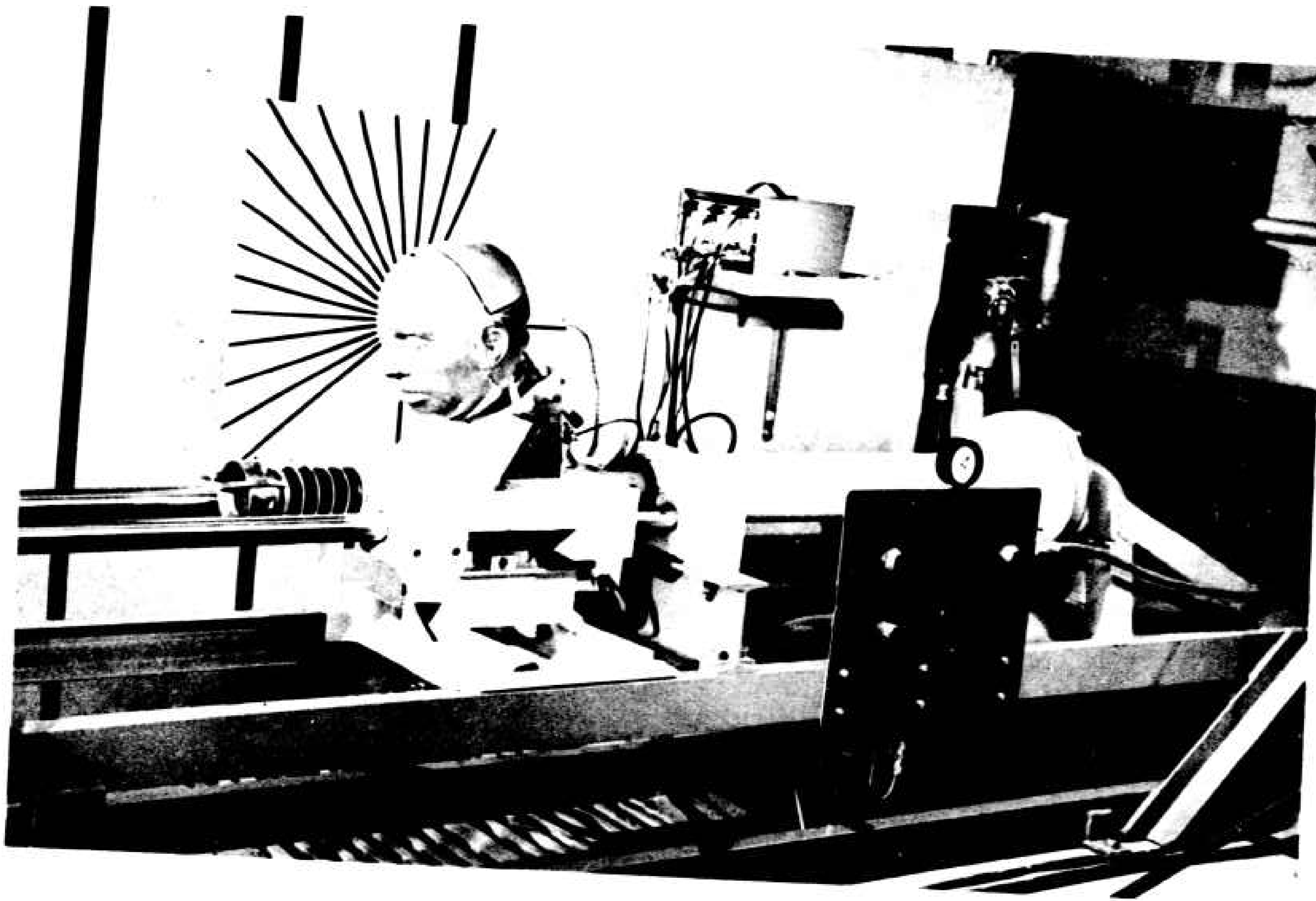

Figure 1
Test sled and launching system

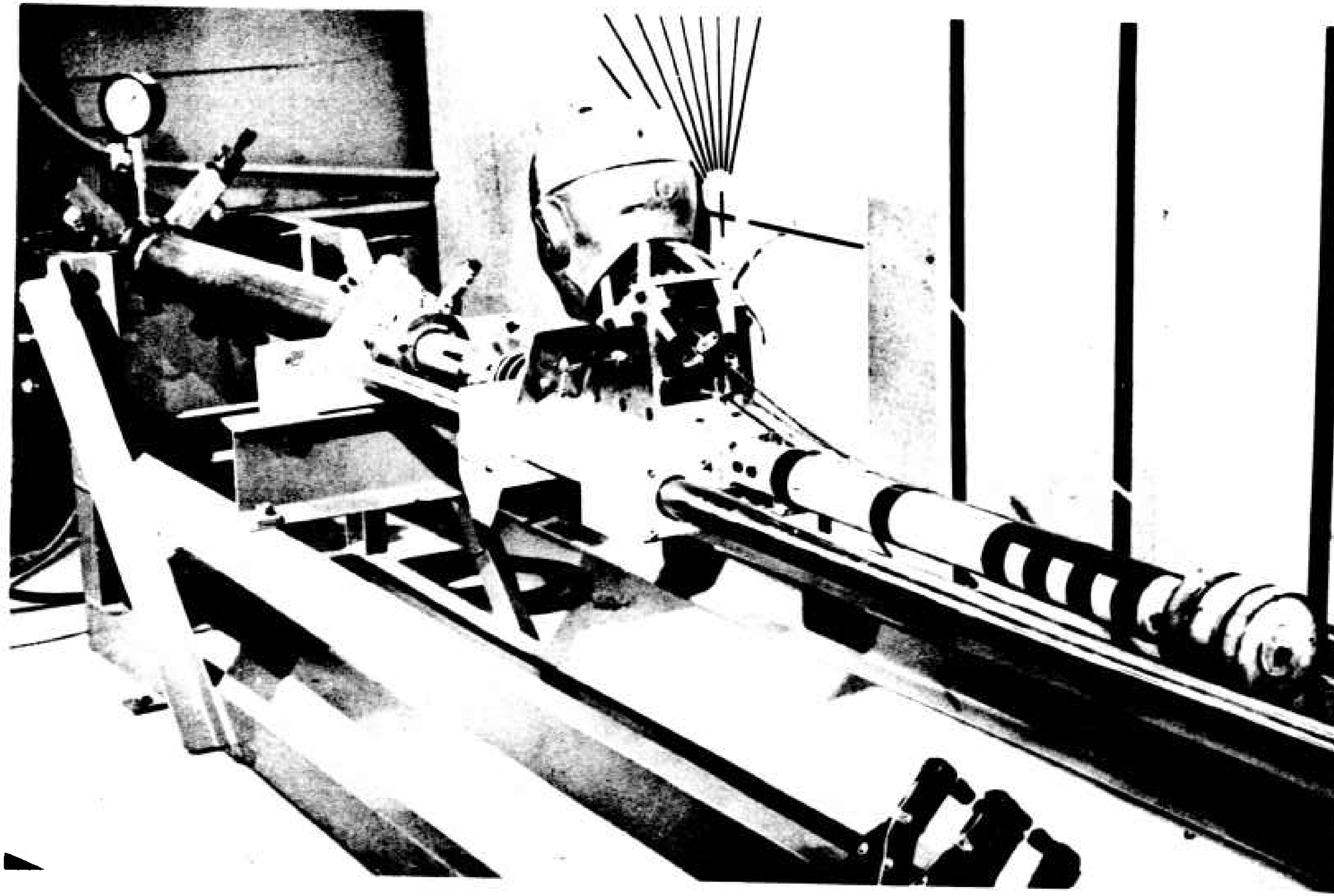

Figure 2
Test sled and snubbing system

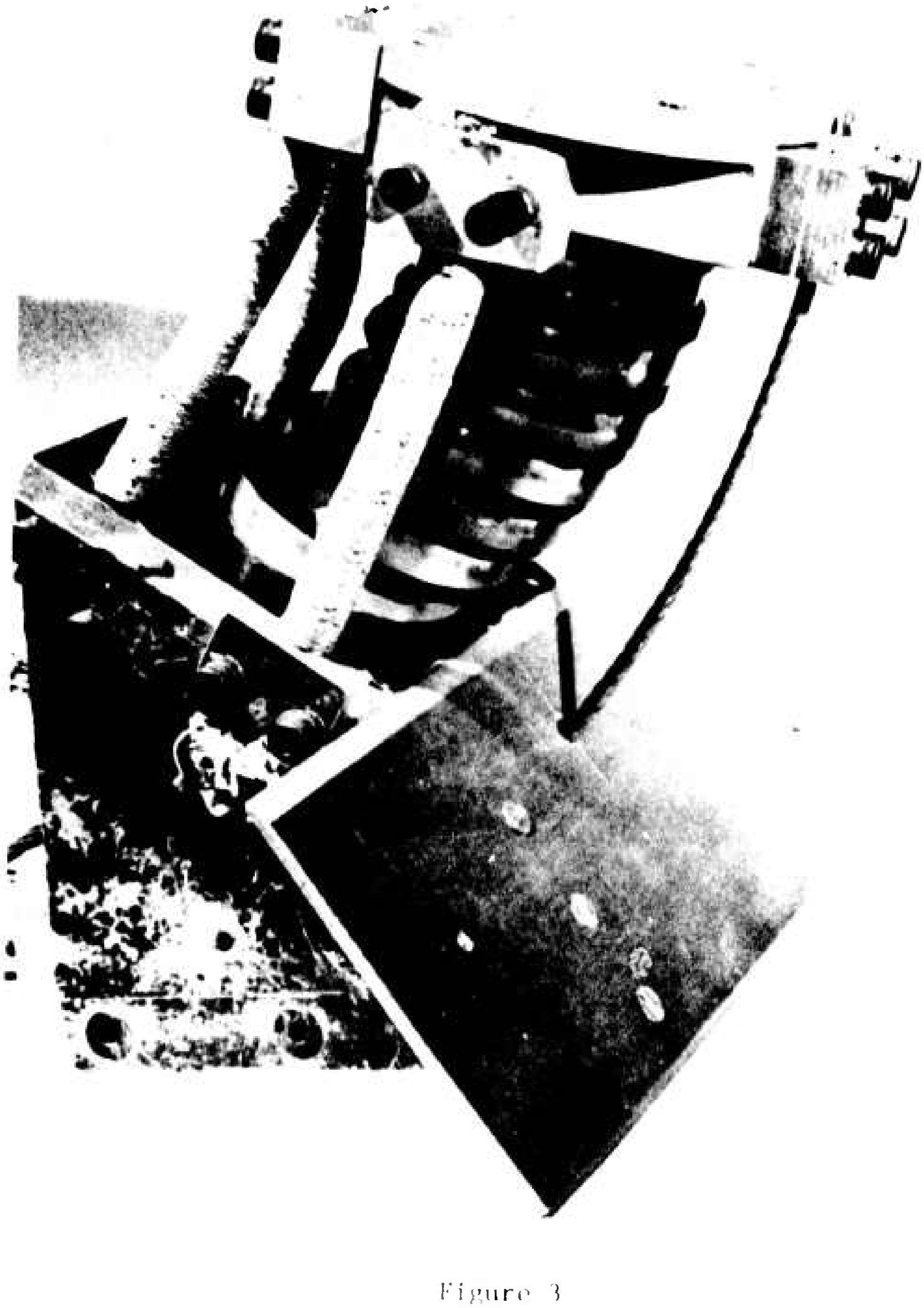

Figure 3
Mechanical neck assembly

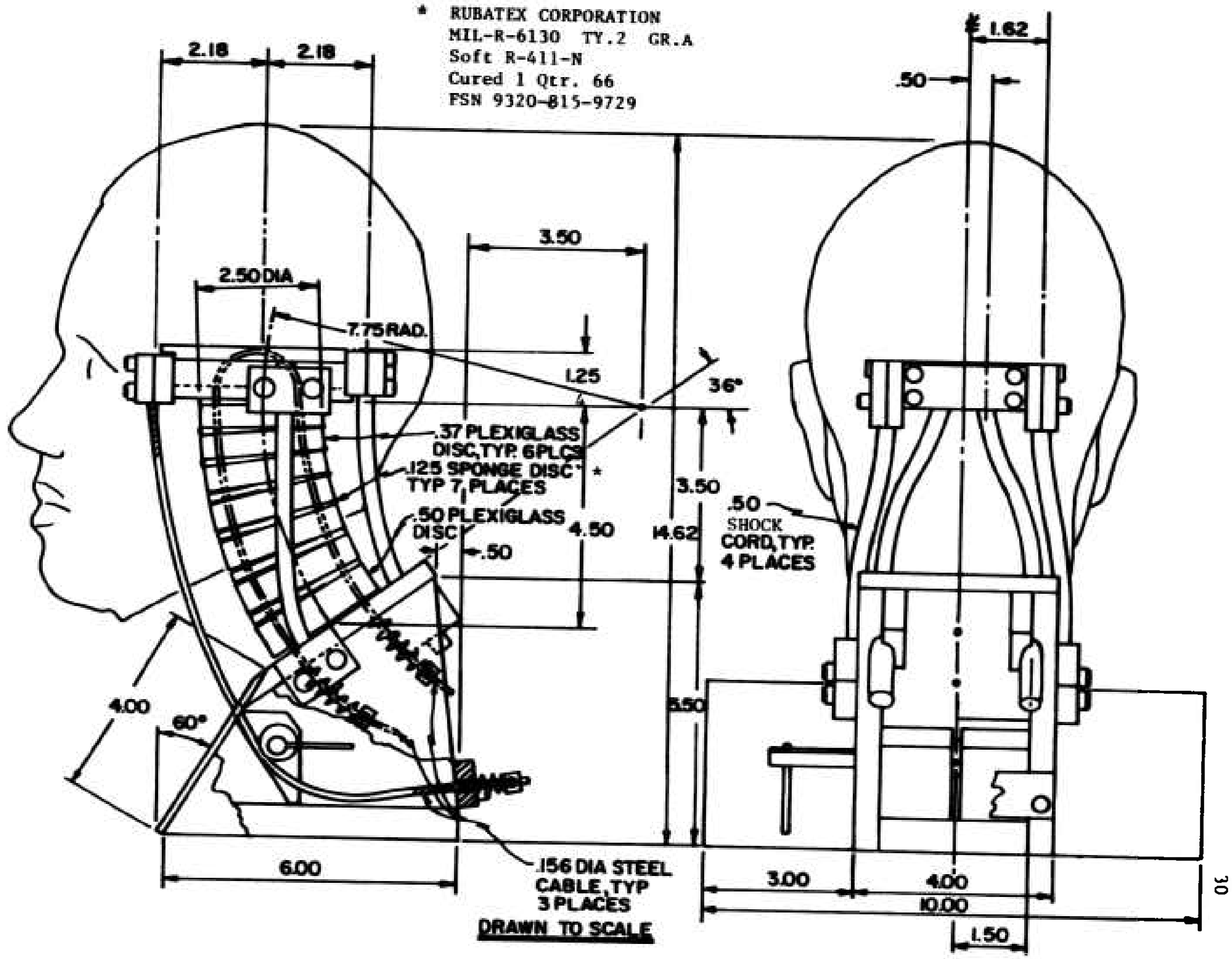
* RUBATEX CORPORATION
MIL-R-6130 TY.2 GR.A
Soft R-411-N
Cured 1 Qtr. 66
FSN 9320-815-9729
2.18
2.18
2.50 DIA
7.75 RAD.
3.50
1.25
36°
.37 PLEXIGLASS DISC, TYP. 6 PLCS
.125 SPONGE DISC * TYP 7 PLACES
.50 PLEXIGLASS DISC
.50
4.50
3.50
14.62
5.50
.50 SHOCK CORD, TYP. 4 PLACES
4.00
60°
6.00
.156 DIA STEEL CABLE, TYP 3 PLACES
DRAWN TO SCALE
1.62
.50
3.00
4.00
10.00
1.50
30

FIGURE 4

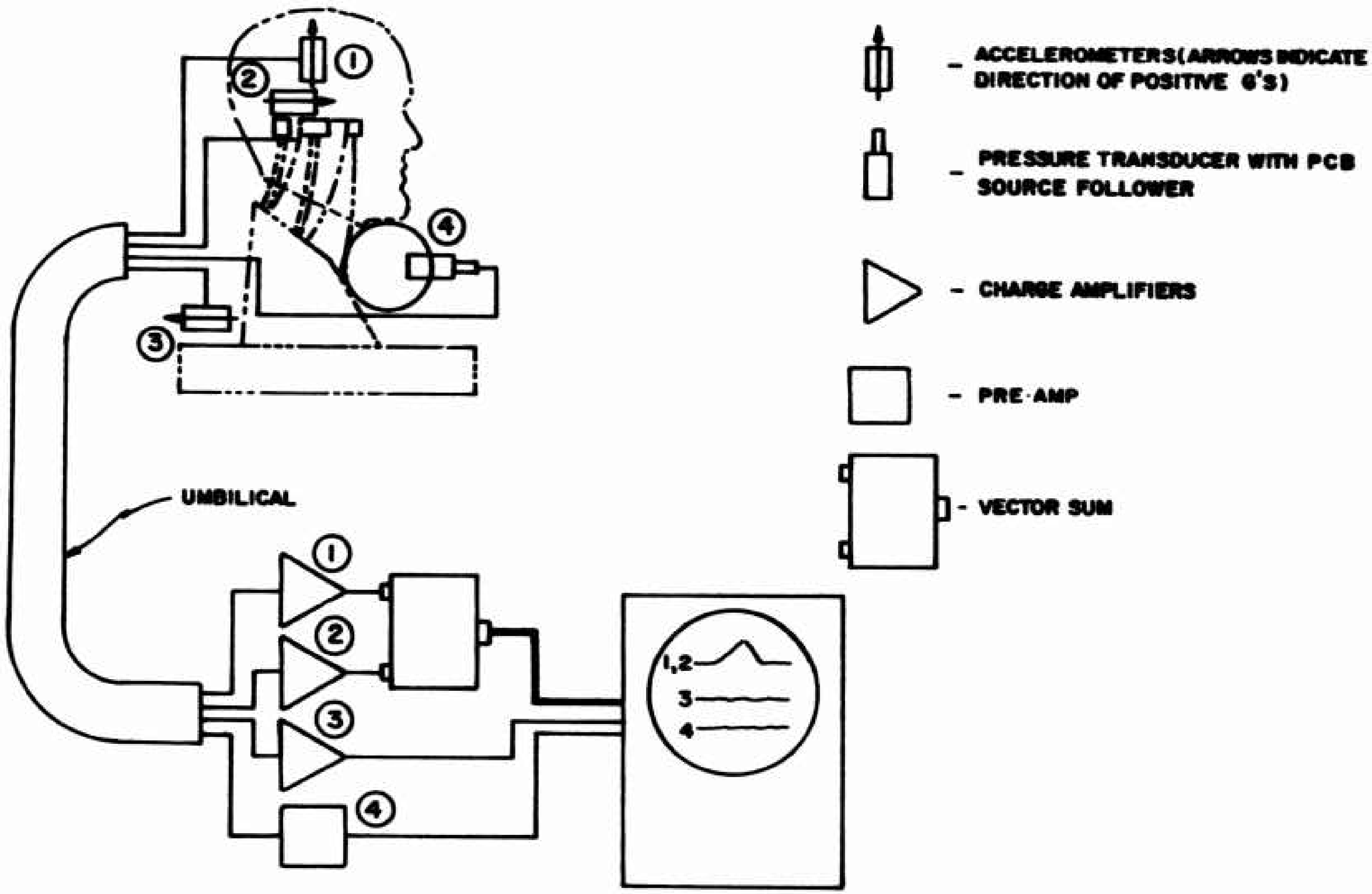

FIGURE 5
Instrumentation schematic

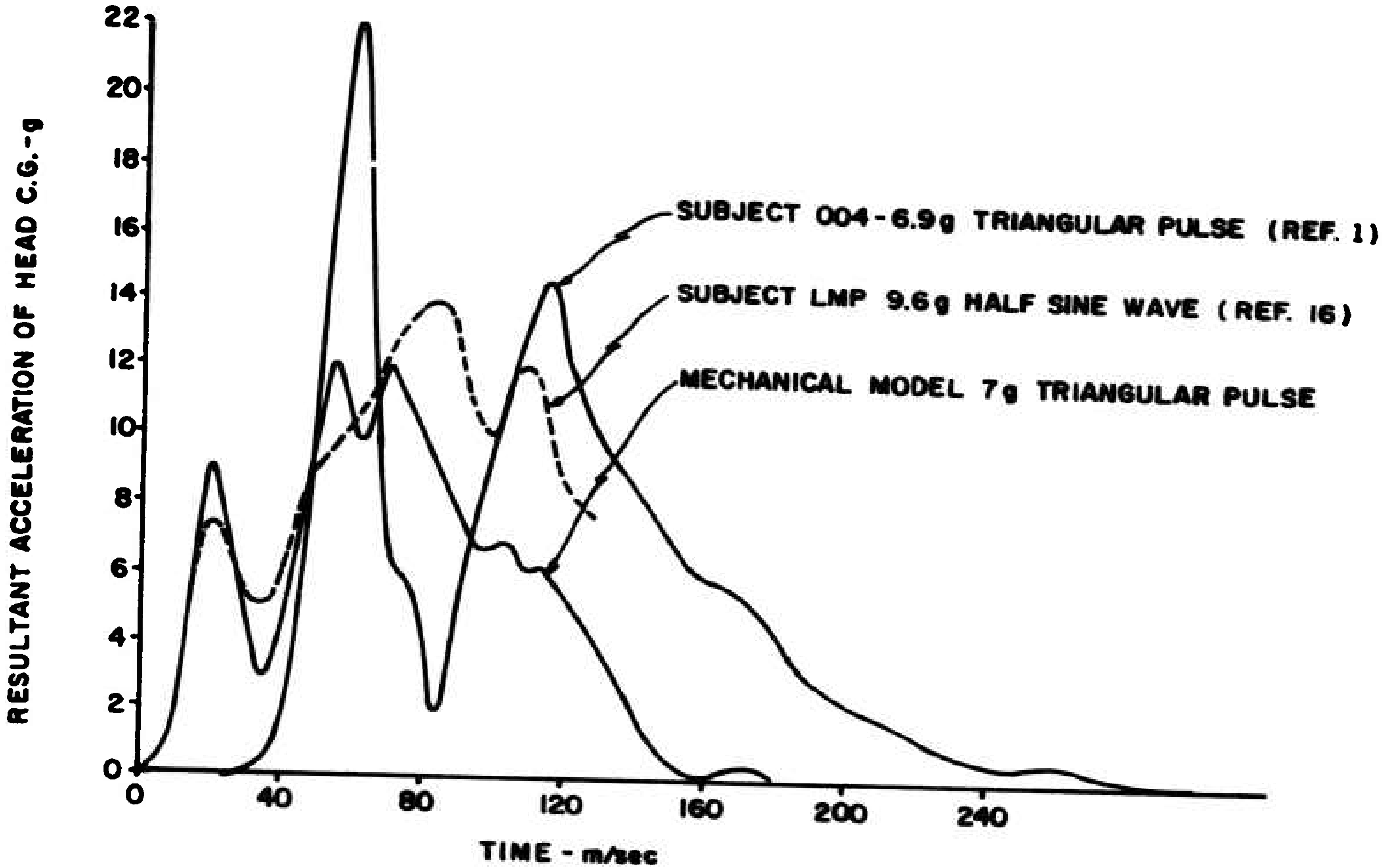

FIGURE 6. Resultant head acceleration of model and live subject with neck base impulse of Figure 7.

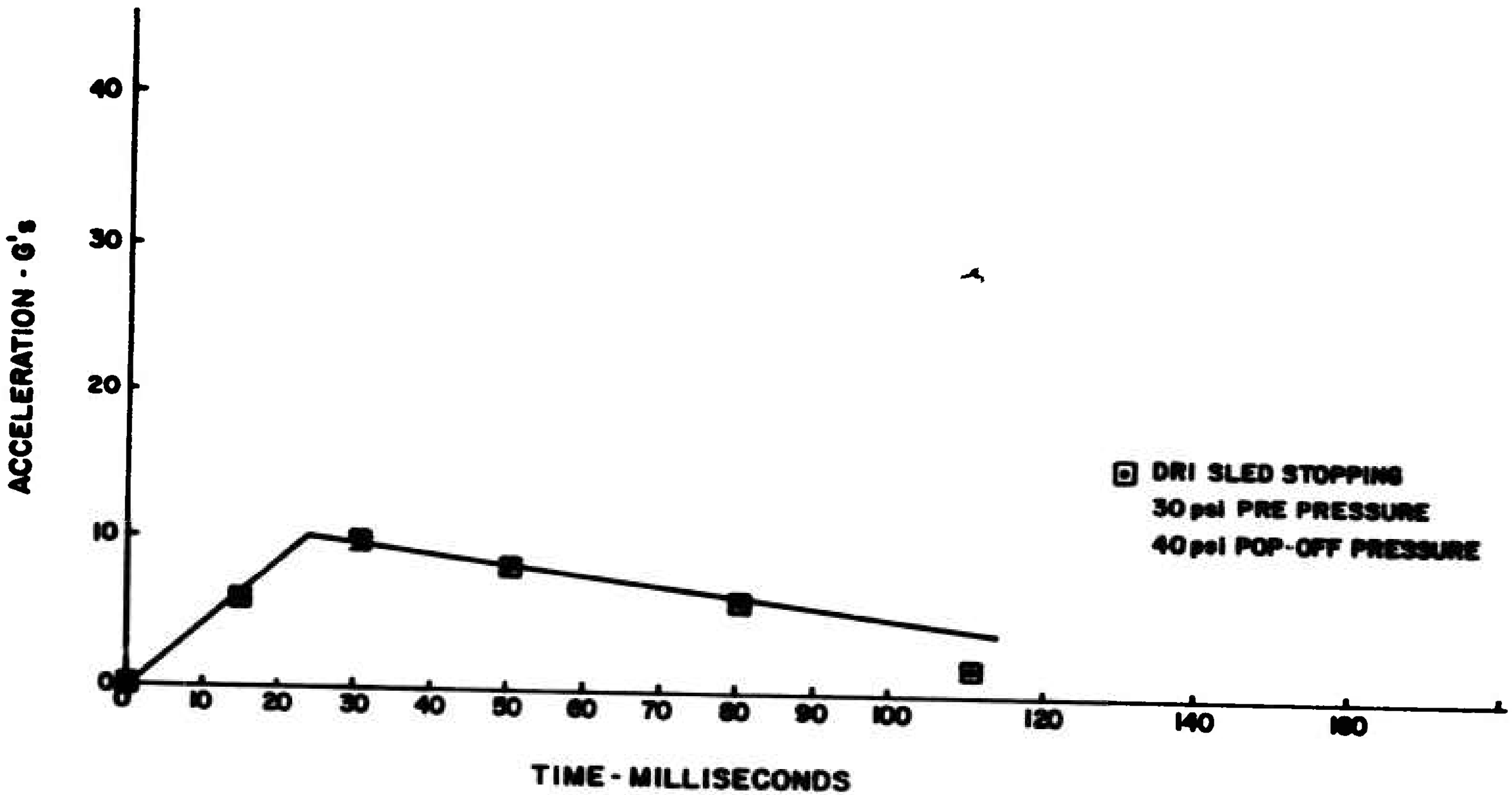

FIGURE 7. Plot of acceleration impulses on base of model and human necks.

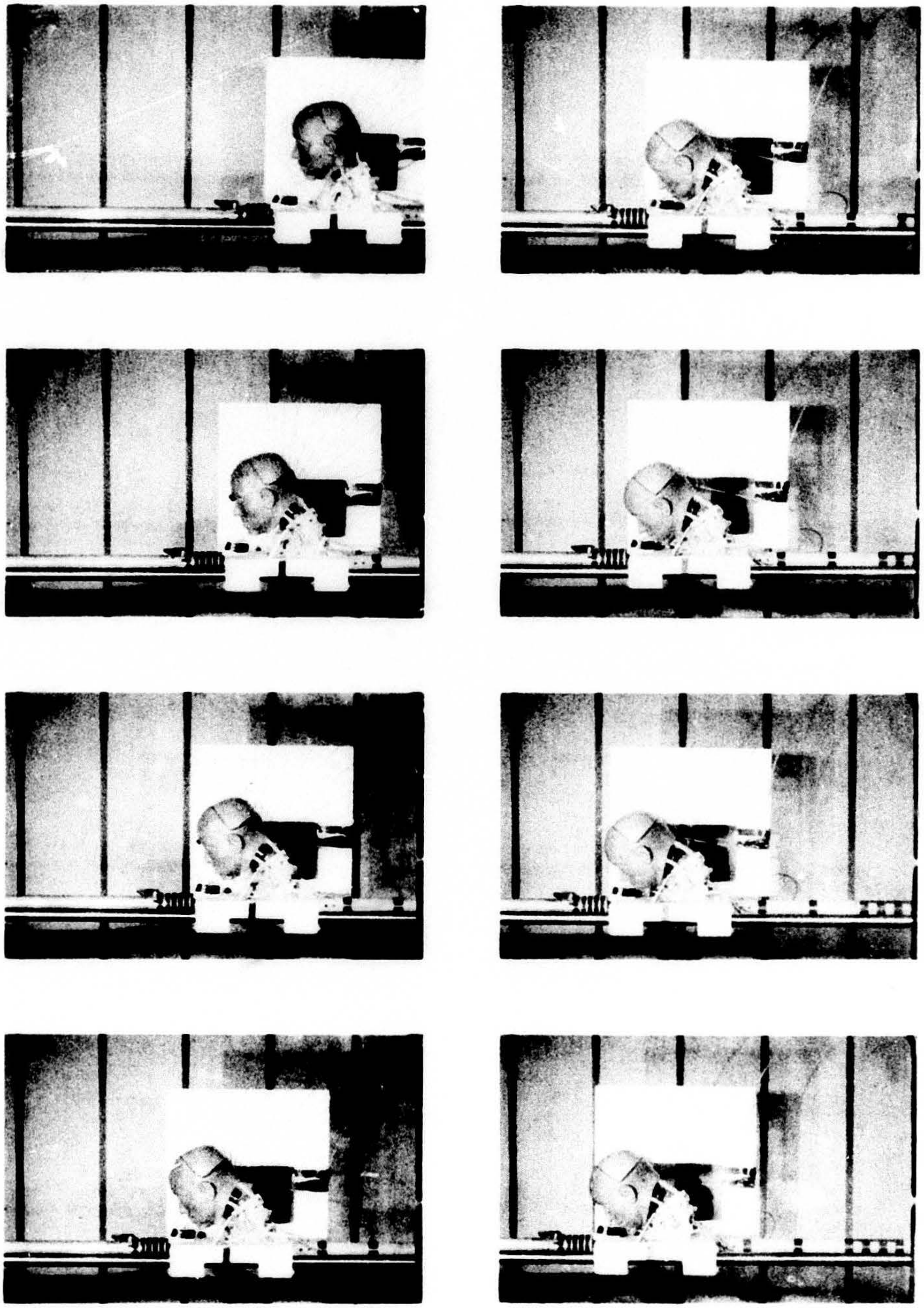

FIGURE 8

High Speed Film Sequence of Model Test

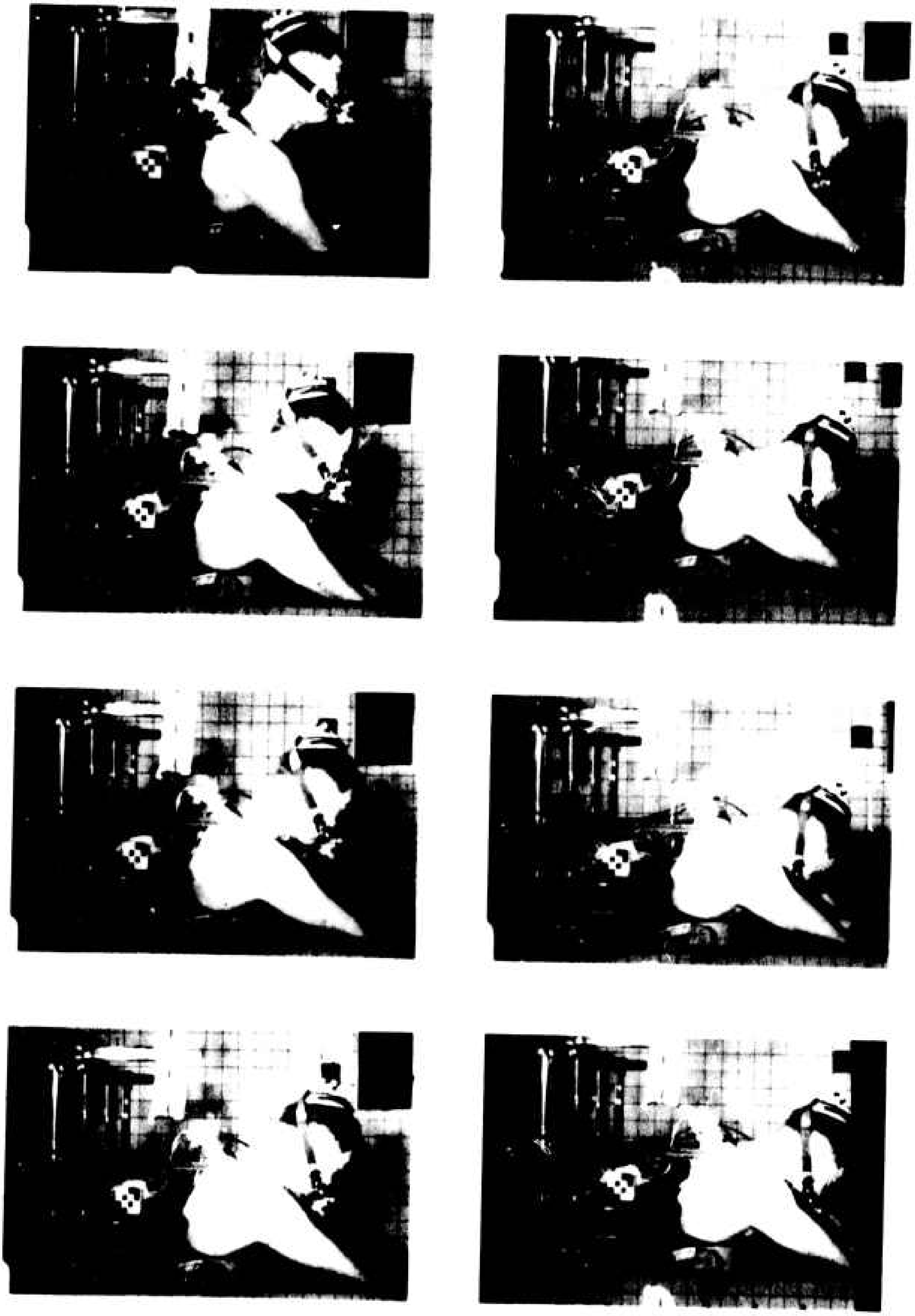

FIGURE 9
High speed of film sequence of live subject on sled (See Ref. 1, Subject 04, 7 g test).

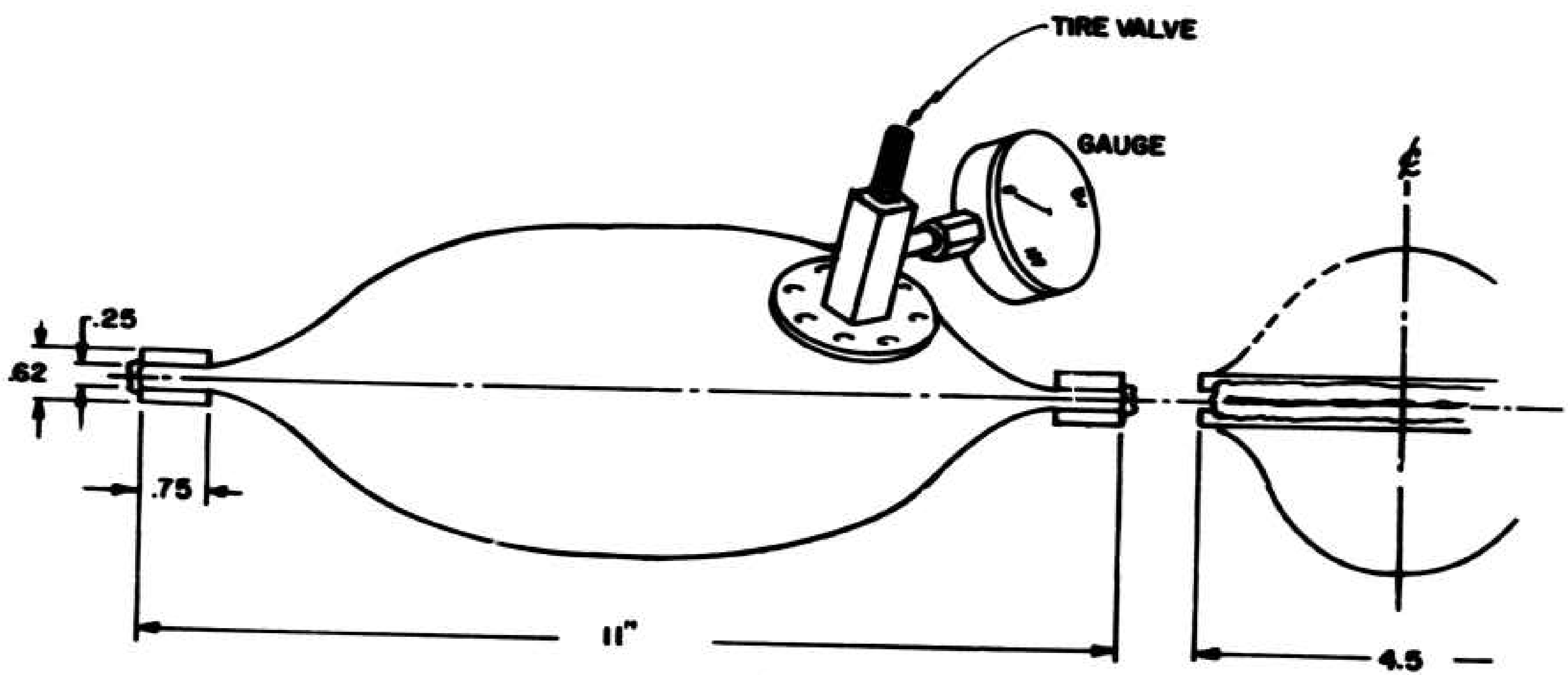

FIGURE 10. Chin Bag

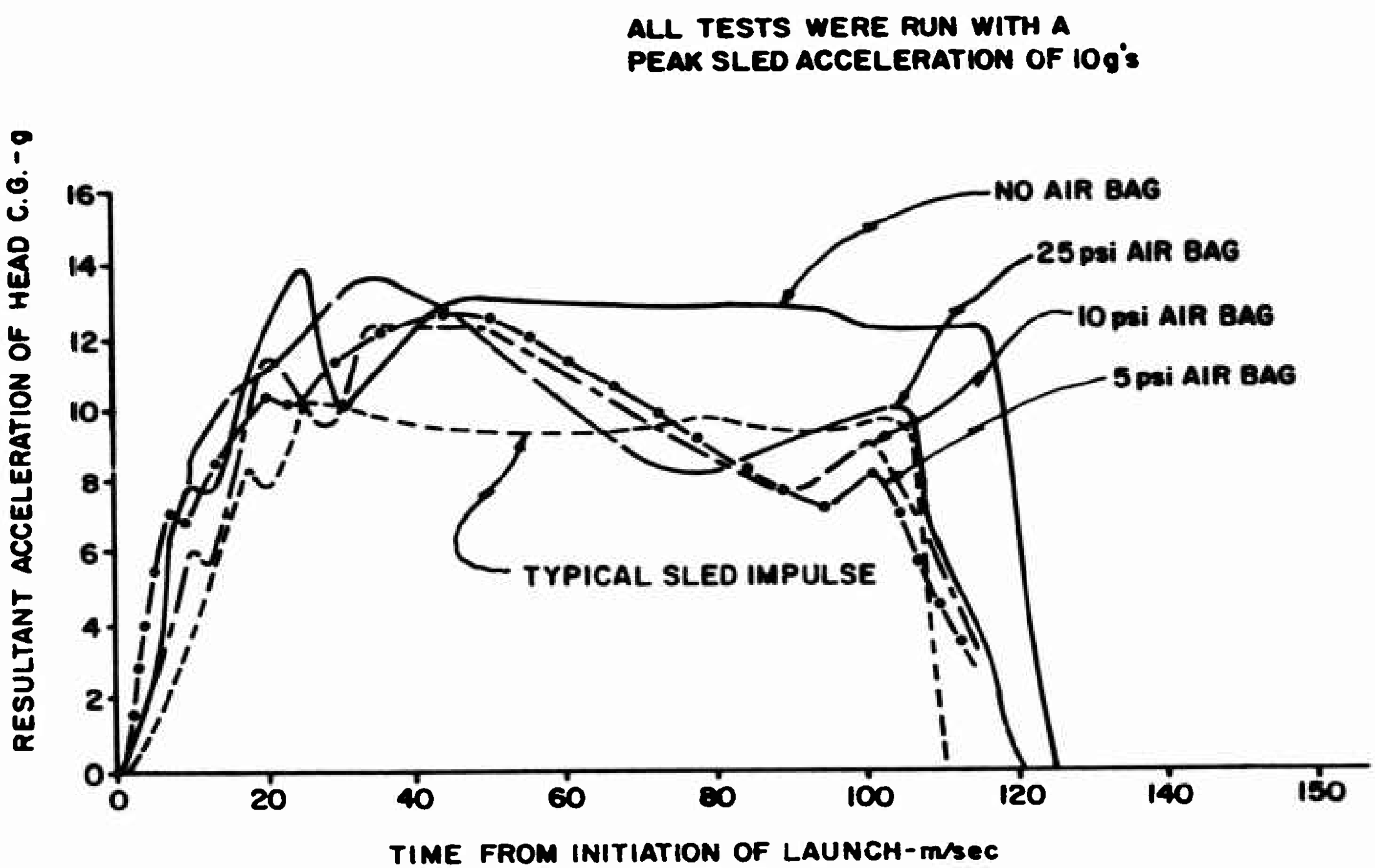

FIGURE 11
Resultant head acceleration of model with and without chin bag; 10 g square wave sled impulse.

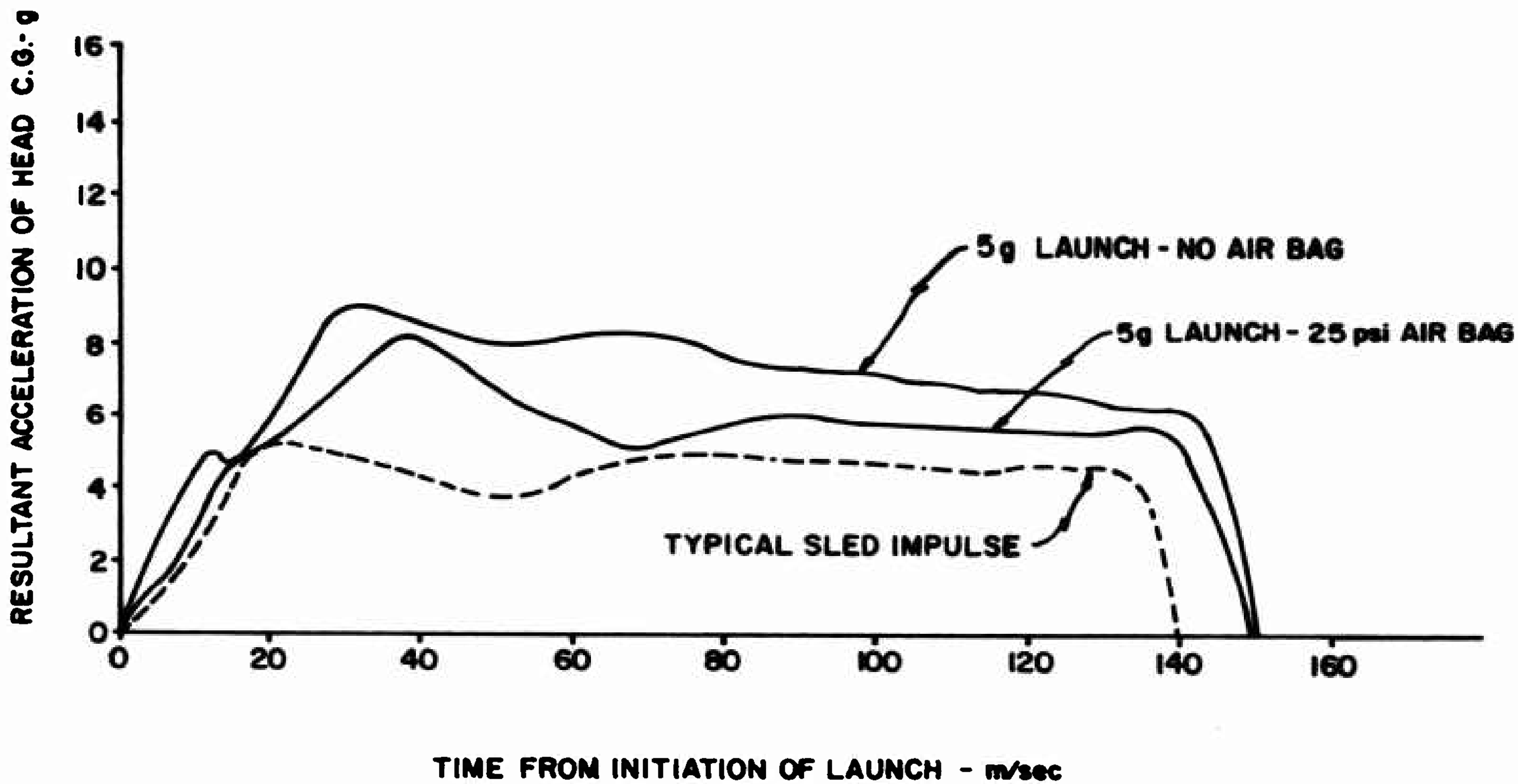

FIGURE 12

Resultant head acceleration of model with and without chin bag; 5 g square wave sled impulse.

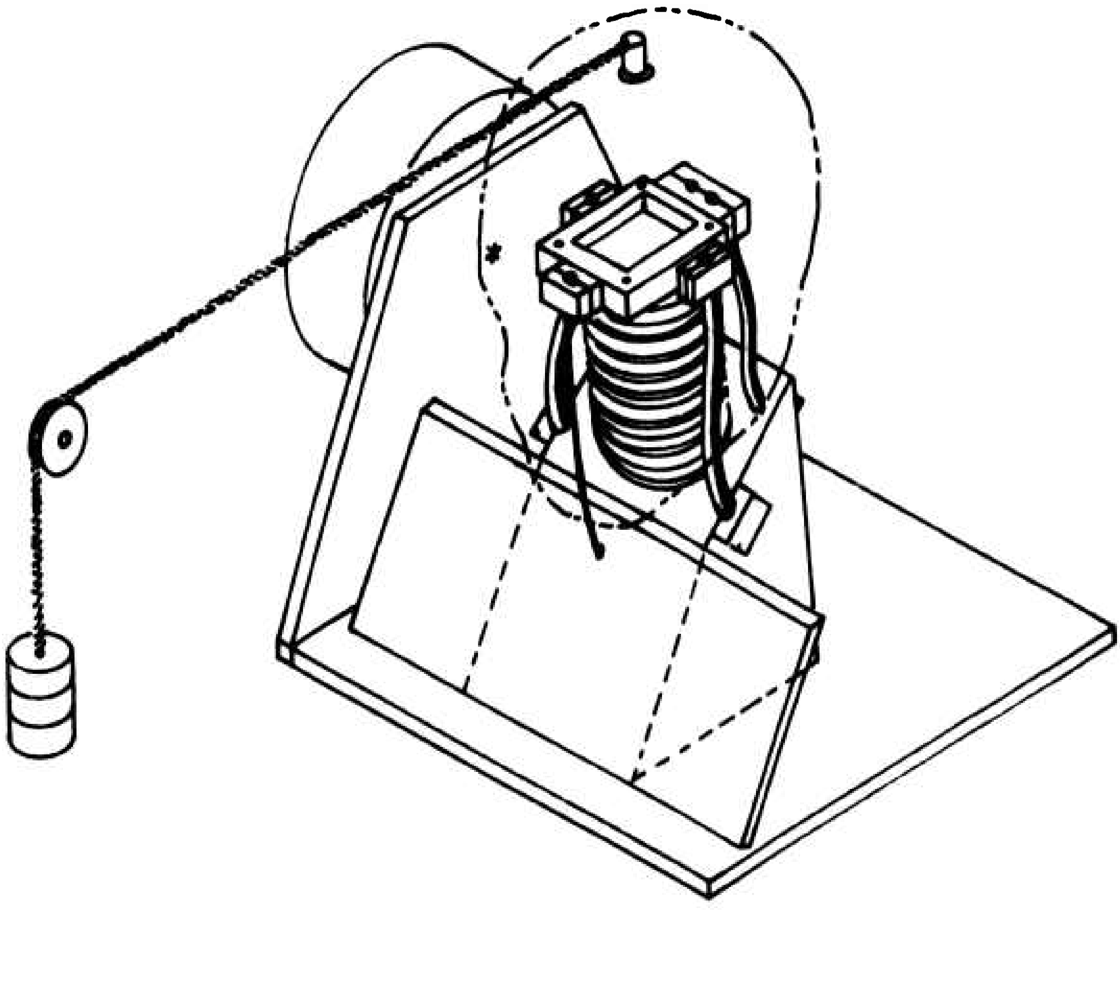

FIGURE 13
Test set up, static chin bag tests

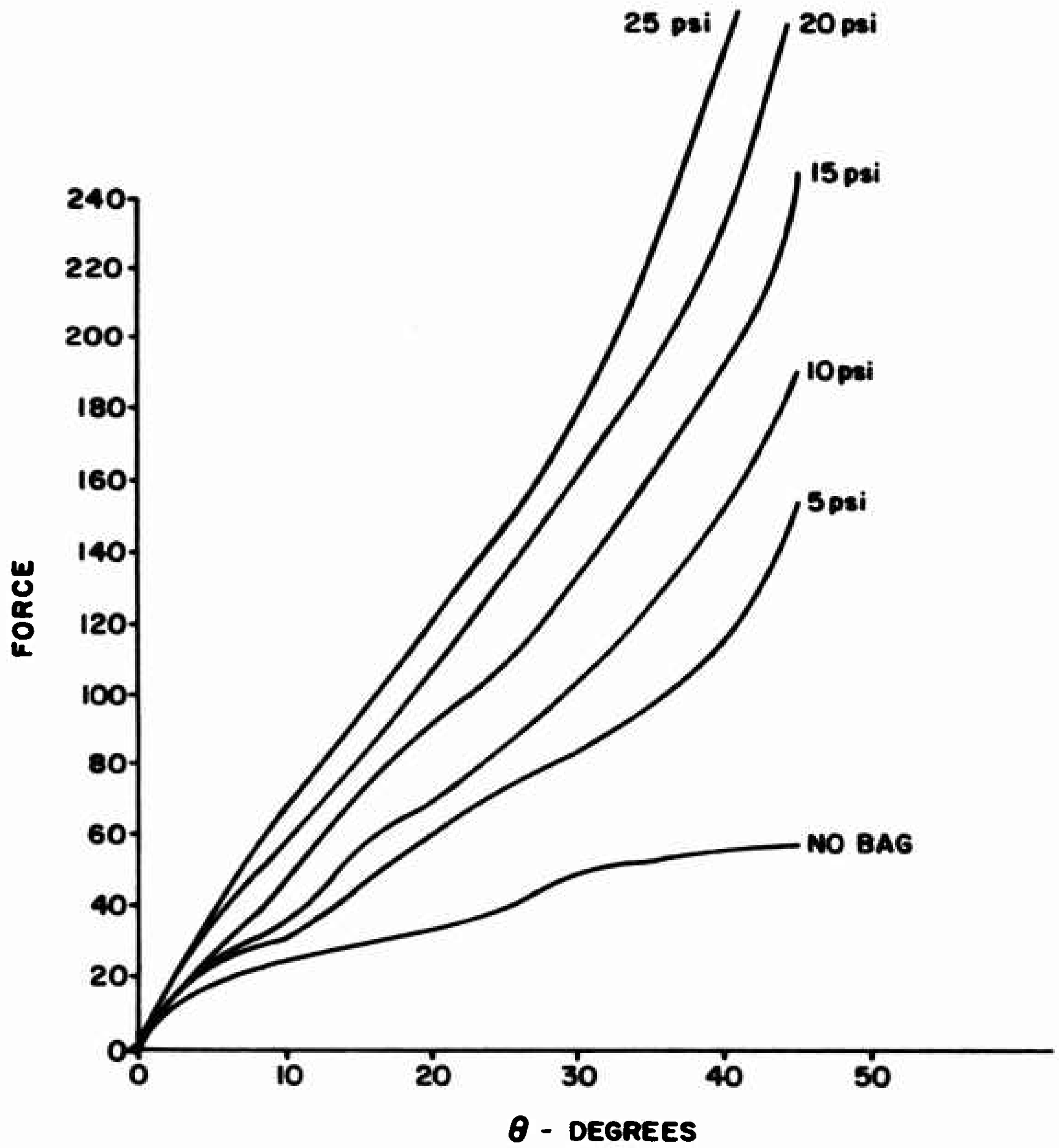

25 psi
20 psi
15 psi
10 psi
5 psi
NO BAG
FORCE
240
220
200
180
160
140
120
100
80
60
40
20
0
0
10
20
30
40
50
θ - DEGREES

FIGURE 14

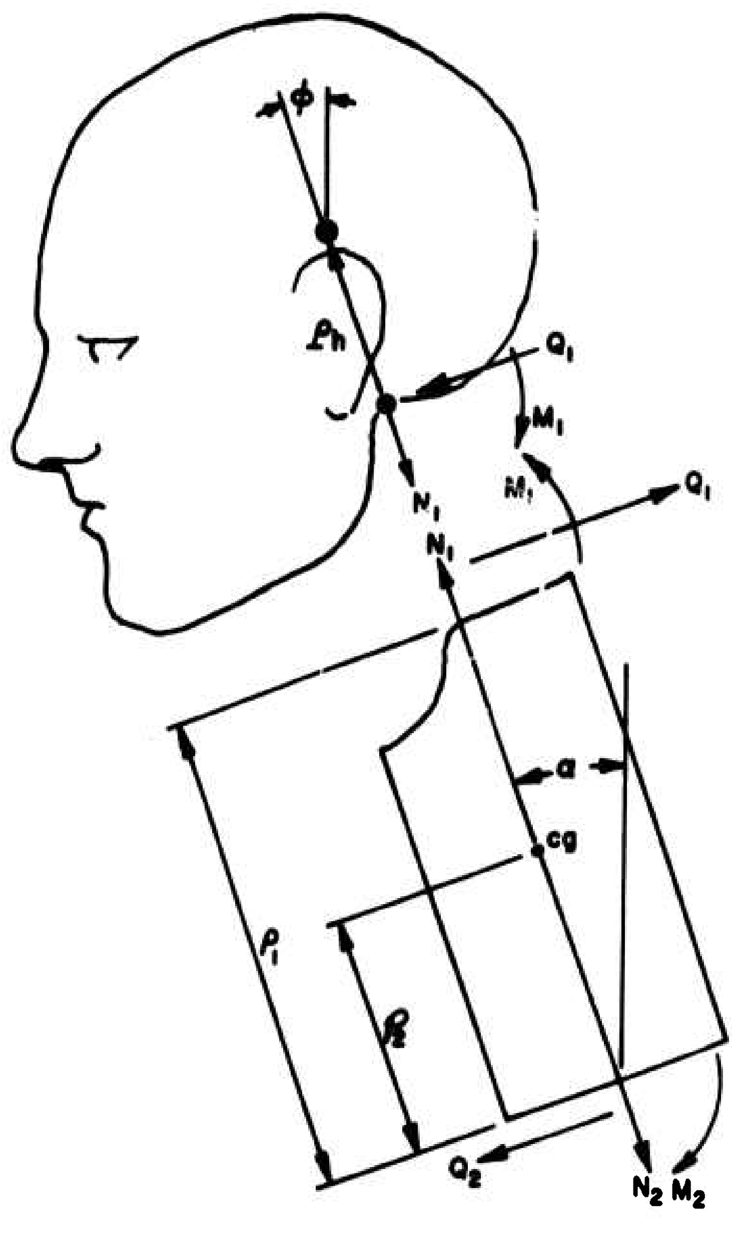

FIGURE 15
Simplified mathematical model of head and neck

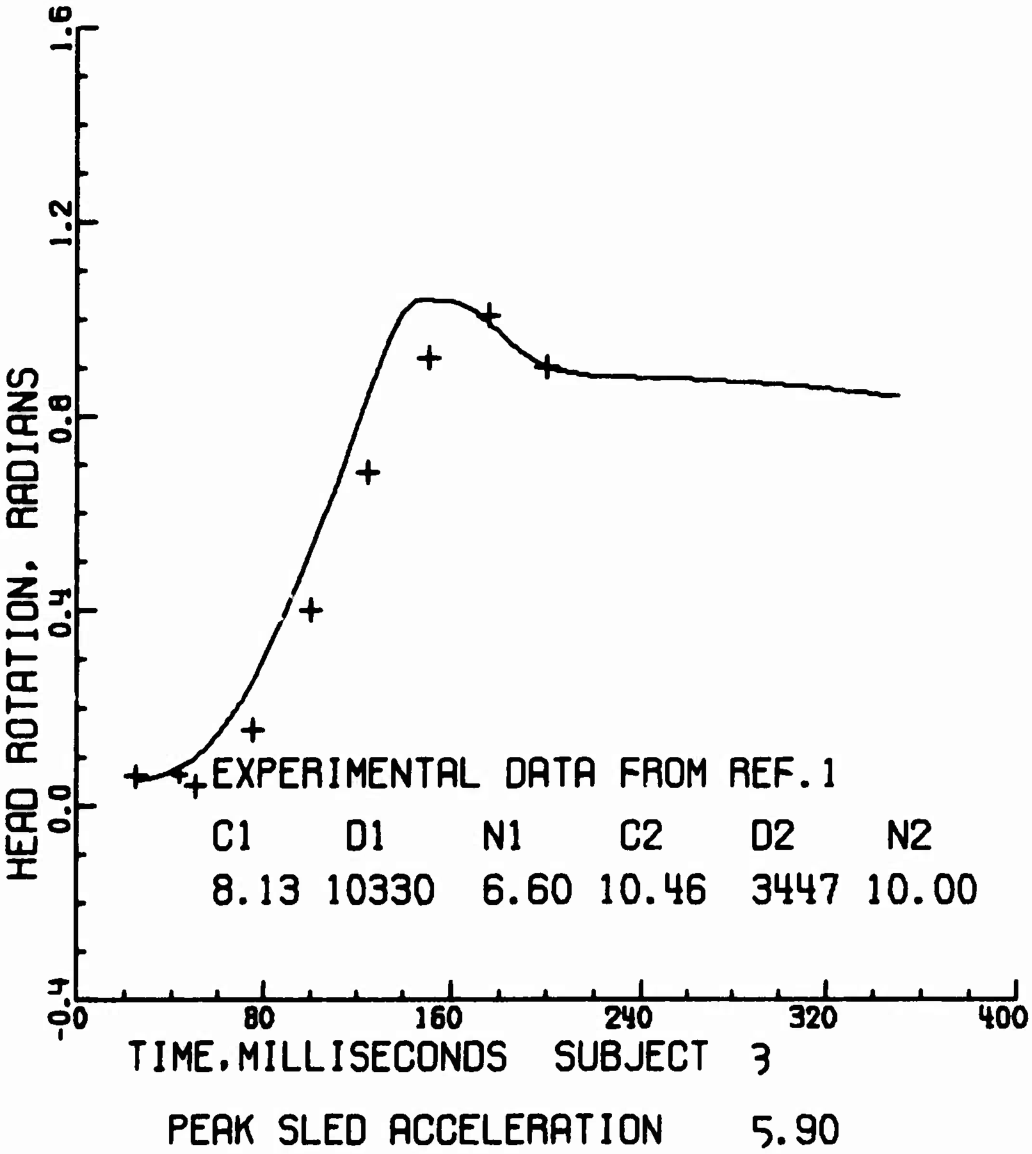
1.6
1.2
0.8
0.4
0.0
-0.4
HEAD ROTATION, RADIANS
EXPERIMENTAL DATA FROM REF. 1
C1 D1 N1 C2 D2 N2
8.13 10330 6.60 10.46 3447 10.00
0
80
160
240
320
400
TIME, MILLISECONDS SUBJECT 3
PEAK SLED ACCELERATION 5.90

FIGURE 16

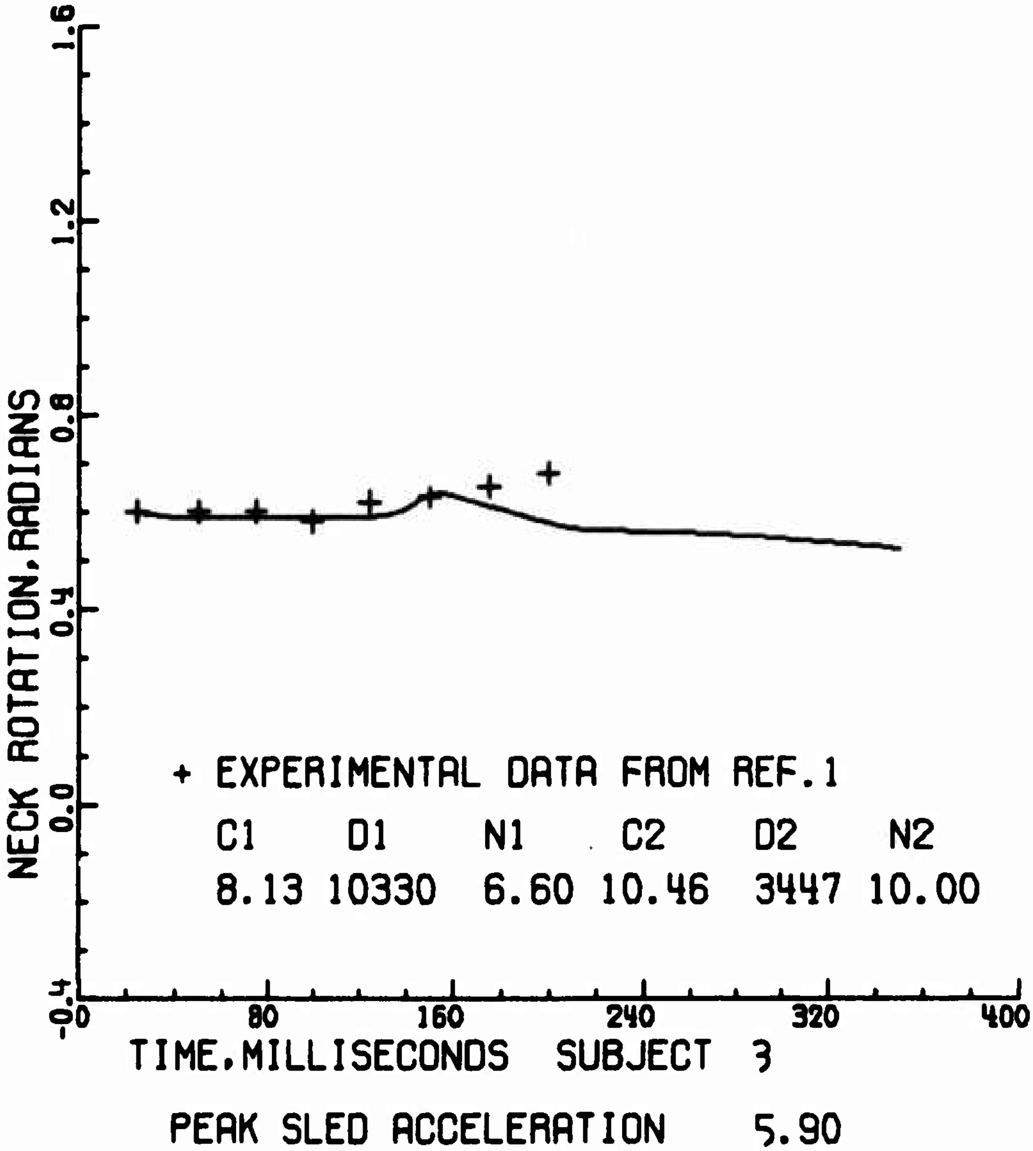
NECK ROTATION, RADIANS
1.6
1.2
0.8
0.4
0.0
-0.4
0
80
160
240
320
400
+ EXPERIMENTAL DATA FROM REF. 1
C1 D1 N1 C2 D2 N2
8.13 10330 6.60 10.46 3447 10.00
TIME, MILLISECONDS SUBJECT 3
PEAK SLED ACCELERATION 5.90

FIGURE 17

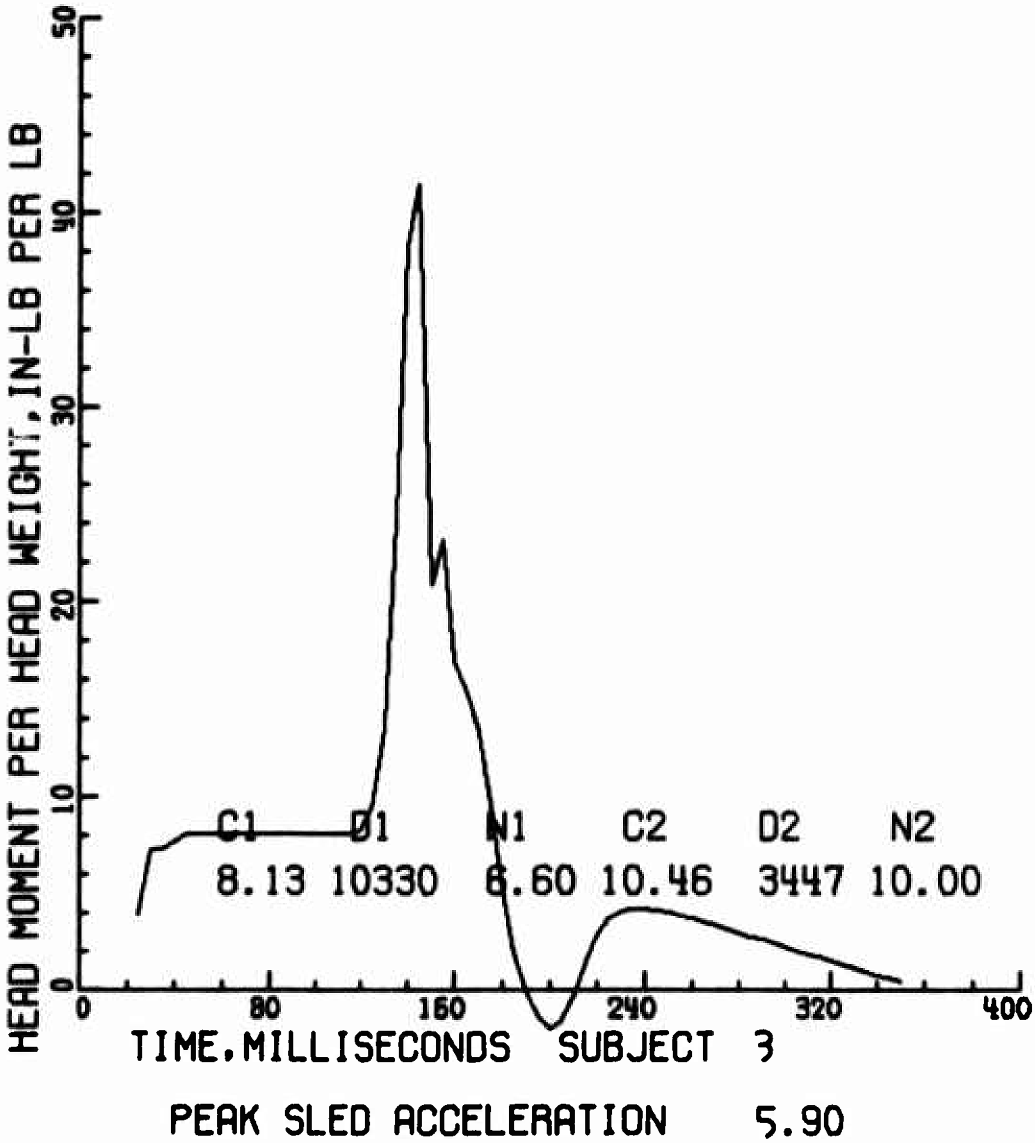
HEAD MOMENT PER HEAD WEIGHT, IN-LB PER LB
0
10
20
30
40
50
0
80
160
240
320
400
C1 D1 N1 C2 D2 N2
8.13 10330 6.60 10.46 3447 10.00
TIME, MILLISECONDS SUBJECT 3
PEAK SLED ACCELERATION 5.90

FIGURE 18

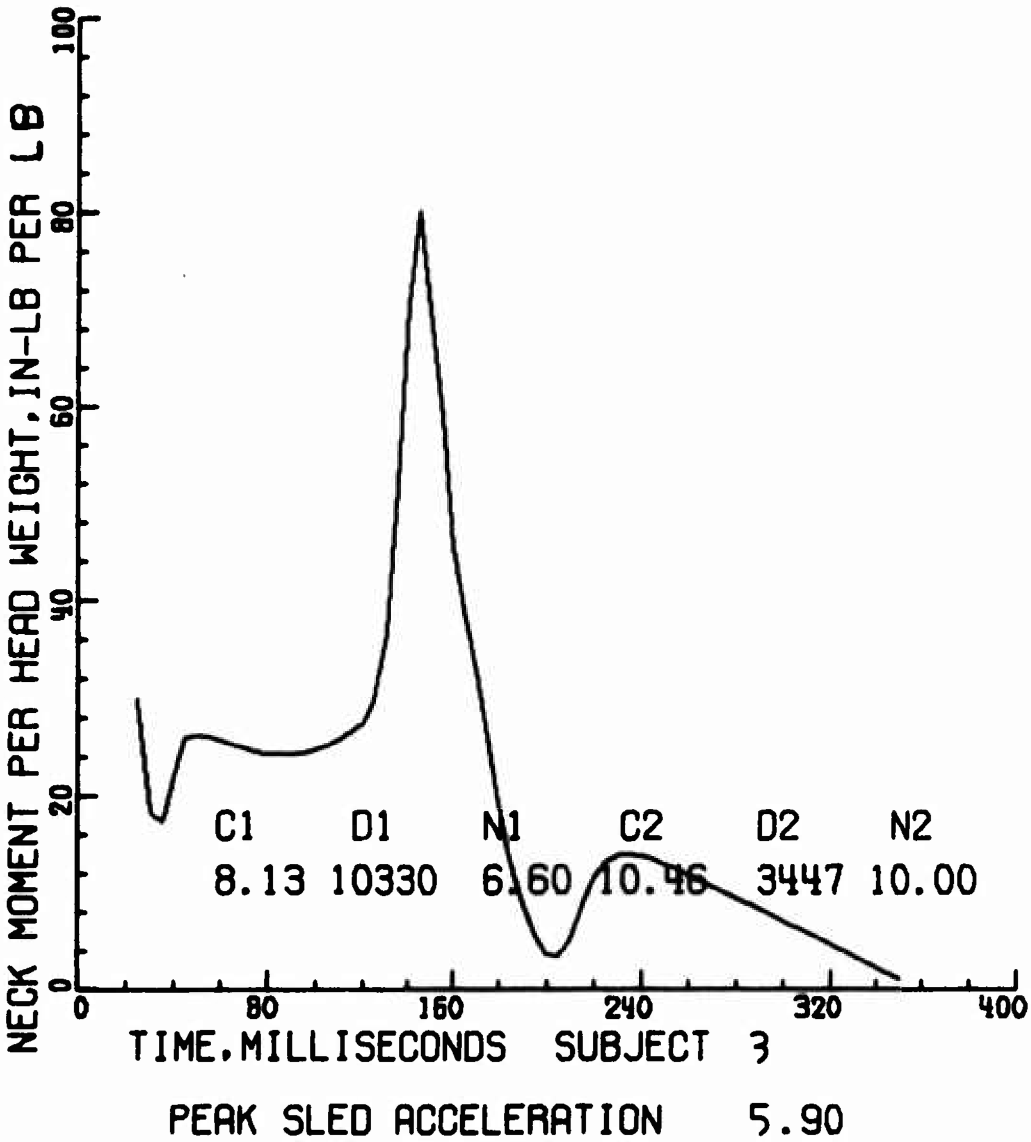
NECK MOMENT PER HEAD WEIGHT, IN-LB PER LB
0
20
40
60
80
100
0
80
160
240
320
400
C1 D1 N1 C2 D2 N2
8.13 10330 6.60 10.46 3447 10.00
TIME, MILLISECONDS SUBJECT 3
PEAK SLED ACCELERATION 5.90

FIGURE 19

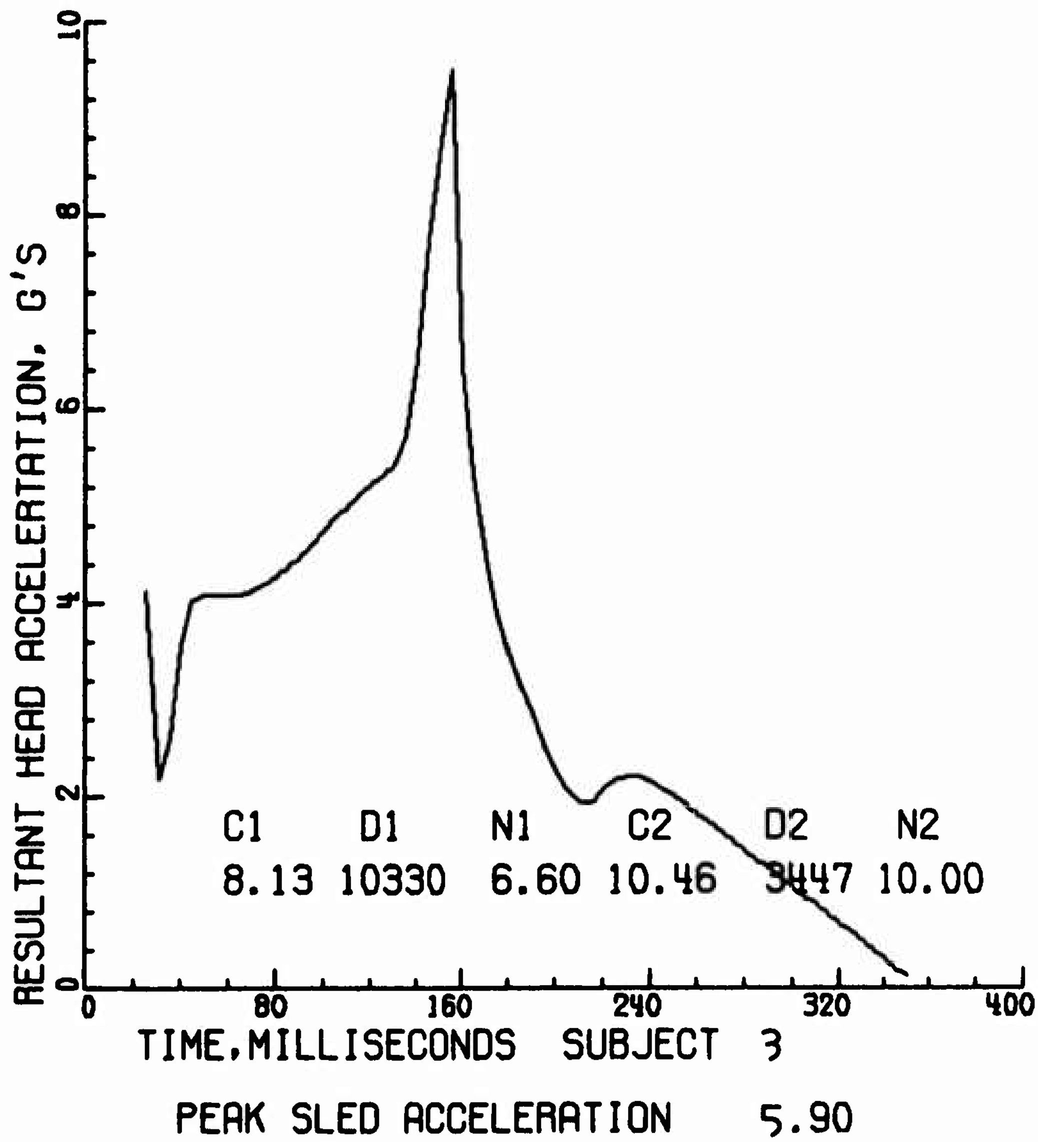

RESULTANT HEAD ACCELERATION, G'S
0
2
4
6
8
10
0
80
160
240
320
400
C1 D1 N1 C2 D2 N2
8.13 10330 6.60 10.46 3447 10.00
TIME, MILLISECONDS SUBJECT 3
PEAK SLED ACCELERATION 5.90

FIGURE 20

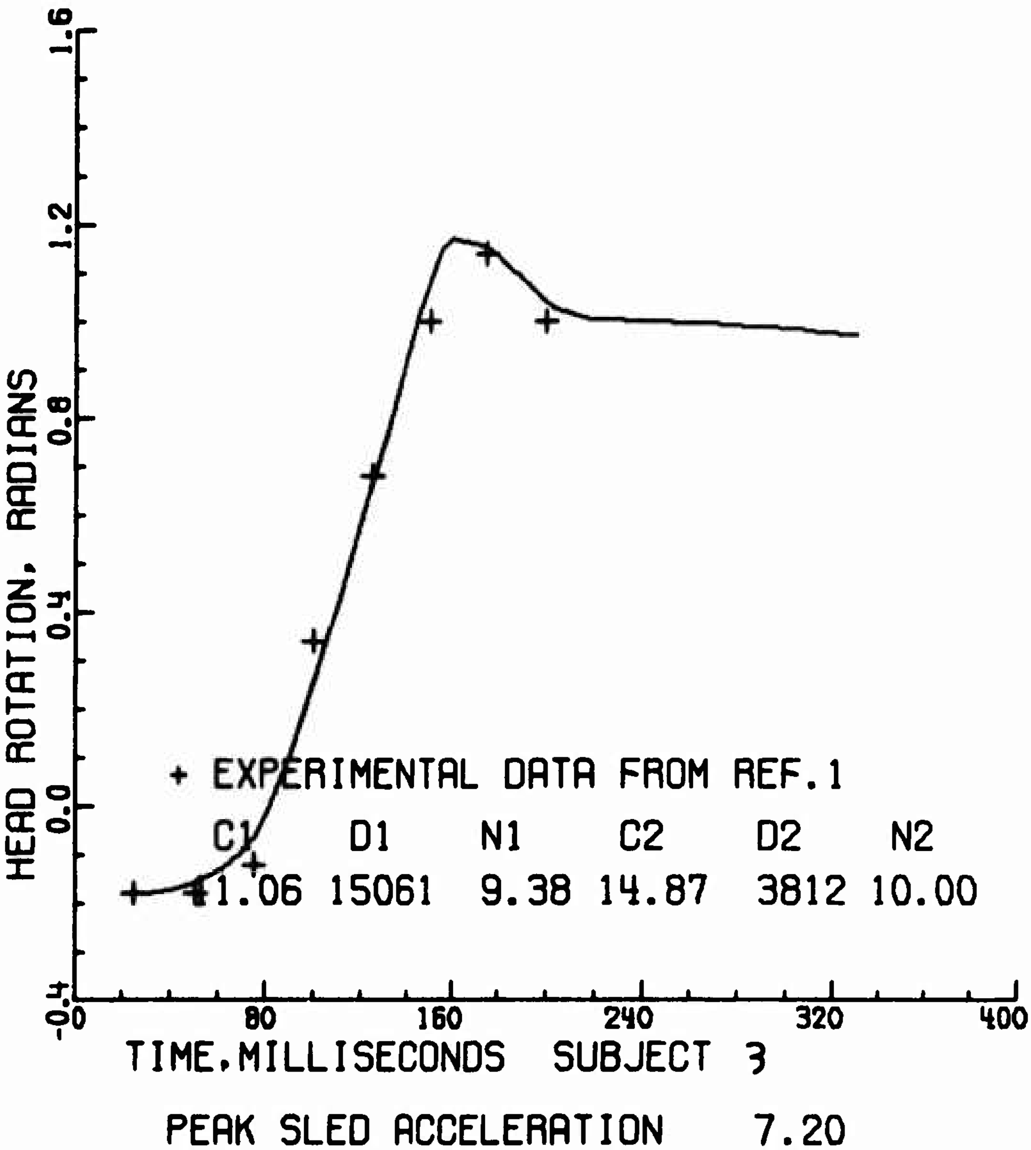
HEAD ROTATION, RADIANS
1.6
1.2
0.8
0.4
0.0
-0.4
0
80
160
240
320
400
+ EXPERIMENTAL DATA FROM REF.1
C1 D1 N1 C2 D2 N2
11.06 15061 9.38 14.87 3812 10.00
TIME,MILLISECONDS SUBJECT 3
PEAK SLED ACCELERATION 7.20

FIGURE 21

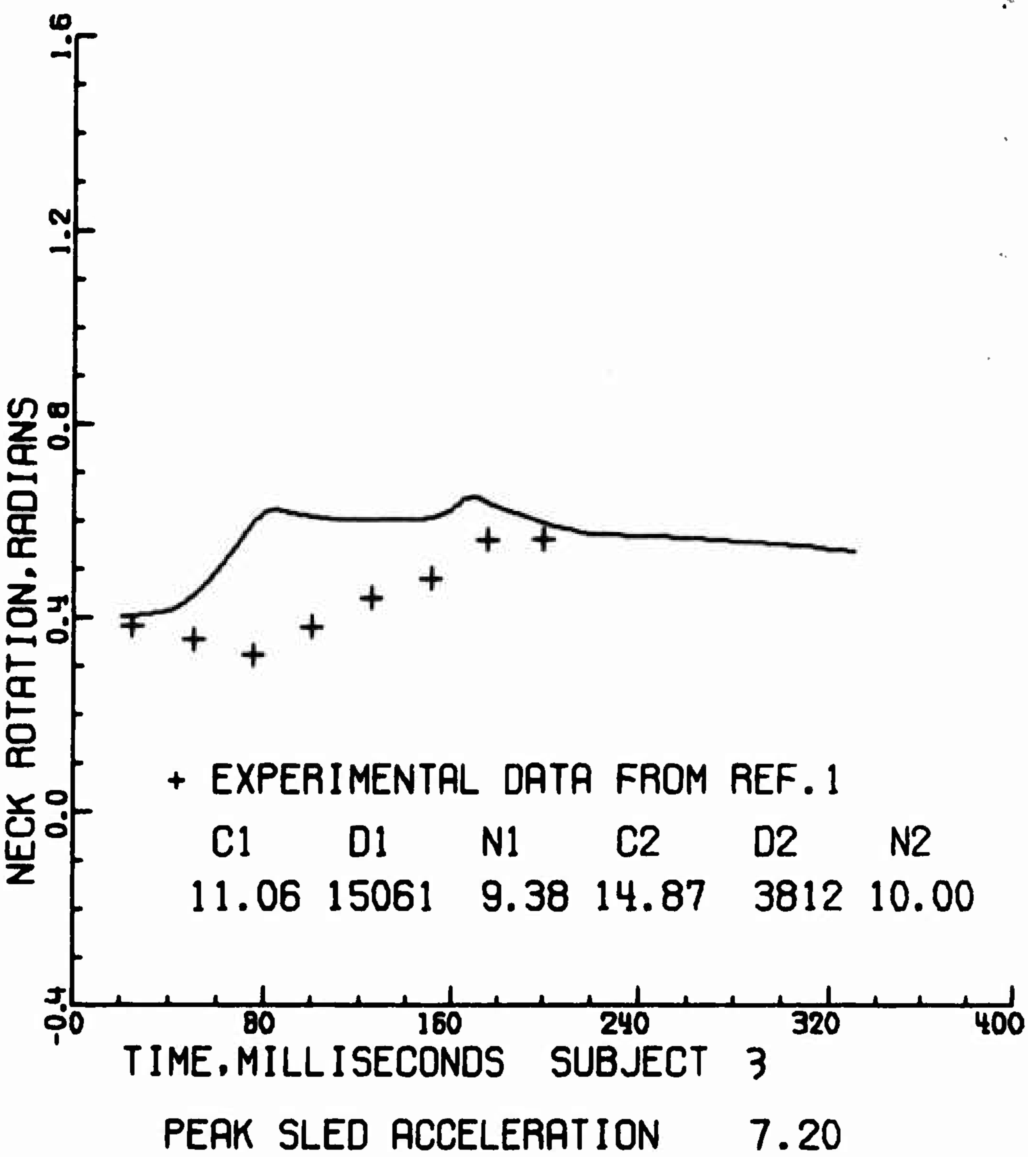
NECK ROTATION, RADIANS
1.6
1.2
0.8
0.4
0.0
-0.4
+ EXPERIMENTAL DATA FROM REF.1
C1 D1 N1 C2 D2 N2
11.06 15061 9.38 14.87 3812 10.00
0.0
80
160
240
320
400
TIME, MILLISECONDS SUBJECT 3
PEAK SLED ACCELERATION 7.20

FIGURE 22

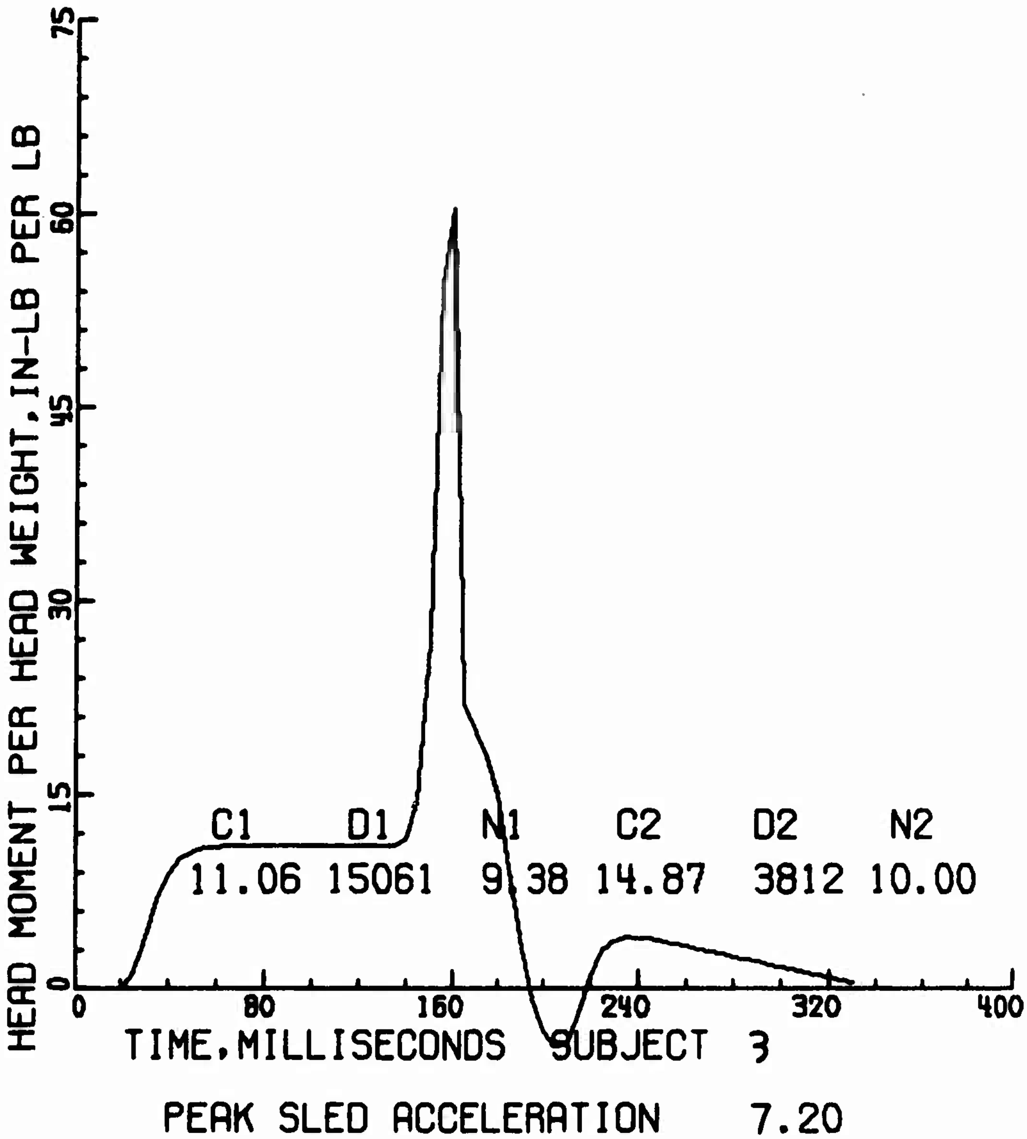
HEAD MOMENT PER HEAD WEIGHT, IN-LB PER LB
0
15
30
45
60
75
0
80
160
240
320
400
C1 D1 N1 C2 D2 N2
11.06 15061 9.38 14.87 3812 10.00
TIME, MILLISECONDS SUBJECT 3
PEAK SLED ACCELERATION 7.20

FIGURE 23

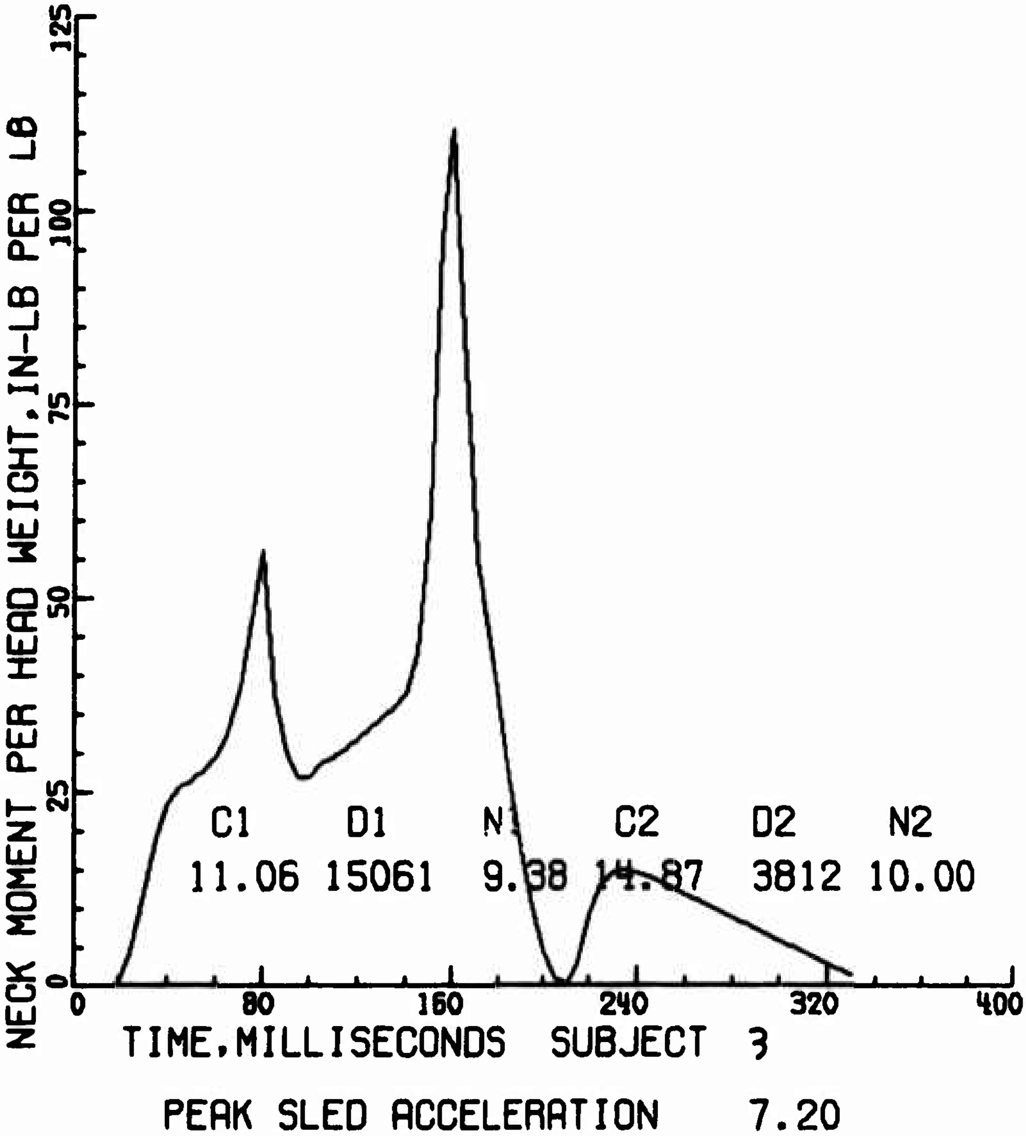
NECK MOMENT PER HEAD WEIGHT, IN-LB PER LB
0
25
50
75
100
125
0
80
160
240
320
400
C1 D1 N1 C2 D2 N2
11.06 15061 9.38 14.87 3812 10.00
TIME, MILLISECONDS SUBJECT 3
PEAK SLED ACCELERATION 7.20

FIGURE 24

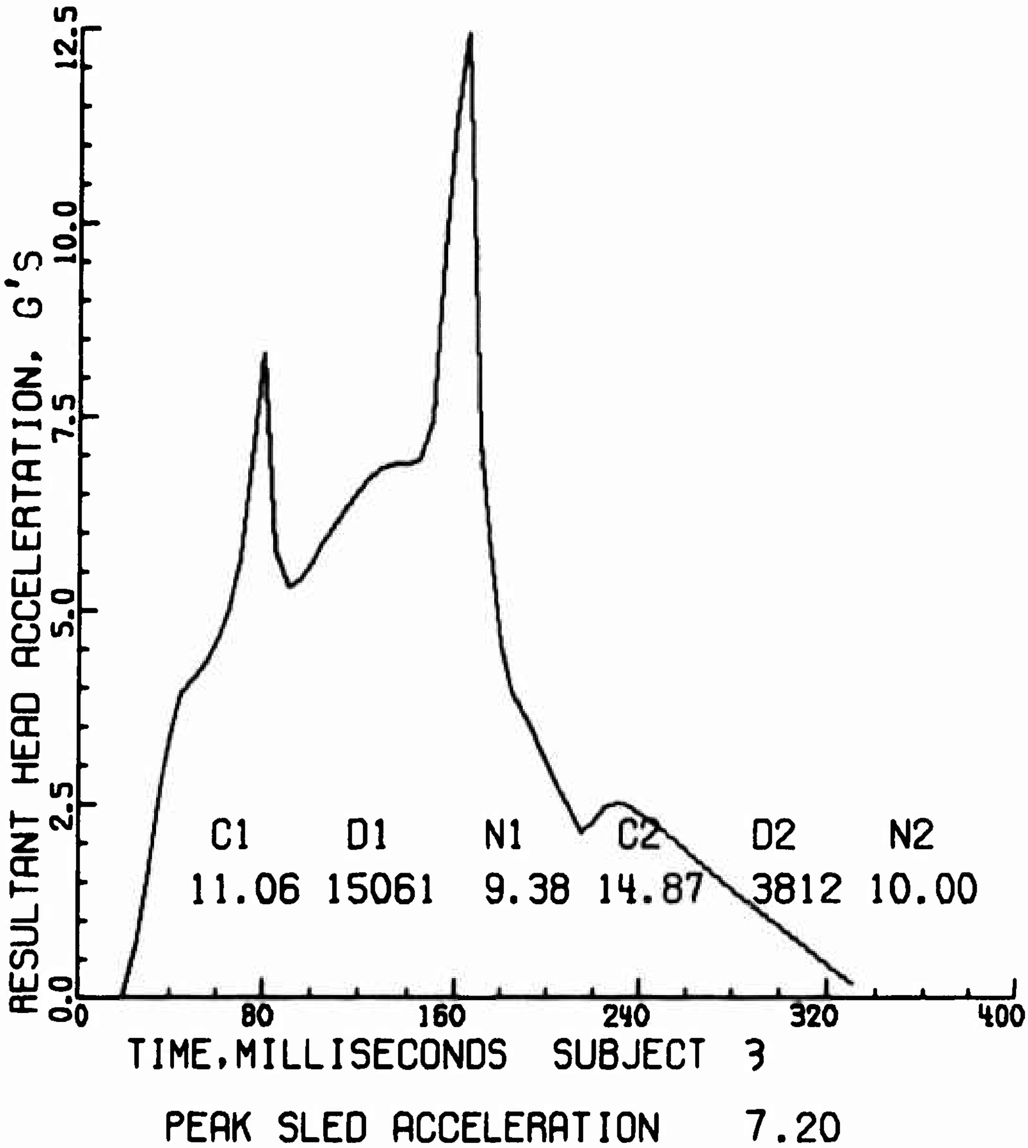
RESULTANT HEAD ACCELERATION, G'S
0.0
2.5
5.0
7.5
10.0
12.5
C1 D1 N1 C2 D2 N2
11.06 15061 9.38 14.87 3812 10.00
0
80
160
240
320
400
TIME,MILLISECONDS SUBJECT 3
PEAK SLED ACCELERATION 7.20

FIGURE 25

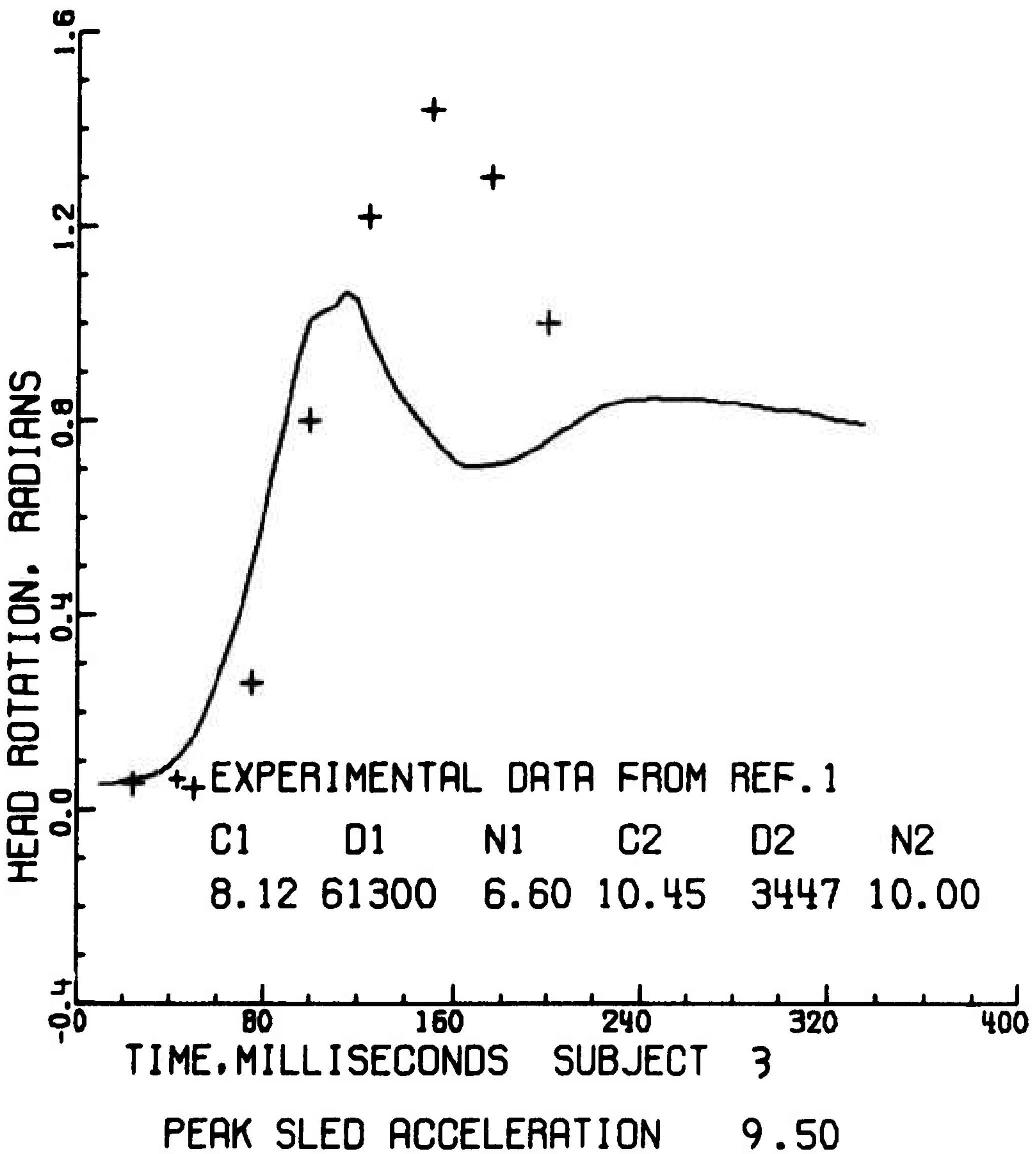
HEAD ROTATION, RADIANS
1.6
1.2
0.8
0.4
0.0
-0.4
0
80
160
240
320
400
+EXPERIMENTAL DATA FROM REF.1
C1 D1 N1 C2 D2 N2
8.12 61300 6.60 10.45 3447 10.00
TIME,MILLISECONDS SUBJECT 3
PEAK SLED ACCELERATION 9.50

FIGURE 26

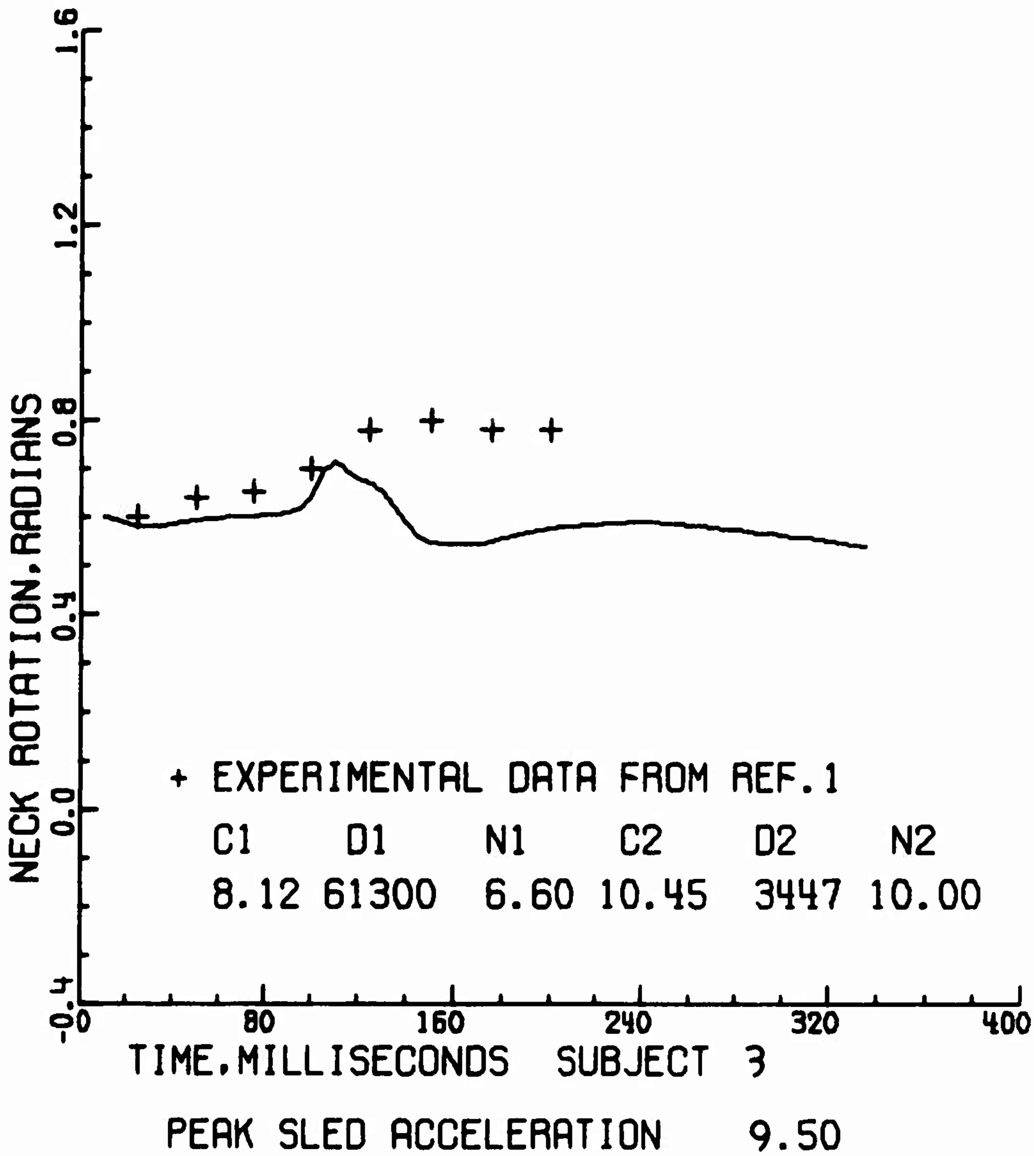
NECK ROTATION, RADIANS
1.6
1.2
0.8
0.4
0.0
-0.4
+ EXPERIMENTAL DATA FROM REF. 1
C1 D1 N1 C2 D2 N2
8.12 61300 6.60 10.45 3447 10.00
0
80
160
240
320
400
TIME, MILLISECONDS SUBJECT 3
PEAK SLED ACCELERATION 9.50

FIGURE 27

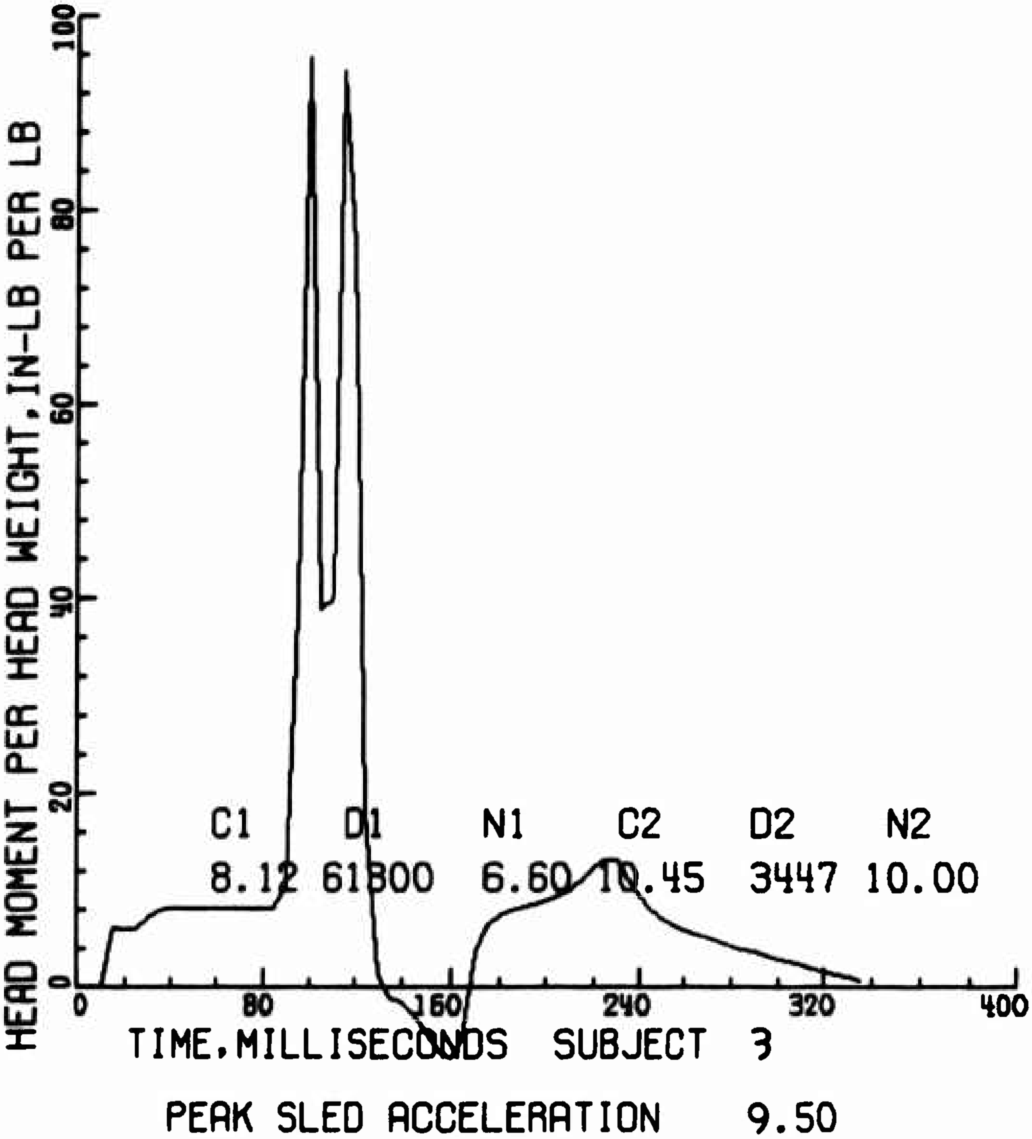
HEAD MOMENT PER HEAD WEIGHT, IN-LB PER LB
0
20
40
60
80
100
C1 D1 N1 C2 D2 N2
8.12 61300 6.60 10.45 3447 10.00
0
80
160
240
320
400
TIME, MILLISECONDS SUBJECT 3
PEAK SLED ACCELERATION 9.50

FIGURE 28

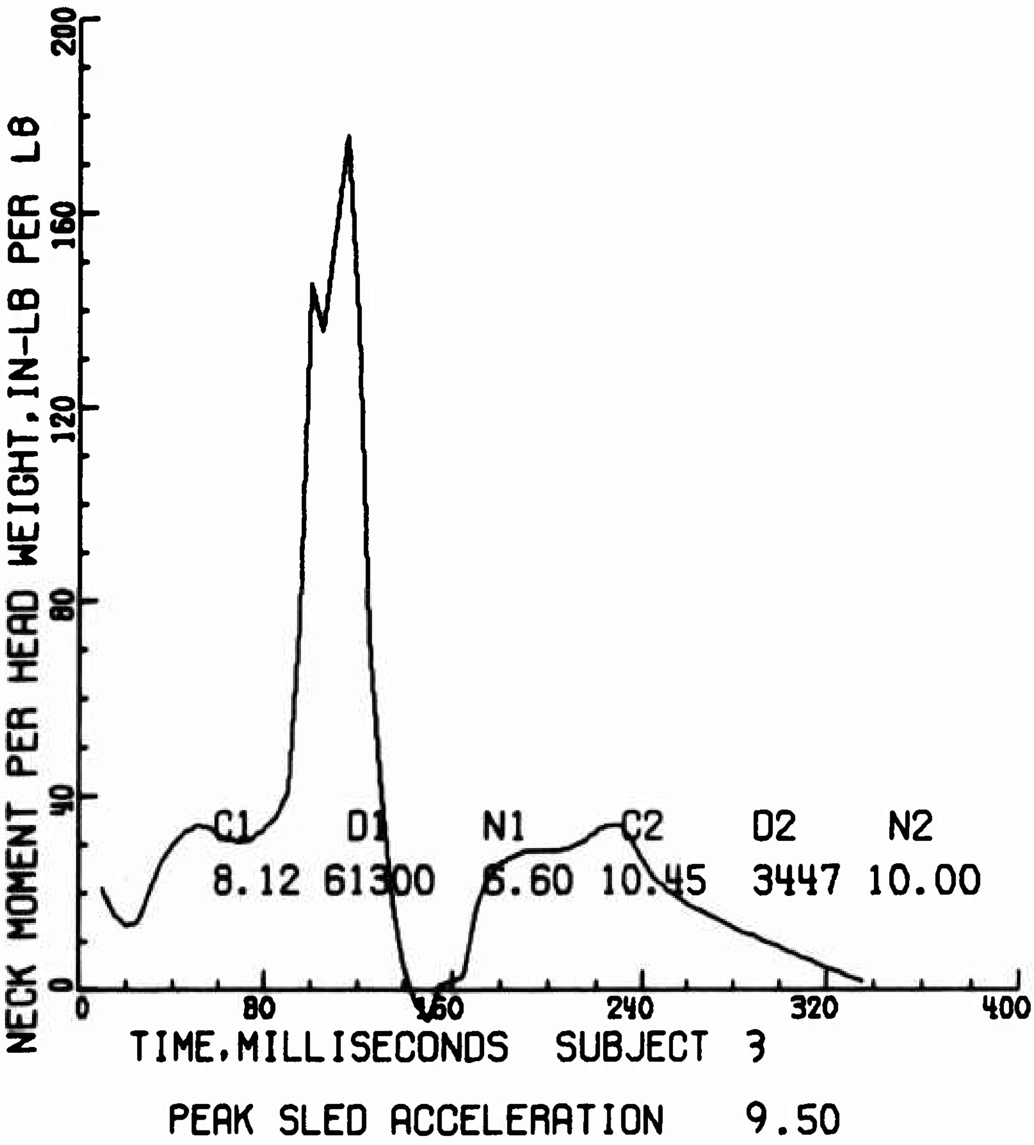
NECK MOMENT PER HEAD WEIGHT, IN-LB PER LB
0
40
80
120
160
200
C1 D1 N1 C2 D2 N2
8.12 61300 5.60 10.45 3447 10.00
0
80
160
240
320
400
TIME, MILLISECONDS SUBJECT 3
PEAK SLED ACCELERATION 9.50

FIGURE 29

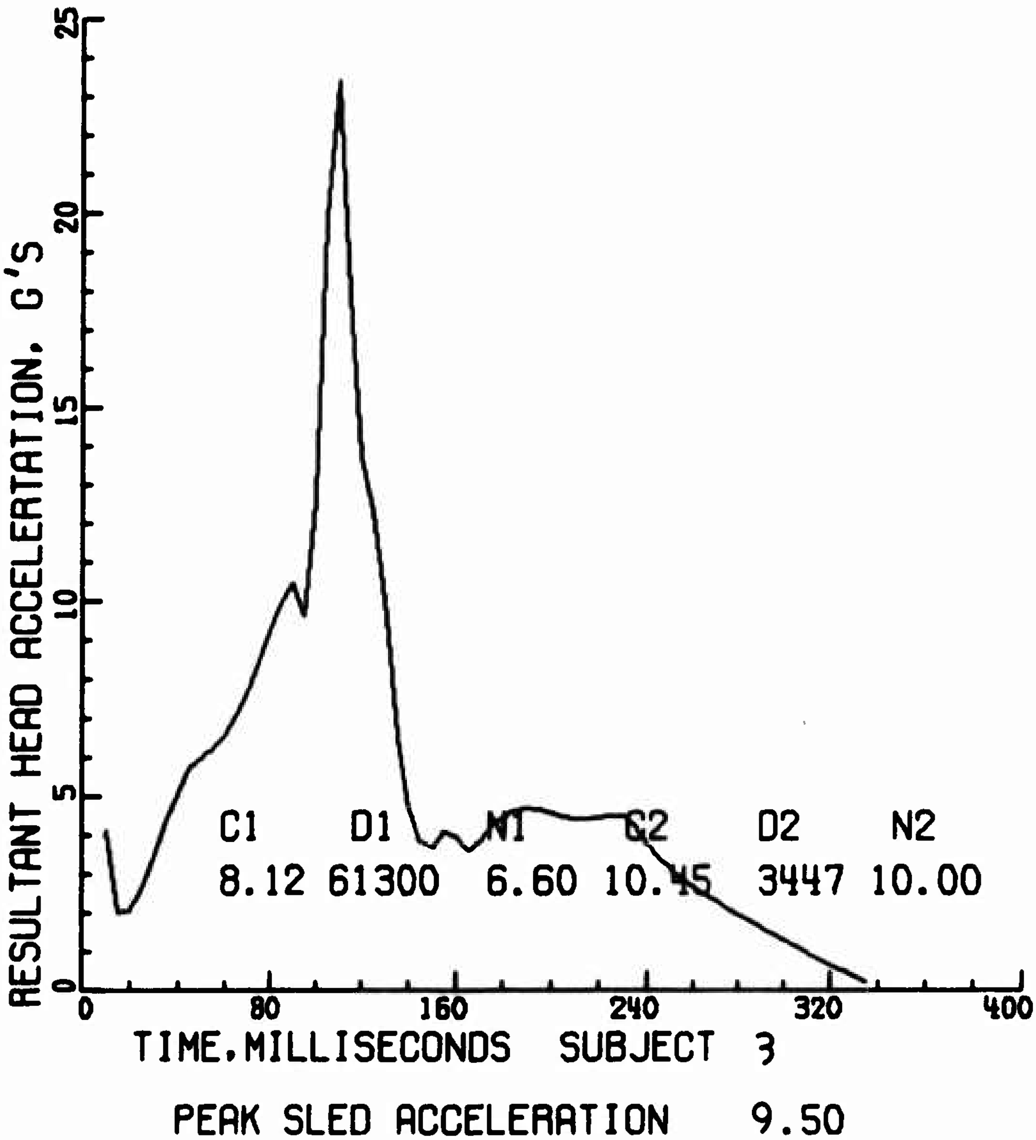
RESULTANT HEAD ACCELERATION, G'S
0
5
10
15
20
25
C1 D1 N1 C2 D2 N2
8.12 61300 6.60 10.45 3447 10.00
0
80
160
240
320
400
TIME, MILLISECONDS SUBJECT 3
PEAK SLED ACCELERATION 9.50

FIGURE 30

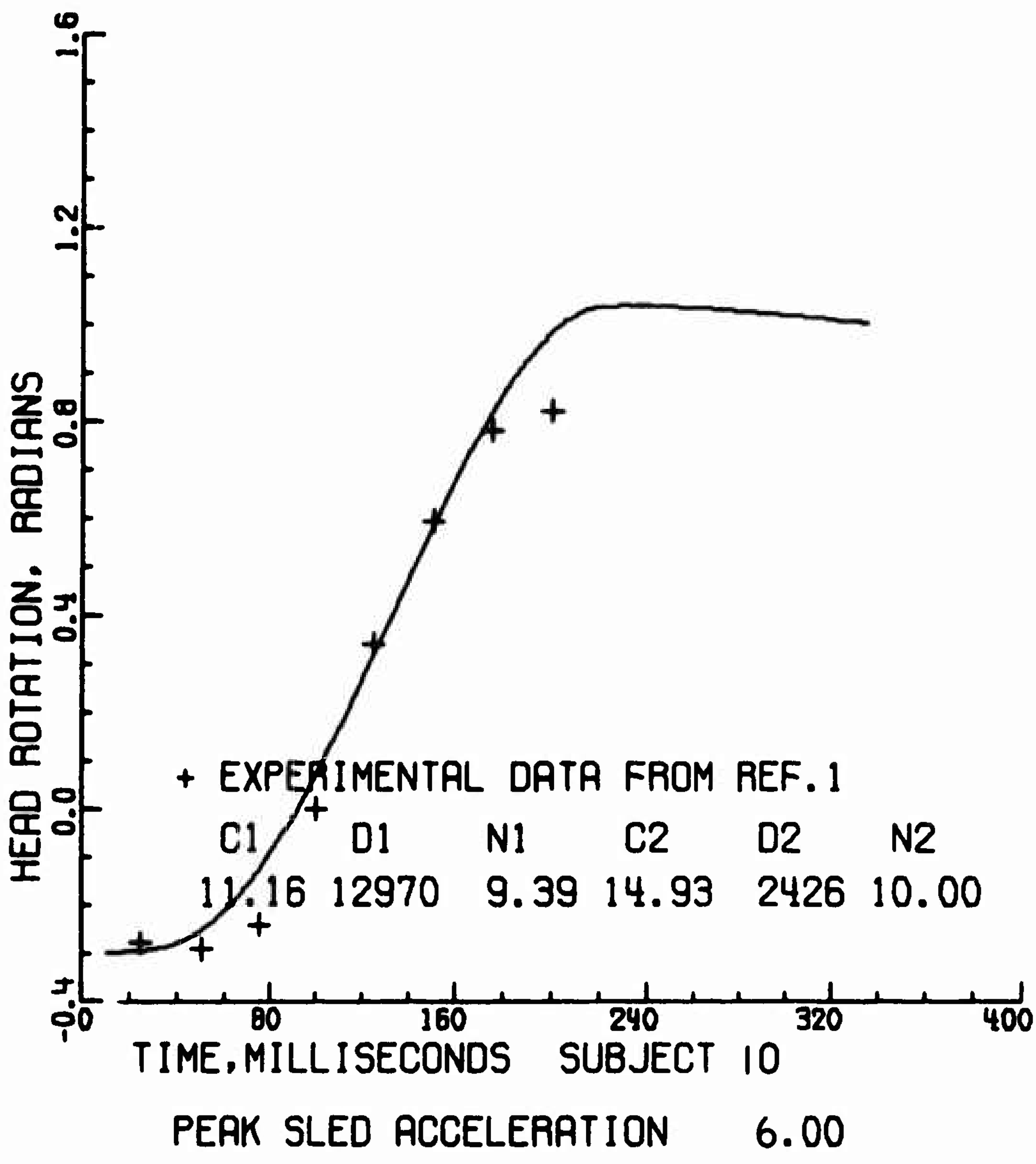
HEAD ROTATION, RADIANS
-0.4
0.0
0.4
0.8
1.2
1.6
+ EXPERIMENTAL DATA FROM REF.1
C1 D1 N1 C2 D2 N2
11.16 12970 9.39 14.93 2426 10.00
-0.0
80
160
240
320
400
TIME,MILLISECONDS SUBJECT 10
PEAK SLED ACCELERATION 6.00

FIGURE 31

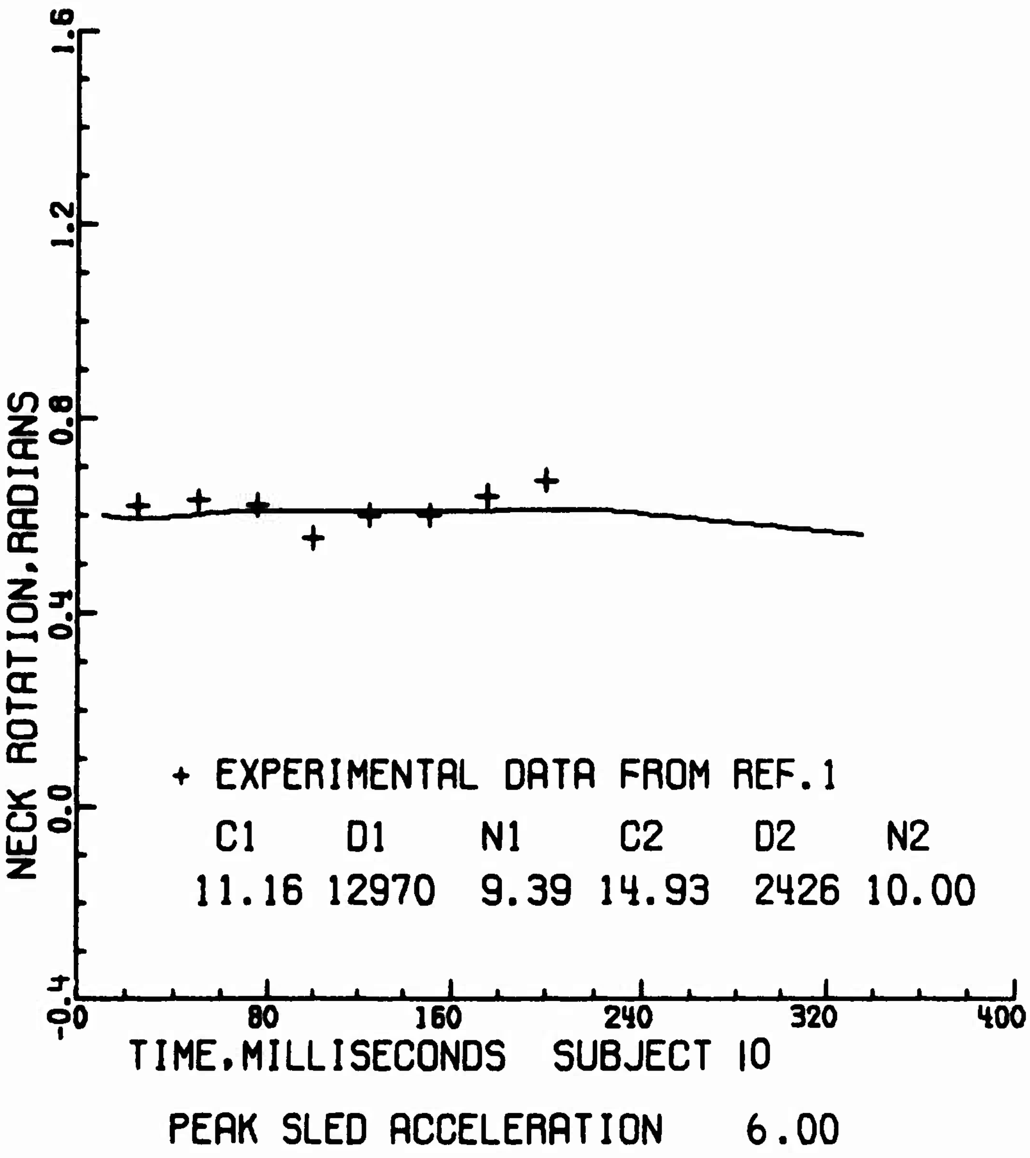
1.6
1.2
0.8
0.4
0.0
-0.4
NECK ROTATION, RADIANS
+ EXPERIMENTAL DATA FROM REF.1
C1 D1 N1 C2 D2 N2
11.16 12970 9.39 14.93 2426 10.00
0
80
160
240
320
400
TIME, MILLISECONDS SUBJECT 10
PEAK SLED ACCELERATION 6.00

FIGURE 32

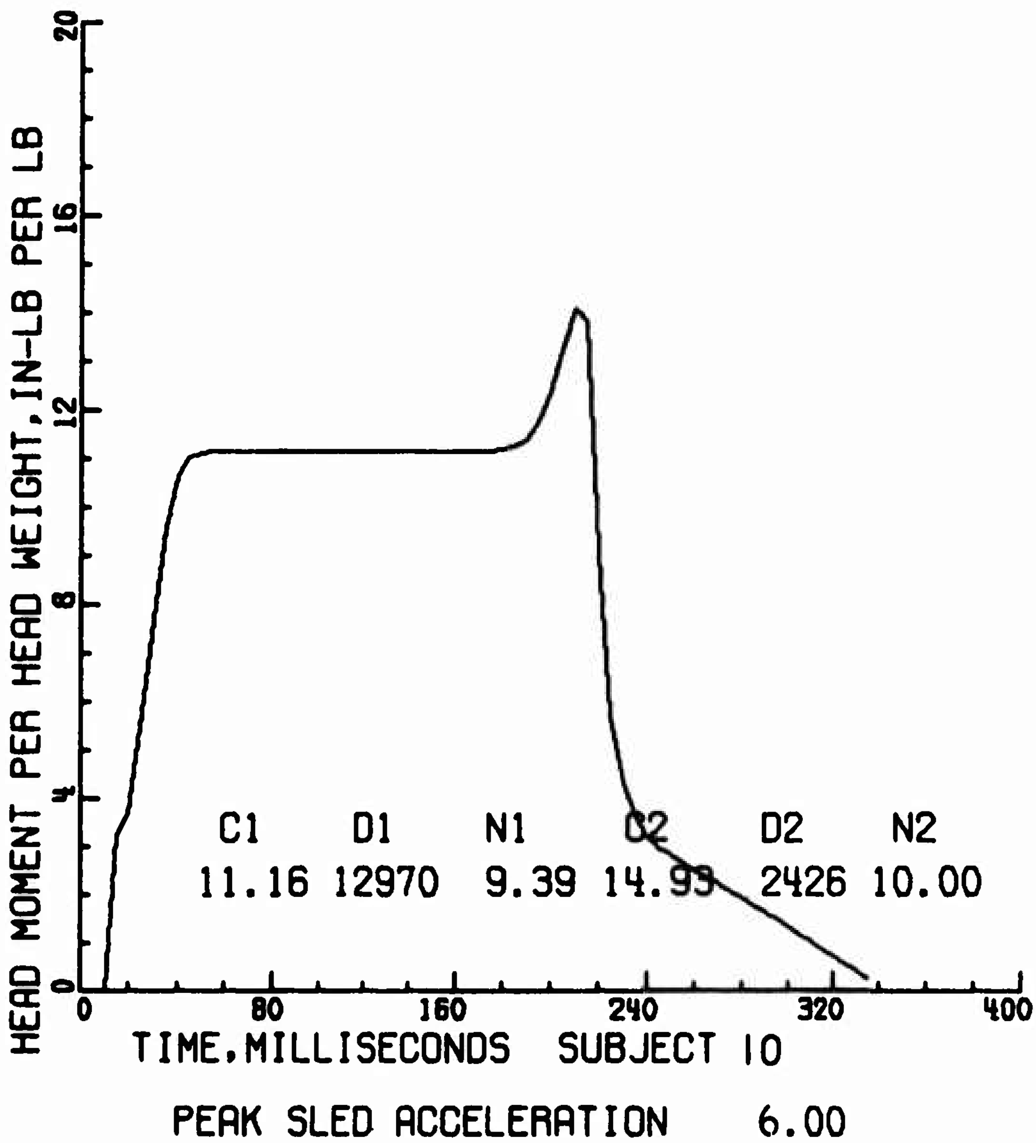
HEAD MOMENT PER HEAD WEIGHT, IN-LB PER LB
0
4
8
12
16
20
C1 D1 N1 C2 D2 N2
11.16 12970 9.39 14.93 2426 10.00
0
80
160
240
320
400
TIME, MILLISECONDS SUBJECT 10
PEAK SLED ACCELERATION 6.00

FIGURE 33

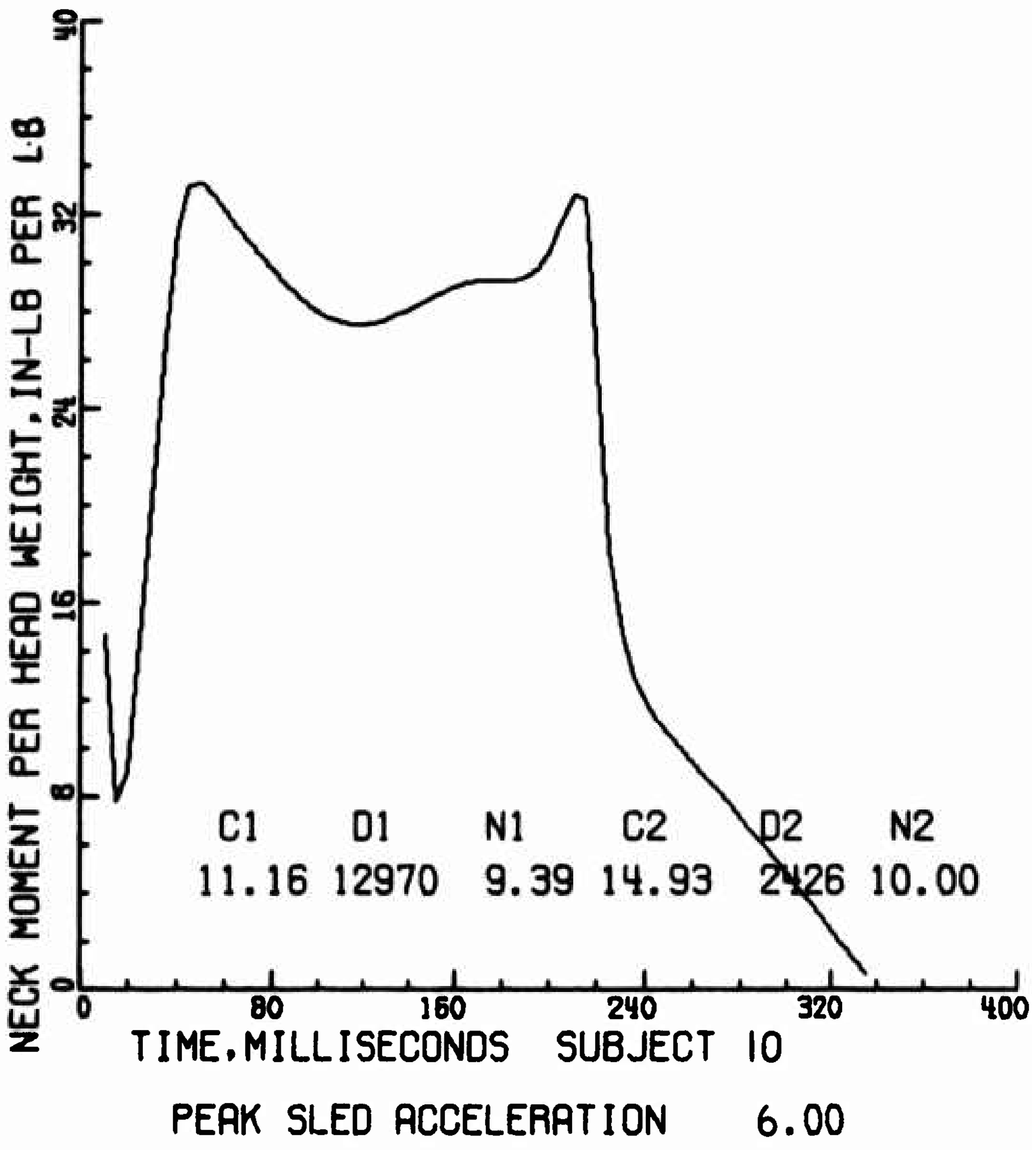
NECK MOMENT PER HEAD WEIGHT, IN-LB PER LB
0
8
16
24
32
40
0
80
160
240
320
400
C1 D1 N1 C2 D2 N2
11.16 12970 9.39 14.93 2426 10.00
TIME, MILLISECONDS SUBJECT 10
PEAK SLED ACCELERATION 6.00

FIGURE 34

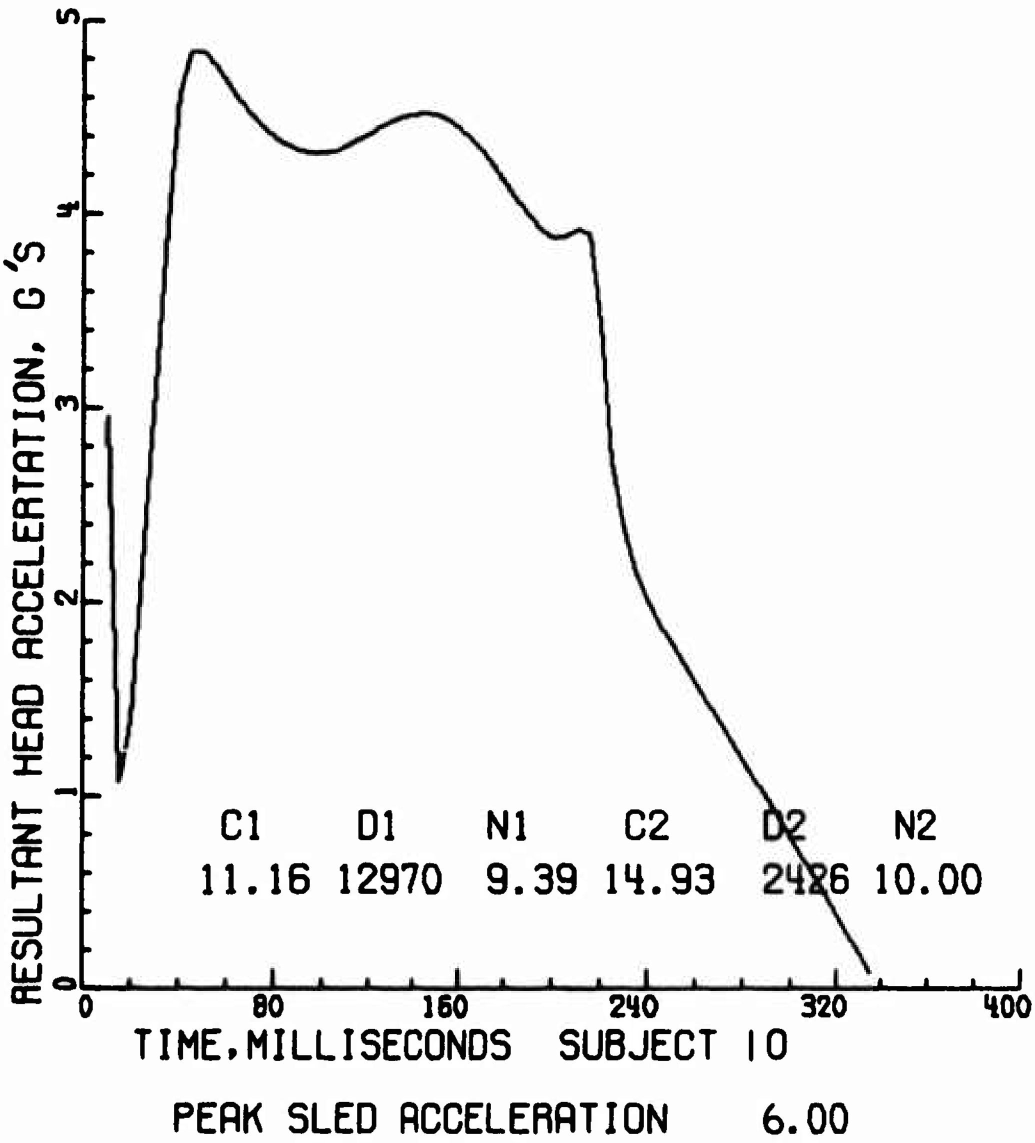
5
4
3
2
1
0
RESULTANT HEAD ACCELERATATION, G'S
C1 D1 N1 C2 D2 N2
11.16 12970 9.39 14.93 2426 10.00
0
80
160
240
320
400
TIME,MILLISECONDS SUBJECT 10
PEAK SLED ACCELERATION 6.00

FIGURE 35

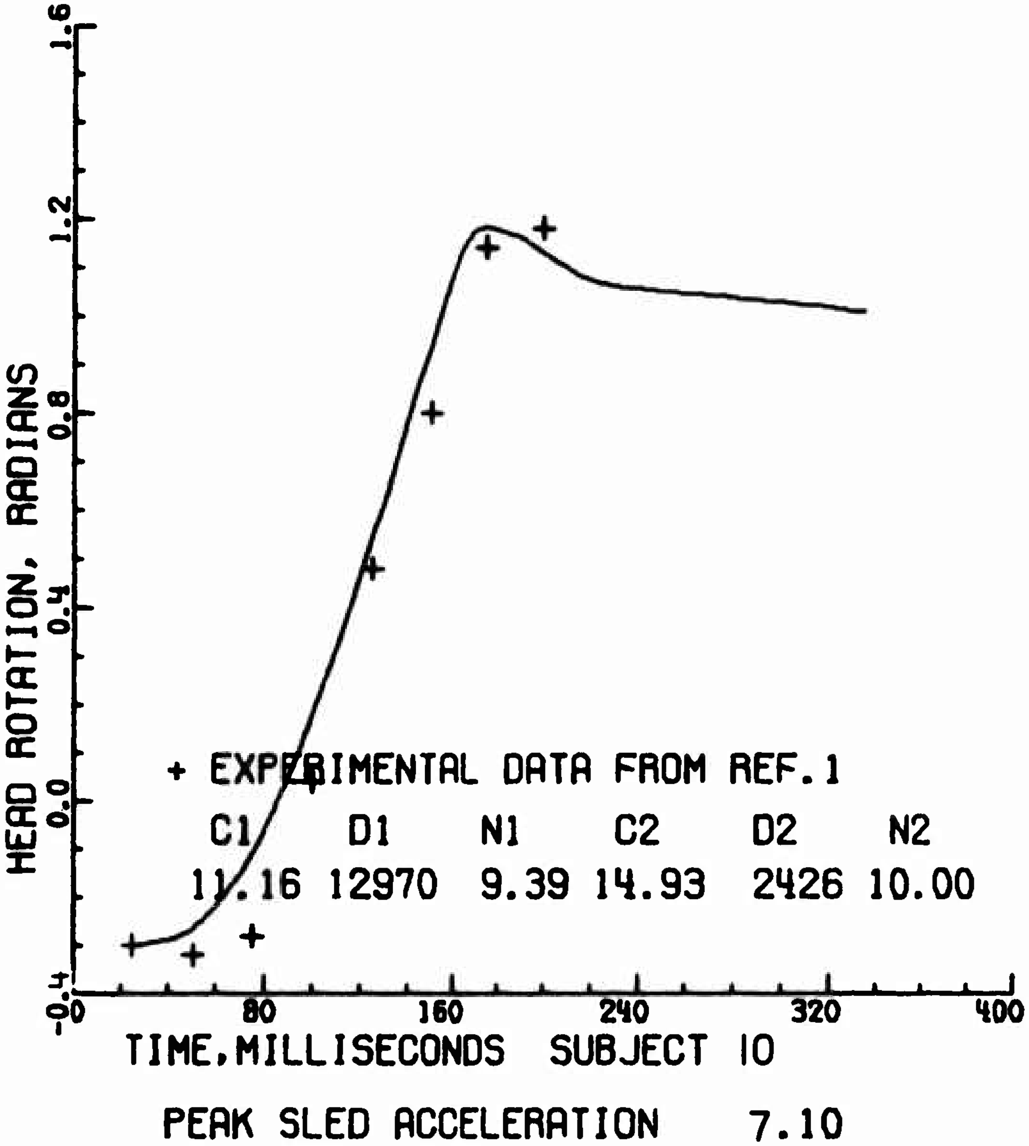
HEAD ROTATION, RADIANS
-0.4
0.0
0.4
0.8
1.2
1.6
0
80
160
240
320
400
+ EXPERIMENTAL DATA FROM REF. 1
C1 D1 N1 C2 D2 N2
11.16 12970 9.39 14.93 2426 10.00
TIME, MILLISECONDS SUBJECT 10
PEAK SLED ACCELERATION 7.10

FIGURE 36

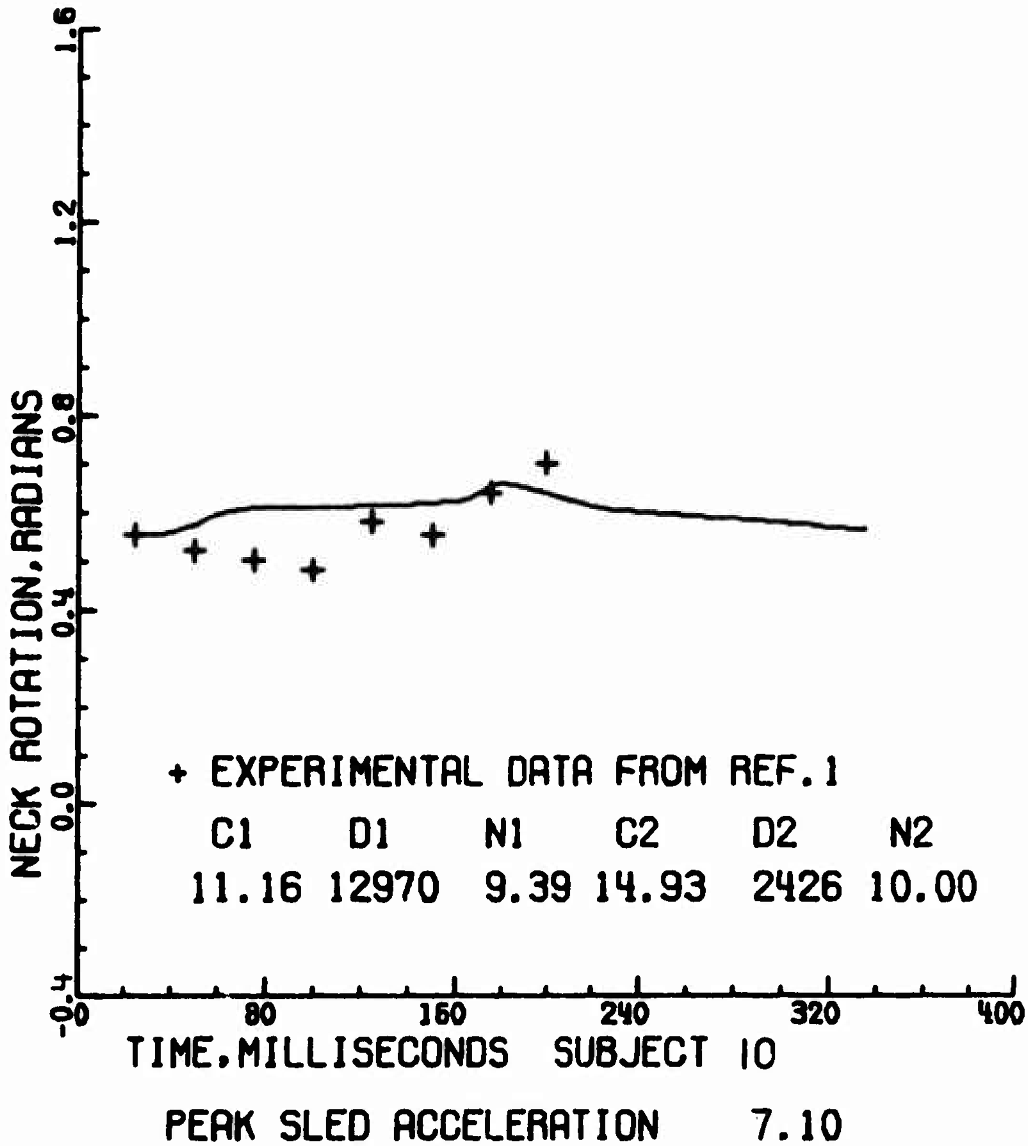

NECK ROTATION, RADIANS
1.6
1.2
0.8
0.4
0.0
-0.4
0.0
80
160
240
320
400
+ EXPERIMENTAL DATA FROM REF. 1
C1 D1 N1 C2 D2 N2
11.16 12970 9.39 14.93 2426 10.00
TIME, MILLISECONDS SUBJECT 10
PEAK SLED ACCELERATION 7.10

FIGURE 37

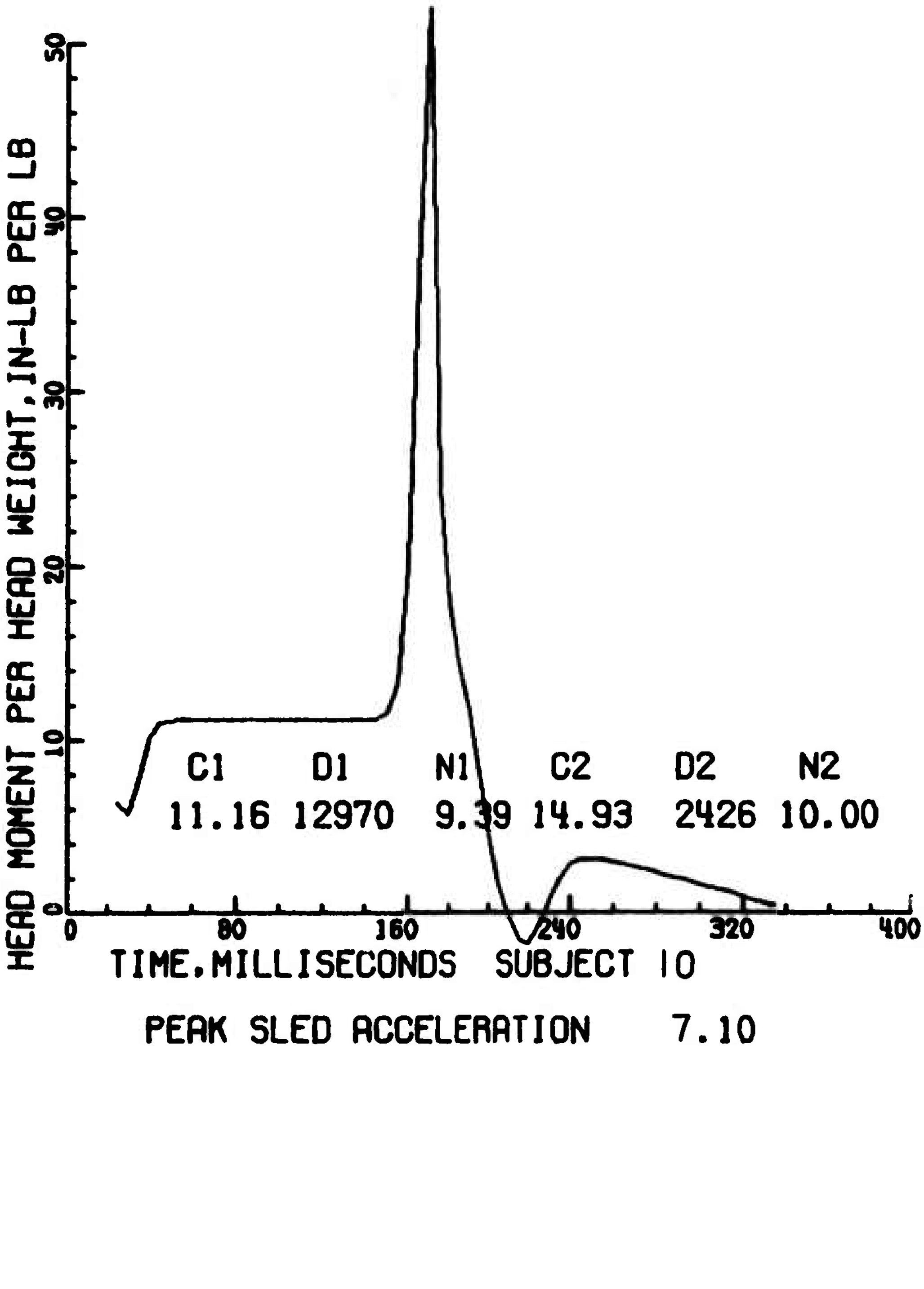
HEAD MOMENT PER HEAD WEIGHT, IN-LB PER LB
0
10
20
30
40
50
0
80
160
240
320
400
C1 D1 N1 C2 D2 N2
11.16 12970 9.39 14.93 2426 10.00
TIME, MILLISECONDS SUBJECT 10
PEAK SLED ACCELERATION 7.10

FIGURE 38

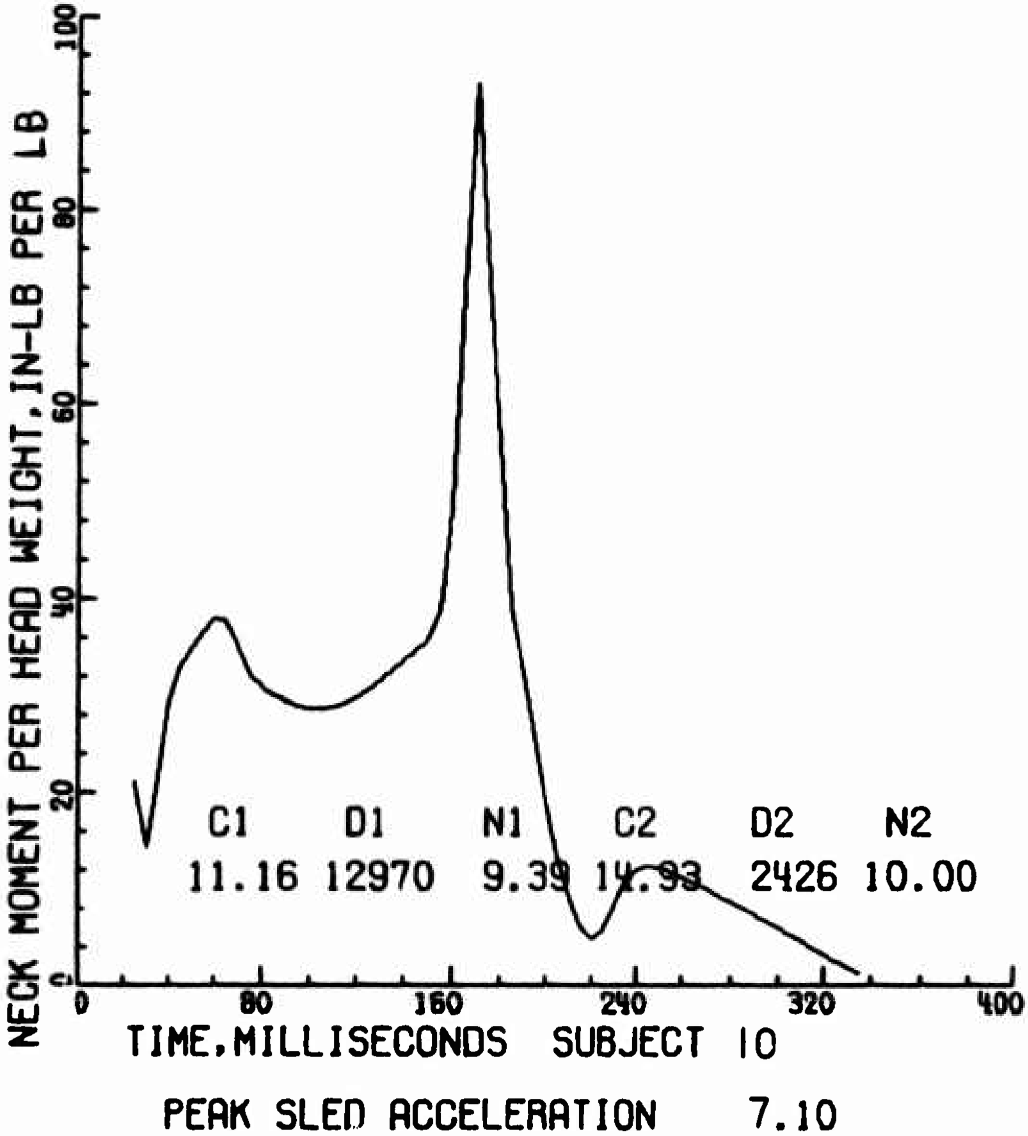
NECK MOMENT PER HEAD WEIGHT,IN-LB PER LB
0
20
40
60
80
100
C1 D1 N1 C2 D2 N2
11.16 12970 9.39 14.93 2426 10.00
0
80
160
240
320
400
TIME,MILLISECONDS SUBJECT 10
PEAK SLED ACCELERATION 7.10

FIGURE 39

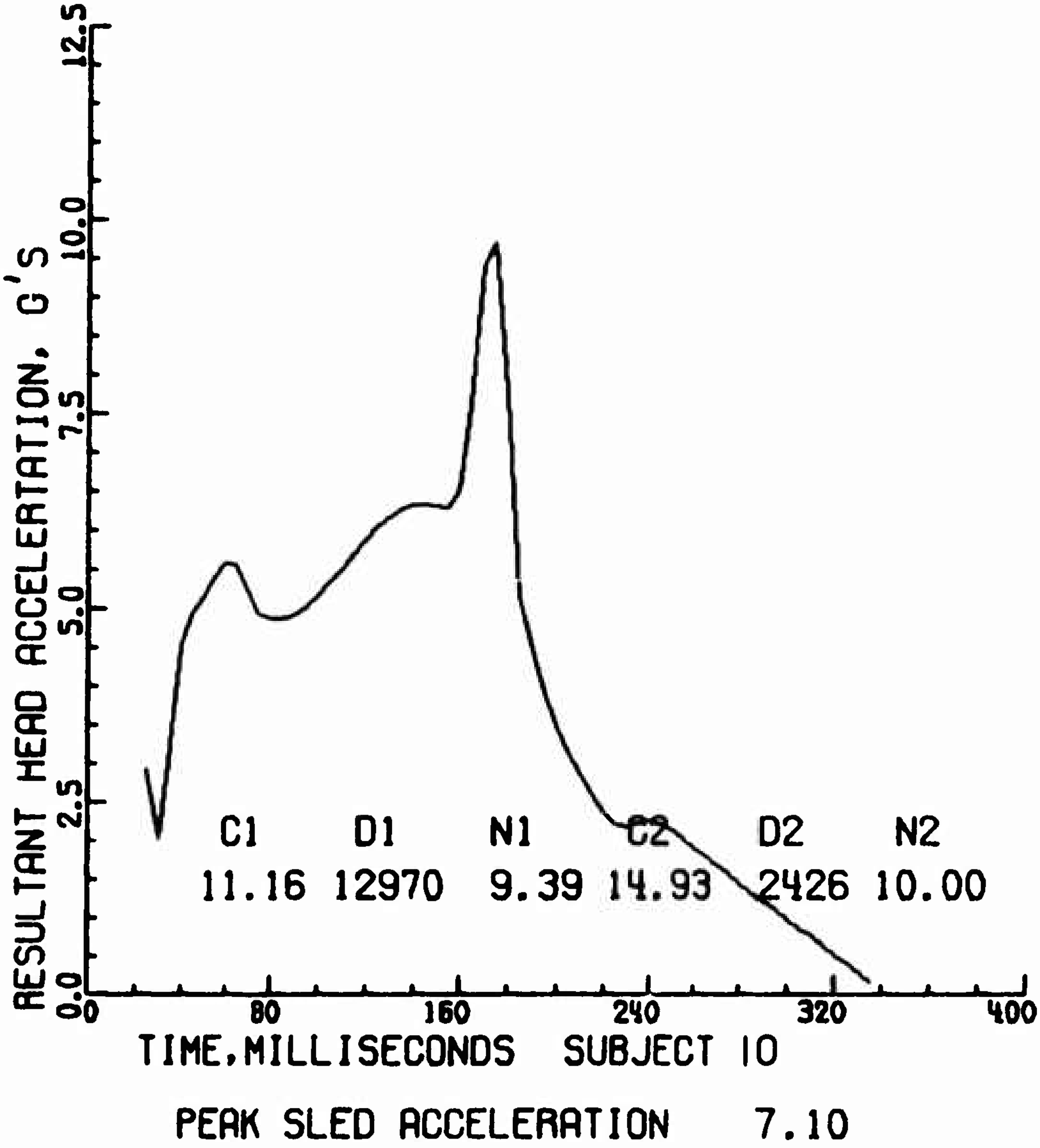
RESULTANT HEAD ACCELERATION, G'S
0.0
2.5
5.0
7.5
10.0
12.5
C1 D1 N1 C2 D2 N2
11.16 12970 9.39 14.93 2426 10.00
0.0
80
160
240
320
400
TIME, MILLISECONDS SUBJECT 10
PEAK SLED ACCELERATION 7.10

FIGURE 40

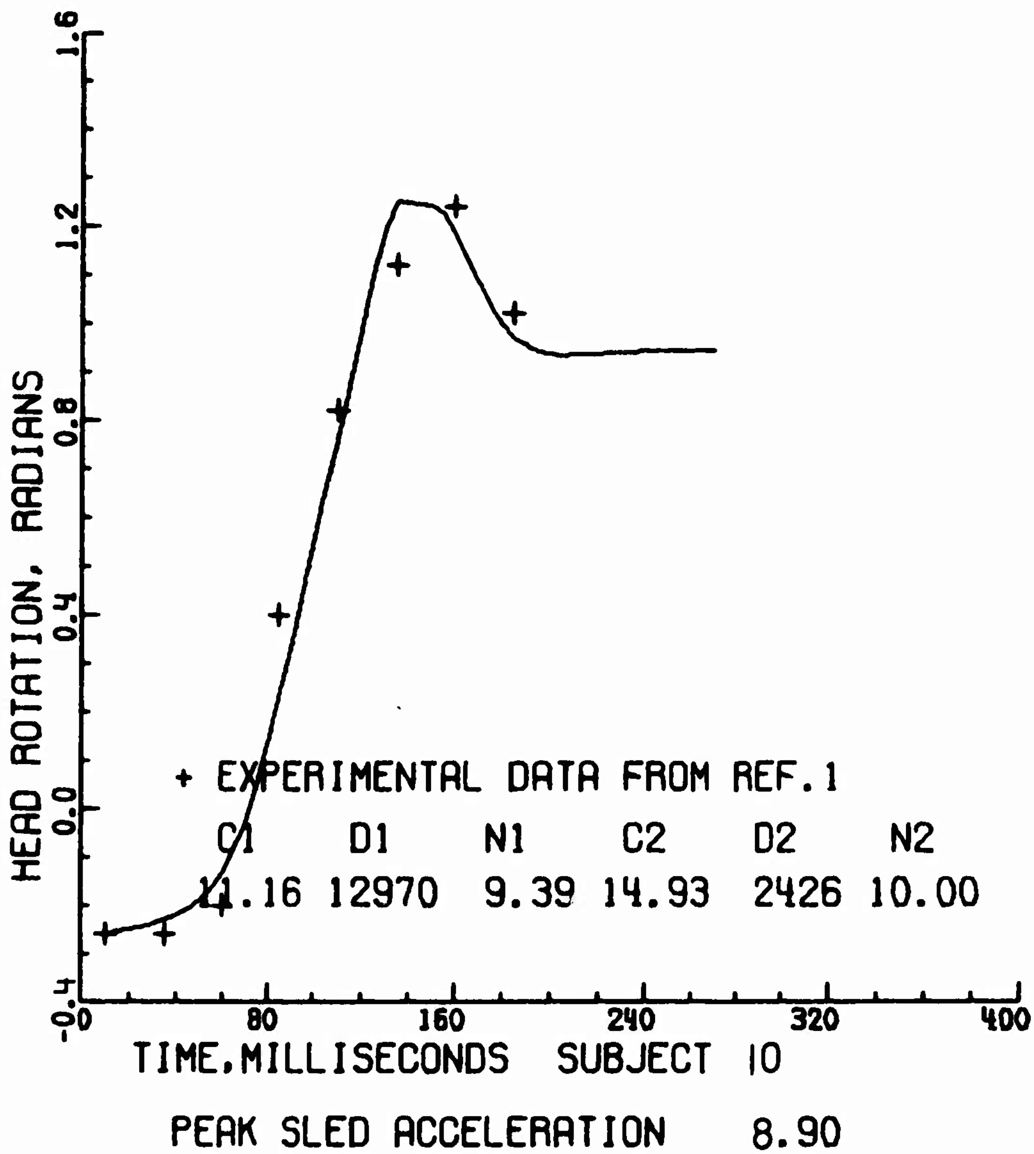

1.6
1.2
0.8
0.4
0.0
-0.4
HEAD ROTATION, RADIANS
+ EXPERIMENTAL DATA FROM REF.1
C1 D1 N1 C2 D2 N2
11.16 12970 9.39 14.93 2426 10.00
0
80
160
240
320
400
TIME,MILLISECONDS SUBJECT 10
PEAK SLED ACCELERATION 8.90

FIGURE 41

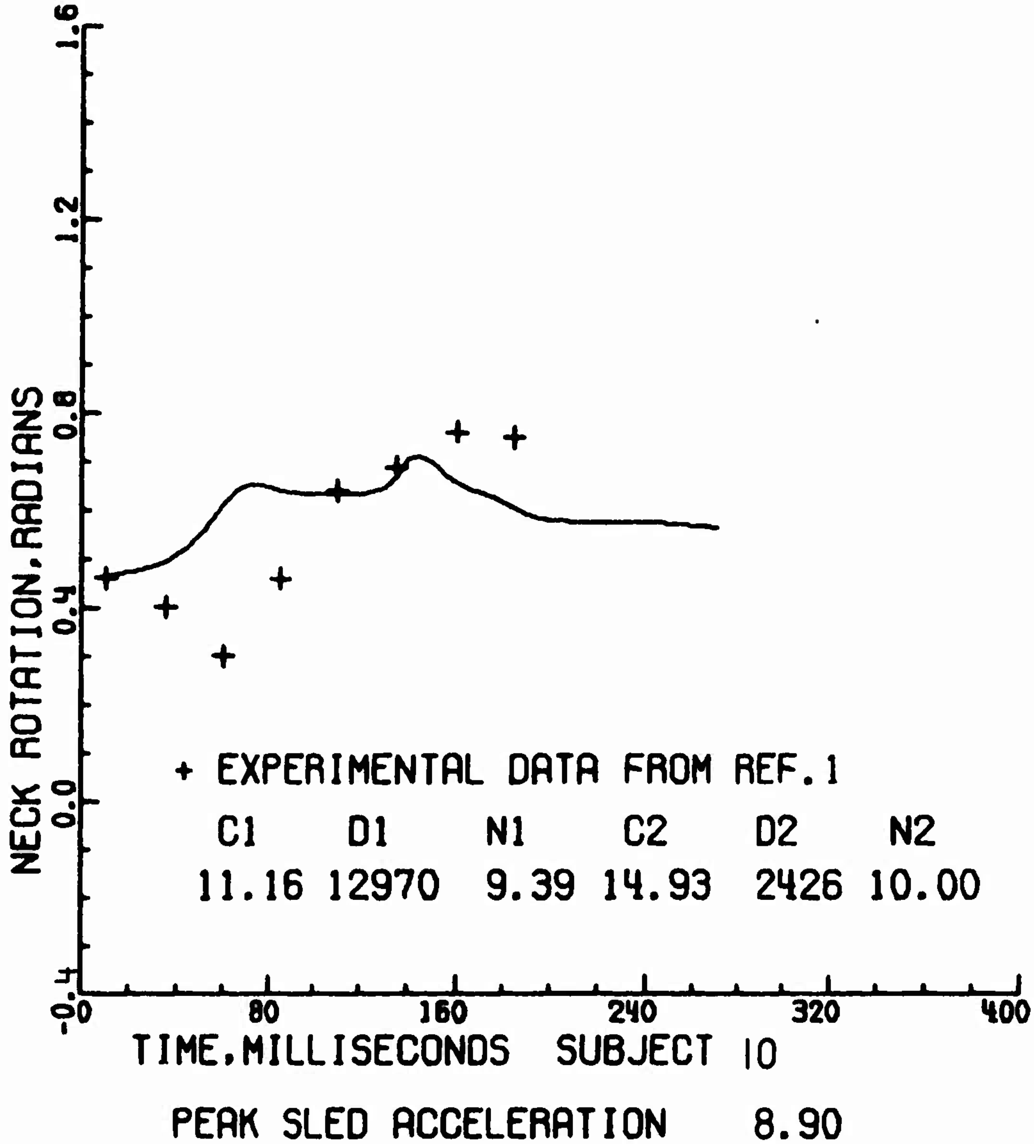
NECK ROTATION, RADIANS
1.6
1.2
0.8
0.4
0.0
-0.4
-0.0
80
160
240
320
400
+ EXPERIMENTAL DATA FROM REF. 1
C1 D1 N1 C2 D2 N2
11.16 12970 9.39 14.93 2426 10.00
TIME, MILLISECONDS SUBJECT 10
PEAK SLED ACCELERATION 8.90

FIGURE 42

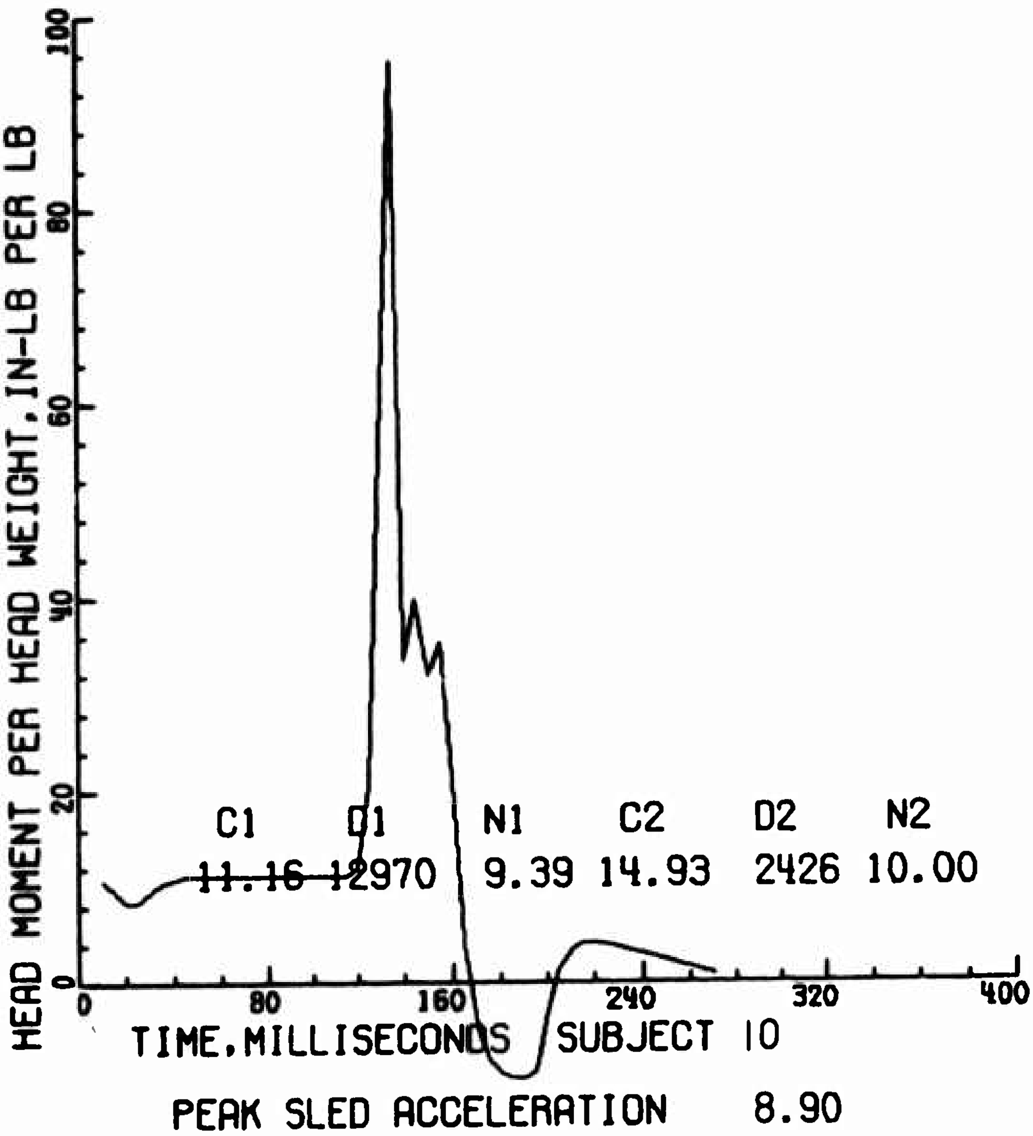
HEAD MOMENT PER HEAD WEIGHT, IN-LB PER LB
0
20
40
60
80
100
0
80
160
240
320
400
TIME, MILLISECONDS
SUBJECT 10
C1 D1 N1 C2 D2 N2
11.16 12970 9.39 14.93 2426 10.00
PEAK SLED ACCELERATION 8.90

FIGURE 43

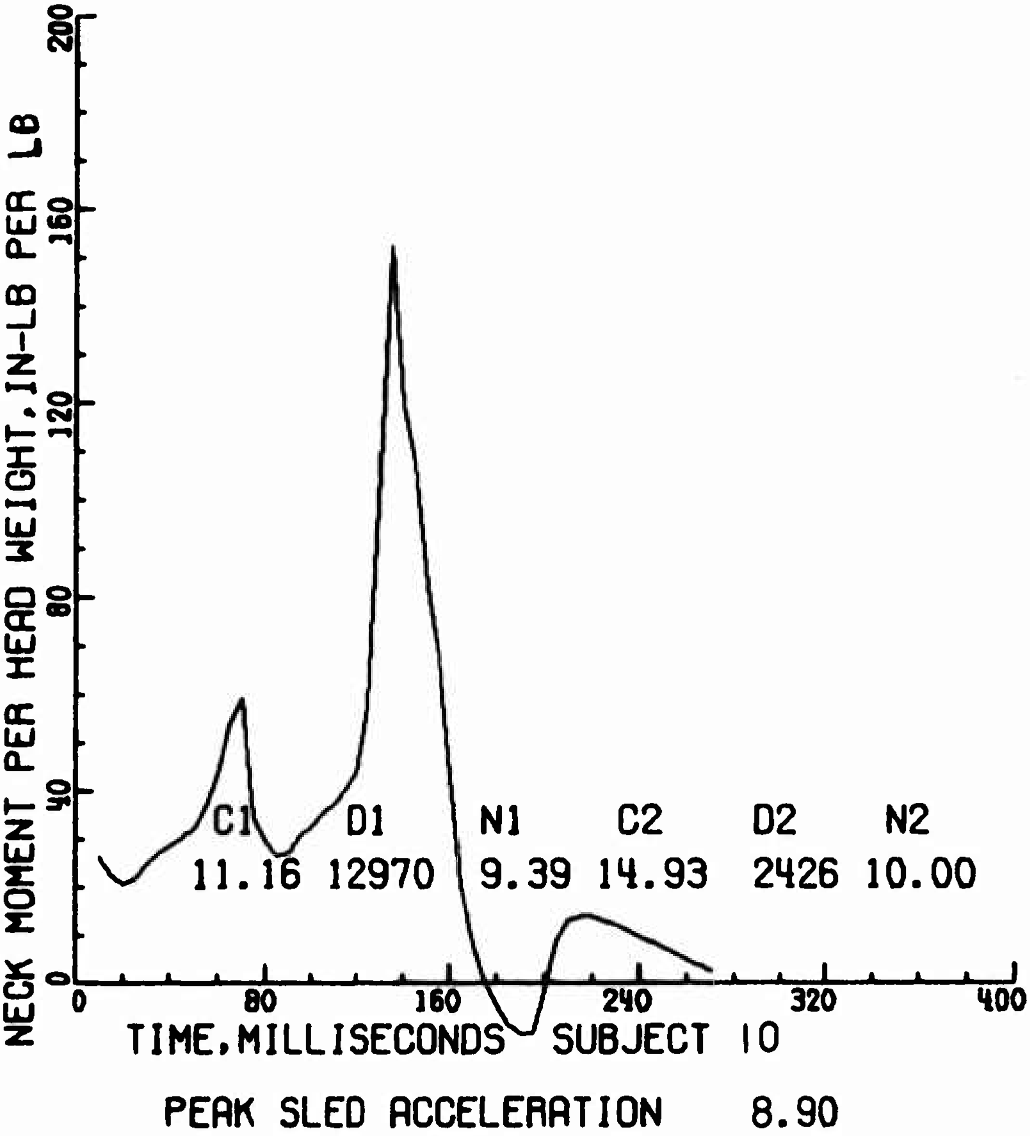
NECK MOMENT PER HEAD WEIGHT, IN-LB PER LB
0
40
80
120
160
200
C1 D1 N1 C2 D2 N2
11.16 12970 9.39 14.93 2426 10.00
0
80
160
240
320
400
TIME, MILLISECONDS SUBJECT 10
PEAK SLED ACCELERATION 8.90

FIGURE 44

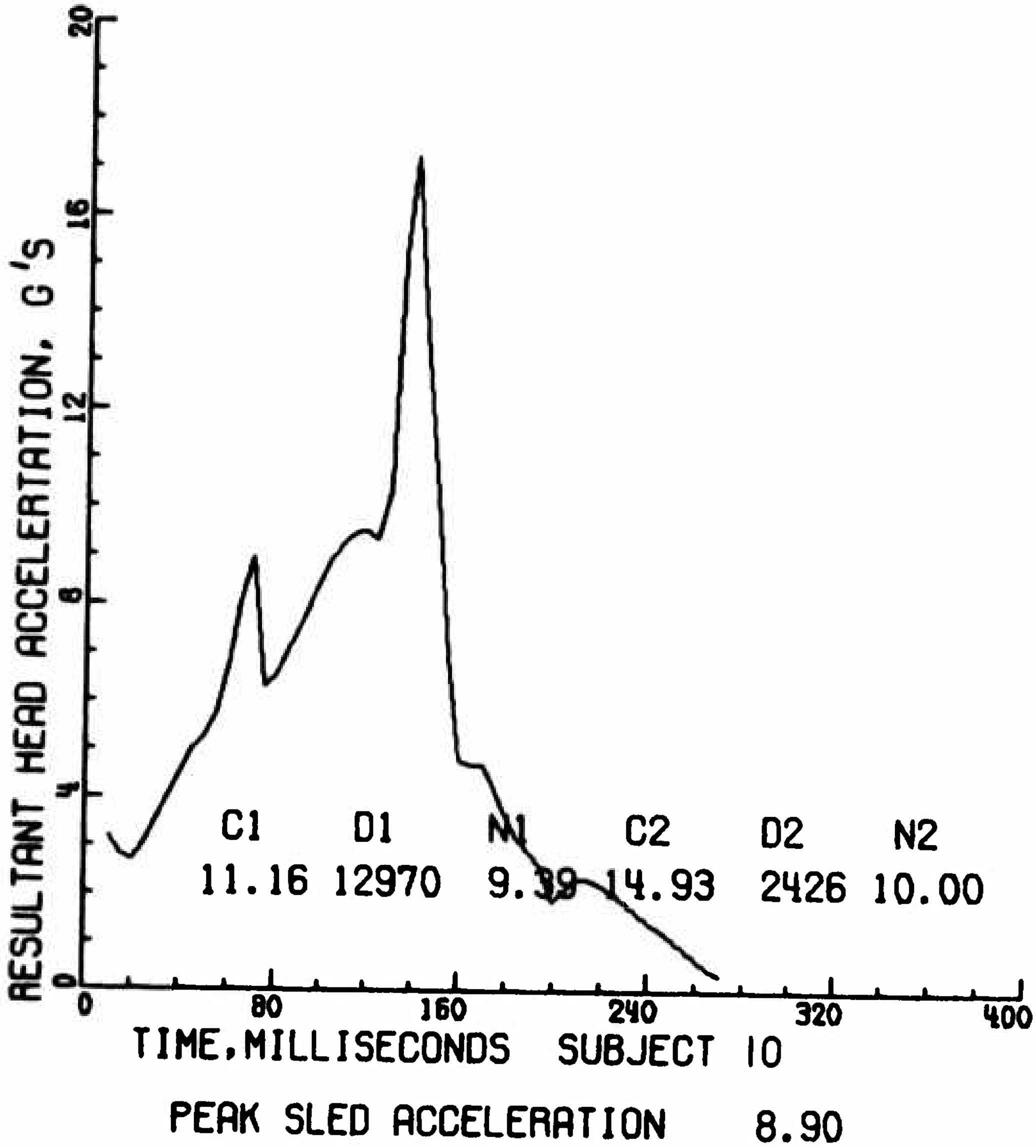
RESULTANT HEAD ACCELERATION, G'S
0
4
8
12
16
20
C1 D1 N1 C2 D2 N2
11.16 12970 9.39 14.93 2426 10.00
0
80
160
240
320
400
TIME, MILLISECONDS SUBJECT 10
PEAK SLED ACCELERATION 8.90

FIGURE 45

PART I - GOVERNMENT

Administrative and Liaison Activities

Chief of Naval Research
Department of the Navy
Arlington, Virginia 22217
Attn: Code 439 (3)
461
444

Director
ONR Branch Office
495 Summer Street
Boston, Massachusetts 02210

Director
ONR Branch Office
536 South Clark Street
Chicago, Illinois 60605

Director
Naval Research Laboratory
Attn: Library, Code 2029 (ONRL)
Washington, D.C. 20390 (6)

U. S. Naval Research Laboratory
Attn: Technical Information Division
Washington, D.C. 20390 (6)

Commanding Officer
ONR Branch Office
207 West 24th Street
New York, New York 10011

Director
ONR Branch Office
1030 E. Green Street
Pasadena, California 91101

Defense Documentation Center
Cameron Station
Alexandria, Virginia 22314 (12)

Navy

Chief of Naval Operations
Dept. of the Navy
Washington, D.C. 20305
Attn: NOP-05F
NOP-506N
NOP-098T

Headquarters
U.S. Marine Corps
Washington, D.C. 20380
Attn: MC-AX-2
MC-AX-4E2 (2)
MC-AAP-3

Commander
Naval Air Systems Command
Dept. of the Navy
Washington, D.C. 20360
Attn: NAVAIR-320N
NAVAIR-5302
NAVAIR-531
NAVAIR-5311J
NAVAIR-5314
NAVAIR-5315A

Commander
Naval Air Development Center
Warminster, Pennsylvania 18974
Attn: Mr. M. Schulman
Crew Systems Dept.

Naval Air Development Center
Philadelphia, Pennsylvania 19112
Attn: Dr. E. Hendler
Crew Systems Dept.

Director
Naval Research Laboratory
Washington, D.C. 20390
Attn: Code 8440 (Dr. F. Rosenthal)

Commanding Officer
Naval Ship Research and Development Center
Bethesda, Maryland 20034
Attn: Code 745 (Mr. B. Whang)

Commanding Officer
Naval Civil Engineering Laboratory
Port Hueneme, California 93041
Attn: Dr. Warren Shaw, Structures Department

Commander
Naval Safety Center
Naval Air Station
Norfolk, Virginia 23511

Capt. Channing L. Ewing Mclusn
Naval Aerospace Medical Research
Lab.
Michoud Assembly Facility
New Orleans, Louisiana 70129

Army

Commanding Officer
U.S. Army Aviation Materiel
Laboratories
Fort Eustis, Virginia 23604
Attn: VDLEU-SS
(Mr. G. T. Singley, III)

Director
U.S. Army Board for Aviation
Accident Research
Fort Rucker, Alabama 36360
Attn: BAAR-PP (Mr. J. Haley)

Commanding Officer
U.S. Army Research Office Durham
Attn: Mr. J. J. Murray
CRD-AA-IP
Box CM, Duke Station
Durham, North Carolina 27706

Air Force

Air Force Office of Scientific Res.
1400 Wilson Blvd.
Arlington, Virginia 22209
Attn: Mechs. Div.

Commanding Officer
6571 st AMRL
Holloman Air Force Base,
New Mexico
Attn: Mr. C. C. Gragg

NASA

Mr. C. Kubokawa
N239-3
NASA Ames Research Center
Moffett Field, California 94035

Department of Transportation

Mr. R. F. Chandler
Code AC 119
CAMI, FAA Aeronautical Center
P.O. Box 25082
Oklahoma City, Oklahoma 73123

Mr. H. Spicer
Federal Aviation Administration (DS-41)
800 Independence Ave SW
Washington, D.C. 20590

Mr. H. Daiutolo
Federal Aviation Administration
NAFEC (NA541)
Atlantic City, New Jersey 08405

Mr. D. Beyer
Federal Aviation Administration
(RD-730)
800 Independence Ave SW
Washington, D.C. 20590

Headquarters
U.S. Coast Guard
400 7th Street SW
Washington, D.C. 20590
Attn: DAT/62
EAE/63
ENE-5/64
IGS-1/61
NMT-t/82
OSR-2/73

Mr. J. G. Viner
Protective Systems Group (RS-12)
Federal Highway Administration
400 7th Street SW
Washington, D.C. 20590

Mr. W. H. Collins
Computer Technology Group (DV-11)
Federal Highway Administration
400 7th Street SW
Washington, D.C. 20590

Mr. Kenneth Batcheller, Chief
Safety Programs Division (RS-20)
Federal Railroad Administration
400 7th Street, SW
Washington, D.C. 20590

Mr. E. Ward, Chief
Engineering Research and Development
Division (RT-20)
Federal Railroad Administration
400 7th Street, SW
Washington, D.C. 20590

Dr. J. A. Edwards
Associate Administrator for Research
and Development
National Highway Traffic Safety
Administration
400 7th Street, SW
Washington, D.C. 20590

Mr. C. D. Ferguson
Office of Crashworthiness (41-40)
National Highway Traffic Safety
Administration
400 7th Street SW
Washington, D.C. 20590

Mr. L. L. Bradford
Office of Vehicle Structures Research
(43-50)
National Highway Traffic Safety
Administration
400 7th Street SW
Washington, D.C. 20590

National Transportation Safety Board
800 Independence Ave SW
Washington, D.C. 20590
Attn: Mr. A. L. Schmieg, NS-10
Mr. H. L. Morgan, NS-20
Mr. B. C. Doyle, NA-87

Dr. H. E. vonGierke
Aerospace Medical Research
Laboratory
Aerospace Medical Division
Air Force Systems Command
Wright-Patterson Air Force Base,
Ohio 45433

Sal Davis
Fairchild Industries, Inc.
Fairchild Republic Division
Farmingdale, New York 11735

PART 2 - CONTRACTORS AND OTHER TECHNICAL COLLABORATORS

Mr. S. P. Desjardins
Dynamic Science
1800 West Deer Valley Drive
Phoenix, Arizona 85027

Dr. A. A. Ezra, Chairman
Dept. of Mechanical Sciences and
Environmental Engineering
University of Denver
Denver, Colorado 80210

Dr. Albert I. King
Bioengineering Center
Wayne State University
Detroit, Michigan 48202

Dr. R. C. DeHart, Director
Dept. of Structural Research
Southwest Research Institute
P.O. Drawer 28510
San Antonio, Texas 78284

Professor Pedro V. Marcal
Division of Engineering
Brown University
Providence, Rhode Island 02912

Professor J. B. Martin
Division of Engineering
Brown University
Providence, Rhode Island 02912

Dr. J. L. Tocher
Boeing Computer Services (72-80)
P.O. Box 24346
Seattle, Washington 98124

Mr. D. G. Harding, Manager
Survivability Staff
Boeing Company - Vertol Division
Philadelphia, Pennsylvania 19142

Dr. H. E. Lindberg, Manager
Engineering Mechanics Program
Stanford Research Institute
Menlo Park, California 94025

Mr. John W. Freyler
Beta Industries, Inc.
2763 Culver Avenue
Dayton, Ohio 45429

Dr. L. E. Hulbert, Chief
Advanced Solid Mechanics Division
505 King Avenue
Columbus, Ohio 43201

Professor George Sih
Department of Mechanics
Lehigh University
Bethlehem, Pennsylvania 18015

Dr. Harold Liebowitz, Dean
School of Engrg. and Applied
Science
George Washington University
725 23rd Street
Washington, D. C. 20006

Professor S. B. Dong
University of California
Department of Mechanics
Los Angeles, California 90024

Professor A. J. Durelli
Mechanics Division
The Catholic University of
America
Washington, D.C. 20017

Professor H. H. Bleich
Department of Civil Engineering
Columbia University
Amsterdam & 120th Street
New York, New York 10027

Professor A. M. Freudenthal
George Washington University
School of Engrg. and Applied
Science
Washington, D.C. 20006

Professor P. G. Hodge
Department of Mechanics
Illinois Institute of Technology
Chicago, Illinois 60616

Dr. D. C. Drucker
Dean of Engineering
University of Illinois
Urbana, Illinois 61801

Professor N. M. Newmark
Department of Civil Engineering
University of Illinois
Urbana, Illinois 61801

Library (Code 0384)
U. S. Naval Postgraduate School
Monterey, California 93940

Dr. Francis Cozzarelli
Division of Interdisciplinary Studies
and Research
School of Engineering
State University of N. Y.
Buffalo, New York 14214

Dr. George Herrmann
Stanford University
Department of Applied Mechanics
Stanford, California 94305

Professor J. D. Achenbach
Technological Institute
Northwestern University
Evanston, Illinois 60201

Professor J. Kempner
Dept. of Aero. Engrg. and
Applied Mech.
Polytechnic Institute of Brooklyn
333 Jay Street
Brooklyn, New York 11201

Dr. Nicholas J. Hoff
Dept. of Aero. and Astro.
Stanford University
Stanford, California 94305

Professor Norman Jones
Massachusetts Institute of Technology
Dept. of Naval Architecture and Marine
Engineering
Cambridge, Massachusetts 02139

Professor Werner Goldsmith
Department of Mechanical Engineering
Division of Applied Mechanics
University of California
Berkeley, California 94720

Professor W. D. Pilkey
Department of Aerospace Engrg.
University of Virginia
Charolottesville, Virginia 22903

Dr. H. N. Abramson
Southwest Research Institute
8500 Culebra Road
San Antonio, Texas 78206

Mr. John Scowcroft
Automobile Manufacturers Association
330 New Center Building
Detroit, Michigan 48202

Dr. R. D. Young
Texas Transportation Institute
Texas A & M University
College Station, Texas 77840

Professor J. A. Collins
Mechanical Engineering Department
Arizona State University
Tempe, Arizona 85281